OPTIMIZATION OF THERMAL COOLING PARAMETERS APPLIED TO ROCK STORAGE SYSTEMS

Alex Xavery Matofali

PhD (Mathematics) Thesis
University of Dar es Salaam

April, 2015

OPTIMIZATION OF THERMAL COOLING PARAMETERS APPLIED TO ROCK STORAGE SYSTEMS

By

Alex Xavery Matofali

A Thesis Submitted in Fulfilment of the Requirements for the Degree of Doctor of Philosophy (Mathematics) of the University of Dar es Salaam

University of Dar es Salaam

April, 2015

CERTIFICATION

The undersigned certifies that they have read and hereby recommends for acceptance by the University of Dar es Salaam the thesis titled: ***Optimization of Thermal Cooling Parameters Applied to Rock Storage Systems***, in fulfilment of the requirements for the degree of Doctor of Philosophy of the University of Dar es Salaam.

Prof. Estomih S. Massawe

(Supervisor)

Date: 13/5/2015

DECLARATION

AND

COPYRIGHT

I, **Alex Xavery Matofali,** declare that this thesis is my own original work and has not been presented and will not be presented to any other university for a similar or any other degree award.

Signature:

ACKNOWLEDGEMENTS

First and foremost, I would like to express my sincere appreciation to my supervisor, Prof. Estomih S. Massawe. His guidance, hard work and infectious enthusiasm were essential to complete this work. Recognition and thanks is also due to COSTECH for the financial support in undertaking the work presented here.

I am also grateful to Dr. Gerald Tendayi Marewo of the Department of Mathematics at the University of Swaziland for his support and advice during my research and great support in getting the data and the MATLAB software. Finally, I would like to thank my family and all my friends, for their encouragement, support and understanding during my study.

DEDICATION

This thesis is dedicated to my late father Xavery Lucas Nandi.

ABSTRACT

This study presents a mathematical model for thermal energy storage in low energy buildings. The cooling system which uses rock bed for storing night cooling to be used later for daytime air conditioning is presented. The work initially focuses on the mathematical descriptions of the thermal cooling applied to rock storage system. A numerical method of solution is outlined and the results are compared with measured data at the outlet of the bed both using the measured inlet temperature. A good agreement of trend is observed. The results show two effects of the cooling system on the air temperature, which are damping and time delay of the peaking. The differences are examined through sensitivity analyses for both the convective heat transfer coefficient and mass flow rate. A parametric study for heat storage with materials and bed size is given.

A genetic algorithm (GA) is used as a tool to identify the thermal cooling system parameters related to the mathematical model, including the radius of the sphere (rocks), mass flow rate, convective heat transfer coefficient and length of the rock bed. The simulation results have shown an improvement on the performance of the model with identified parameters compared to the performance before parameter optimization. In general, the model with optimal parameters has shown robustness to predict the performance of the cooling system by reducing the input (air) temperature as much as possible at the time when the temperature is hottest.

TABLE OF CONTENTS

LIST OF FIGURES

LIST OF TABLES

LIST OF ABBREVIATIONS

COSTECH	=	Commission for Science and Technology
GA	=	Genetic Algorithm
TES	=	Thermal Energy Storage
HVAC	=	Heating, Ventilating and Air Conditioning
LHTES	=	Latent Heat Thermal Energy Storage
FES	=	Fabric Energy Storage

CHAPTER ONE

INTRODUCTION

1.1 General Introduction

The demand of air conditioning has increased greatly during the last decade, and large demands of electric power and limited reserves of fossil fuels have led to a surge of interest in efficient energy application (Pasupathy and Velraj, 2006). The debate on global warming has led to increased attention on energy efficient cooling systems utilizing renewable energy sources. Cooling demand has already been increasing due to the evolving comfort expectations and technological development around the world. Furthermore, climate changes have brought additional challenges to cooling systems designers, since most environmental problems related to energy utilization are the results of climate changes (Ravikumar and Srinivasan, 2005). Therefore, there is a need to find a better way to utilize energy: not only in the field of energy production, transmission, distribution, and consumption, but also in the area of energy storage.

Efficient, environmental friendly and economical technology that can be used to store large amounts of heat or cold in a definite volume has been the subject of research for a long time. A long-term solution in the form of new low-cost technology that relies only on renewable sources of energy and on locally available materials is needed. Thermal energy storage plays an important role in building energy conservation initiatives, which are greatly enhanced by incorporation of latent heat storage in building products. Thermal energy storage deals with selecting media/devices that absorb and store heat/cold during peak power operation and releases the same during reduced power operation. Building fabric or packed beds (rock pile, pebble bed and rock bed) materials are some of the thermal storage devices (Ravikumar and Srinivasan, 2005).

The thermal storage capacity of buildings if increased can increase human comfort by decreasing the frequency of internal air temperature swings so that indoor air temperature is closer to the desired temperature for a longer period of time (Dincer *et al.*, 1997). It has been shown that heating, ventilating and air conditioning equipment size and associated capital, operating energy and maintenance costs are lower for a building designed to take advantage of its thermal mass than for a conventional building. Thermal mass are materials having the capacity to store thermal energy for extended periods and are most easily achieved using denser construction materials such as masonry walls or concrete slabs. Balaras (1996), defined thermal mass as that part of the construction mass of a building that is used to store thermal energy. In addition, integration of the air delivery system with structural elements offers the potential to reduce costs (Hui and Cheung, 1998).

Developing efficient and inexpensive energy storage devices is as important as developing new sources of energy. Thermal Energy Storage (TES) has been defined as the temporary storage of thermal energy at high or low temperatures. TES systems provide the potential to attain energy savings, which in turn reduce the environmental impact related to non-renewable energy use. In fact, these systems can reduce time or rate mismatch that is often found between energy supply and energy demand (Ataer, 2006; Pasupathy and Velraj, 2006; Manohar and Adeyanju, 2009). Energy storage improves performance of energy systems by smoothing supply and increasing reliability. The higher efficiency would lead to energy conservation and improve cost effectiveness (Manohar and Adeyanju, 2009). This technology is highly needed especially in developing countries such as Tanzania because its poorest people are the most vulnerable to the ongoing climate change. Climate change is the most serious environmental problem relating to energy utilization. Thermal energy storage technology is one of the most effective ways of mitigating climate change through reductions in emissions of environmentally harmful pollutants such as CO_2, SO_2, and NO_x and thus slow down global warming. Thermal energy storage is also economically viable because it reduces the amount of power lines that would be constructed in future to keep up with demand (Pasupathy and Velraj, 2006).

In general, in summer period (this means during the day) the temperature in a building increases because of solar and internal gains and does not cool down during the night. To keep temperatures within thermal comfort limits cooling must be introduced. Energy efficient cooling can be provided using natural cooling. With intensive night ventilation, the structure elements can be cooled down thus providing more comfortable living conditions the following day. Such natural cooling is especially efficient in moderate climate conditions, where the daily oscillations of the ambient temperature are high (Arkar *et al.*, 2007).

The efficiency of natural cooling could be further improved using latent heat thermal energy storage (LHTES) integrated into the building's mechanical ventilation system. The LHTES stores coldness of ambient air during the night and supplies it with time delay during the day. According to Arkar *et al.*, (2007), the LHTES air inlet temperature in the ambient air temperature can be approximated by the equation:

$$T_a(t) = \overline{T}_a - A\cos(\omega t - \omega \phi) \qquad (1.1)$$

where $\overline{T}_a$ is the average daily ambient temperature, A is the amplitude of temperature swings, ω is the frequency, and ϕ is the time shift of daily minimal temperature. The value of time shift represents the time interval between midnight and the moment of minimal daily ambient air temperature.

1.2 Examples of energy efficient buildings

i). **Eastgate** (Harare, Zimbabwe)

Mode of operation - unlike the usual High Voltage Air Conditioning, cooling in the summer is achieved by pre-cooling specialized passage ways (ventilated floor slabs) within the building mass (mostly concrete) at night, then on the following day, warm outside air is forced through these slabs and thereby cooled before it enters the offices as part of a displacement ventilation system.

Achievements of the cooling system:

(a) The maximum and minimum temperatures of the outside air for the day are kept within acceptable comfort levels of the occupants in the building.

(b) Peaking of the day time outside air temperature is delayed.

Advantages of the cooling system over conventional systems:

(a) Cheaper to install and maintain.

(b) Lower energy consumption.

ii). **Harare International School** (Harare, Zimbabwe)

Mode of operation - while the energy transporting medium is air, similar to the Eastgate building, the energy storage material is not concrete ventilated floor slabs but a packed bed filled with rocks (rock bed). Also, the rock bed is not part of the building mass but lies underground outside the building.

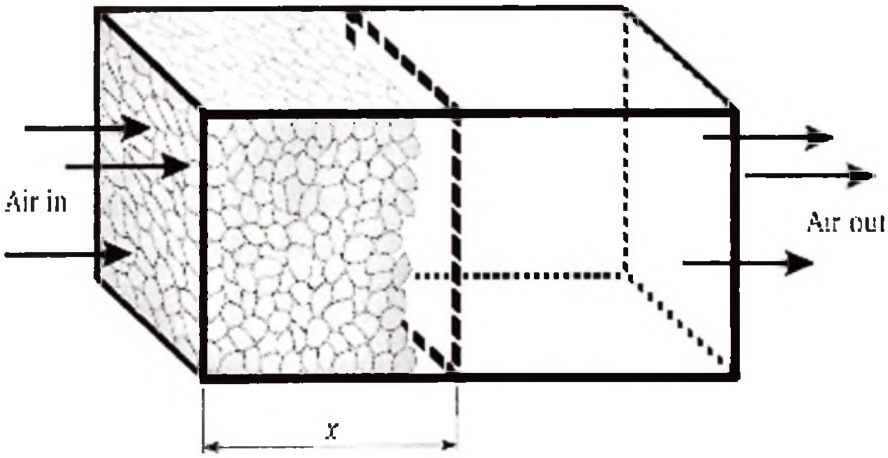

Figure 1.1: The model of a packed bed

Achievements of the cooling system:

(a) The maximum and minimum temperatures of the outside air for the day are kept within acceptable comfort levels of the occupants in the building.

(b) Peaking of the day time outside air temperature is delayed.

Advantages of the cooling system over conventional systems:

This cooling system has the following advantages;

(a) Energy storage material (rocks) is readily available and cheaper for short and long-term storage.

(b) System is easier to modify if there is any need.

(c) More efficient cooling due to higher surface area to volume ratio.

(d) Cheaper to install and maintain.

Compared to the above systems, the existing systems are expensive, difficult to install and usually require external electricity to operate, and hence are not truly applicable in remote areas. The use of construction materials with high thermal admittance in walls, columns and floors, improves the capacity to store and release heat. This method of construction is often termed Fabric Energy Storage (FES) or Thermal Mass, and can be optimized through good design and construction. This technique has been used in many building types to create more comfortable working conditions and reduce energy consumption (Ren and Wright, 1998).

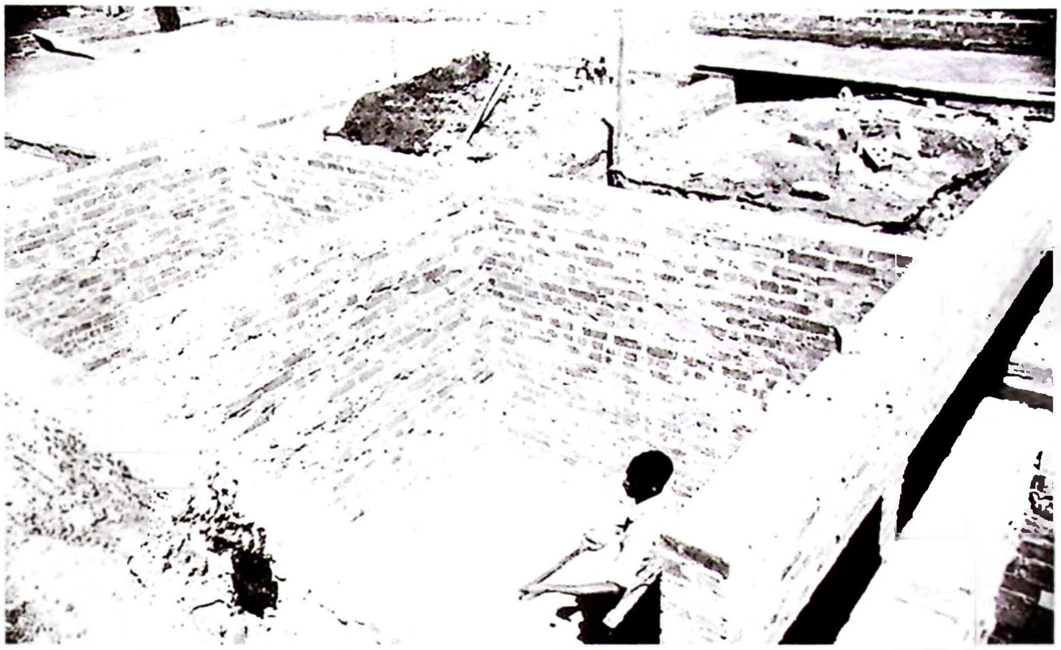

Figure 1.2: Rock-stone compartments (foreground) during construction of the Middle school at Harare international school

The advantage of Fabric Energy Storage or Thermal mass is that it can be used in conjunction with night ventilation of a building to provide passive cooling. Outside air is circulated through the building where it comes into contact with and cools the building fabric. The cooling that is stored in the building fabric is then available to offset the heat gains of the following day and keep temperatures within comfort limits (Barnard, 2006). In particular, thermal mass absorbs excess heat inside buildings during the day, which can be removed by night time ventilation. In this case, peak daytime temperature inside a building can be reduced as much as 6 to 8 °C depending on the heat load, and their onset delayed by up to 6 hours compared to building with low thermal mass (Barnard, 2006).

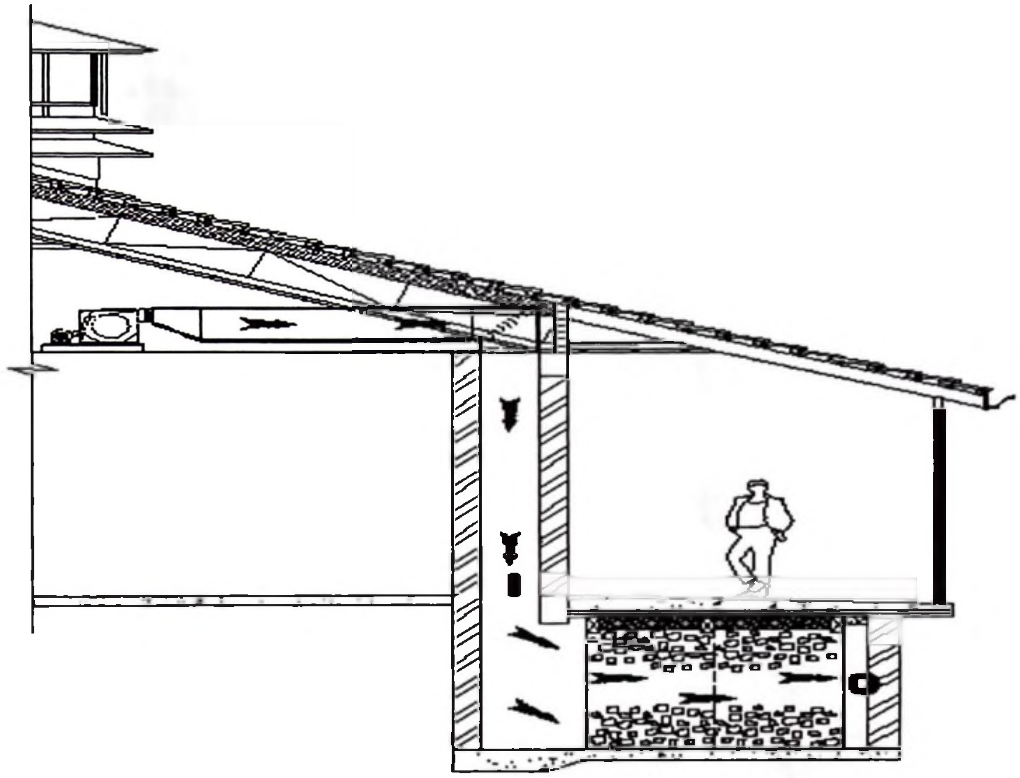

Figure 1.3: An example of Air flow path

Extensive studies have been carried out on the storage of thermal energy as sensible heat in a packed bed (rock bed) useful for low temperature applications such as in the heating and cooling of solar houses. With the increasing interest in the use of solar energy for power production, the use of rock bed for high temperature heat storage has been suggested (Al-Nimr *et al.*, 1996).

Coutier and Farber (1982) mention that packed bed (rock bed) generally represents the most sensible energy storage unit for air based systems. A *packed bed* is a volume of porous media obtained by packing particles of selected materials into a container. A packed bed storage system consists of loosely packed solid materials through which the heat transport fluid is circulated. Heated fluid (usually air) flows from solar collectors into a bed of graded particles from top to bottom in which thermal energy is transferred during the charging phase (Singh *et al.*, 2010).

1.3 Statement of the Research Problem

Passive cooling is defined as the building design approach that focuses on heat gain control and heat dissipation in a building in order to improve the indoor thermal comfort with low or nil energy consumption (Barnard, 2006). Passive cooling systems using rock storage have been used and researched over years, as a way of cooling buildings using less energy compared to electrically powered air-conditioning unit. However, results obtained through different studies such as that of Al-Nimr *et al.*, (1996), Dincer *et al.*, (1997) and Marewo (2006) have little information on how different cooling system parameters applied to rock storage systems such as, dimensions of the rock stone, air velocity, and timing can be chosen to give the best cooling.

Moreover, Singh *et al.*, (2008) reported on the simulated performance of a packed bed energy storage system having storage material elements of large size. The study revealed that, cooling system parameters play an important role by influencing transfer of heat and fluid flow characteristics of a rock bed energy storage system. Despite these findings, more research is needed in order to explore and document information on how best the parameters can be chosen to improve the performance of rock bed storage systems.

The goal of this research is to study thermal cooling with parameter optimization such as, mass flow rate $(\dot{m}_a)$, convective heat transfer coefficient (h_c), radius of the rocks $(R)$and length of the bed (L), by genetic algorithm that can improve the performance of the cooling system applied to rock storage systems. The aim of this study is therefore, to formulate and analyse a mathematical model of the rock bed system with parameter optimization that will improve the performance of thermal cooling systems. Genetic Algorithms (Mitchell, 1996) are used to come up with an optimal strategy (design and operational parameters) that maximizes thermal comfort of occupants and minimizes energy consumption.

1.4 Research Objectives

The main objective of this study is to optimize the thermal cooling parameters applied to rock storage systems.

The specific objectives are:

i. To develop an effective model of optimizing the thermal cooling parameters applied to rock storage systems.
ii. To determine the efficiency of rock storage systems under different climatic conditions.

1.5 Significance of the Research

The need to use sustainable energy technology is of great interest. Using renewable energy and energy efficiency in buildings is techno-economically feasible, and significantly cheaper than other sources of energy such as hydro-power. The need of expanded energy services to meet the growth and development needs is now important, particularly to people living in the developing countries e.g. Tanzania.

In energy systems, where there is a difference between the supply of energy and its utilization, an alternative form of energy storage is important to ensure the community of thermal process. For air systems and in some cases liquid systems, such as solar domestic water and space heating, a rock bed provides effective thermal energy storage (Beasley and Clack, 1984).

This study will come up with a mathematical model that may be used by engineers to improve the performance of cooling systems in the buildings they design and construct.

CHAPTER TWO

LITERATURE REVIEW

This chapter provides a general overview of past research studies and literature on Thermal Energy Storage. Particularly, it reviews the context in which a rock bed store would be used, and previous research studies on the application and efficiency of genetic algorithms.

There have been many analytical and experimental studies on the use and performance analysis of both building fabric and packed bed as thermal energy storage materials. In 1998, Ren and Wright studied hollow core ventilated slab thermal energy systems. Results from this study showed that hollow core ventilated systems provide an effective means of utilizing a building structure as a thermal storage to reduce energy costs while maintaining the thermal comfort of its occupants. The hollow core ventilated slab thermal storage energy has been implemented in several buildings in many parts of the world. One such example is the building housing the laboratory of the Chemical Engineering Department at the National University of Science and Technology in Bulawayo, Zimbabwe.

Studies such as that of Adebiyi *et al.*, (1996) were mainly based on computer simulations involving modelling of a packed bed for thermal energy storage which led to the development of a comprehensive computer model for the sensible heat storage media and parametric study. Athienitis (1997) established that the use of building fabric for storing thermal energy is an effective way of cooling (heating) the internal environment of a building.

In 1996, Al-Nimr *et al.* developed an analytical model that predicts the dynamic response of a packed bed (cylindrical) column to a variable inlet fluid temperature. The energy equation for the fluid includes heat loss to the environment:

$$\varepsilon\rho_f c_f S_{fr} L\frac{\partial T_f}{\partial t} + Gc_f S_{fr} L\frac{\partial T_f}{\partial z} = h_v S_{fr} L(T_m - T_f) + UPL(T_{env} - T_f) \quad (2.1)$$

where $G = \dfrac{\dot{m}_f}{S_{fr}}$ and the energy equation for the solid is

$$(1-\varepsilon)\rho_m c_m S_{fr} L\frac{\partial T_m}{\partial t} = h_v S_{fr} L(T_f - T_m). \quad (2.2)$$

where c is the specific heat capacity, ε is the bed void fraction (which is defined as the volume of gas per unit volume of rock-bed), h_v is the volumetric heat transfer coefficient, L is the bed length, P is the bed perimeter, r is the radial distance, ρ is the density, S_{fr} is the surface frontal area, T_m is the temperature of the packed material, T_f is the temperature of the fluid, T_{env} is the temperature of the surrounding environment t is time, U is the heat loss coefficient from bed to surrounding, z is the distance in direction of fluid flow, $\dot{m}_f$ is the mass flow rate of heat transfer fluid.

By introducing the dimensionless quantities

$$\theta_f = \frac{T_f - T_{env}}{T_{fi} - T_{env}},\ \theta_m = \frac{T_m - T_{env}}{T_{fi} - T_{env}},\ \tau = \frac{h_v t}{\rho_f c_f \varepsilon},\ Z = \frac{h_v z}{Gc_f}$$

the energy equations for the solid and fluid phases assume the forms

$$\frac{\partial \theta_f}{\partial \tau} + \frac{\partial \theta_f}{\partial Z} + (1+\beta_1)\theta_f - \theta_m = 0 \tag{2.3}$$

$$\frac{\partial \theta_m}{\partial \tau} - \beta_2(\theta_f - \theta_m) = 0 \tag{2.4}$$

where $\beta_1 = \frac{UP}{h_v S_{fr}}$, $\beta_2 = \frac{\rho_f c_f \varepsilon}{\rho_m c_m (1-\varepsilon)}$, θ_f is the dimensionless fluid temperature θ_m is dimensionless material temperature, τ is dimensionless time and Z is the dimensionless distance in direction of fluid flow. The mathematical problem considered by Al-Nimr *et al.* was of heat transfer (in the packed bed column) governed by equations (2.3) and (2.4) subject to a constant temperature profile at initial instant and a given temperature of the fluid at the inlet. The solution to this problem was found using Laplace transforms. The model results were validated using measured data.

Ståhl in 2009 carried out a detailed study of the thermal properties of building thermal mass, their influences on the energy efficiency and the heating demand based on the indoor temperature. The term "thermal inertia" is defined as the degree of slowness with which the temperature of a body approaches that of its surrounding. Mathematically, thermal inertia is defined as $P = \sqrt{k\rho c}$, where k represents the thermal conductivity of the material, ρ being the density of material and c corresponding to specific heat capacity. The study suggested that the most important parameter for evaluating energy storage potential of the thermal mass is "thermal inertia". The use of thermal mass with high thermal inertial exposed to the interior environment in the so-called "heavy building" would help to reduce the overall heat consumption, as surplus heat from the internal gain is effectively stored.

Dincer *et al.*, (1997) studied the performance analysis of sensible heat storage systems for thermal applications. They found that rock beds, water and phase-change materials are the most suitable media for solar thermal energy storage. The results also indicated that rocks are the best known and most widely used heat storage medium for air collectors. The study also listed the advantages of using rock beds in thermal energy storage systems. In this thesis, it is intended to develop a mathematical model that predicts the dynamic response of a packed bed which uses rocks as thermal energy storage medium.

In 1991, Bhardwaj *et al.*, made an extensive review of various models for packed bed thermal energy storage systems. Also in 2010, Singh *et al.*, made a review on packed bed solar energy storage systems and observed that a number of analytical studies were carried out to investigate the effects of various parameters on the performance of a packed bed. Athienitis and Chen in 2000 conducted a numerical experiment on the transient heat transfer in floor heating systems using a three-dimensional explicit mathematical model. The study established that solar radiation stored in the floor thermal reduce heating energy consumption significantly (30% or more).

Aly and El-Sharkawy (1990) studied the effects of storage material properties on the thermal behaviour of packed beds during charging. A transient one-dimensional two-phase mathematical model was used to describe the temperature fields in the air and solid media constituting the bed. They concluded that one of the main sets of parameters affecting the design of solid packed beds is the physical properties of the solid phase used as storage material and choice of material is particularly important.

Crandall and Thacher (2004) performed numerical simulations of solar energy storage with rock in stratified beds. They reported that the packed beds can have a higher stratification, which is a major advantage. Stratification provides highest temperature at the top of the bed and coolest at the bottom. This allowed the warmest air to be delivered from the top of packed bed.

In 2001, Nsofor *et al.*, conducted an experimental study for high temperature sensible heat storage. An experimental investigation of forced gas-particle heat transfer coefficient in a packed bed has been done and correlations have been given for Nusselt number. Chen and Liu (2004), studied the use of an air-based rock bed for passive heating in a cold climate. The results indicated that if the porosity of the storage materials (rocks) is kept within a certain range, increasing the rock size will cause an increase of the capability of thermal storage and heating effects.

In 1995, Sanderson and Cunningham studied theoretically a simple model of packed bed which explains how varying the sphere diameter of the packing will influence the degree of axial dispersion. The results showed that, spheres with smaller diameter store more heating/cooling than larger diameter spheres. Also, smaller diameter spheres make more efficient use of the packing storage volume.

Hessari *et al.*, in 2004 studied the behaviour of packed bed by a set of differential equations. A numerical solution of the mathematical model for the packed bed storage tank was accounting to the thermal losses and conduction effect was found. The effect of heat loss to the surrounding, conduction effect and air capacities was examined by the numerical solution. Denok *et al.,* (2011) made theoretical study on thermal performance of rock bed storage. The effect of diameter of the rock, and mass of air flow rate on the thermal performance of the cylindrical thermal storage, as well as on the pressure drop, were examined.

To understand and improve the performance of the cooling system in an energy efficient building, a suitable mathematical model is an essential tool. For example in 2005, Marewo proposed a model for the cooling system at Eastgate building in Harare, Zimbabwe. The model consists of coupled linear partial differential equations (for both the slab and the air) subject to prescribed boundary conditions and time dependent supply of air temperature. The mathematical model was in the form of a parabolic partial differential equation of the form

$$\frac{\partial u}{\partial t} = \alpha \nabla^2 u \quad \text{on} \quad \Omega, t > 0, \tag{2.5}$$

whose solution $u(\mathbf{x}, t)$ is the slab temperature at point $\mathbf{x}$ and time t with boundary conditions,

$$-\frac{\partial u}{\partial n} = h(u - v) \quad \text{on} \quad \partial\Omega^c, \tag{2.6}$$

$$-\frac{\partial u}{\partial n} = 0 \quad \text{on} \quad \partial\Omega^i, \tag{2.7}$$

and initial condition $u(\mathbf{x}, 0) = u_0(\mathbf{x})$.

Also, to find the surrounding air temperature $v(x,t)$, satisfying the equation

$$\frac{\partial v}{\partial t}+\gamma\frac{\partial v}{\partial x}=\beta(u-v) \qquad \text{on} \quad \Pi,\ t>0, \tag{2.8}$$

with boundary condition

$$v(0,\ t)=f(t), \tag{2.9}$$

and initial condition

$$v(x,\ 0)=g(x), \tag{2.10}$$

$f(t)$, $g(x)$ are given functions of t and x respectively, γ is the air velocity, h is the convective heat transfer coefficient between the slab and air, k is the thermal conductivity of the slab, $\alpha=\dfrac{k}{\rho_s c_s}$ is the thermal diffusivity of slab, $\beta=\dfrac{h}{\rho_a c_a g_a}$, ρ_a is the density of air, ρ_s is the density of slab, c_s is the specific heat capacity of the slab, c_a is the specific heat capacity of the air and $\partial\Omega$ is the surface of Ω (domain) and is made of two parts; one which experiences convection $\partial\Omega^c$, the remaining surface $\partial\Omega^i$, is an insulated boundary and Π represents the air void domain. Based on the numerical results of the mathematical model, the model was considered to be a good representation of the heat transfer in the slab system.

Moreover, for the cooling system at Harare International School in 2006, Marewo proposed a model also consisting of an initial-boundary value problem which uses a packed bed system for storing the coldness of the night-time to be used later for day-time air-conditioning. The results from this study showed that, the measured and the predicted outlet temperatures of the bed were generally in agreement. However, the study recommended that an optimization of the design and operational parameters should be considered to improve the performance of the cooling system, which is the purpose of this thesis.

Recently, in 2010, Phueakphum and Fuenkajorn conducted a study to assess the performance of a solar thermal energy storage system using rock fills without electricity supply. The results indicated that throughout the night the system increases the house temperature up to 4-6°C more than surroundings. The study also showed that, the efficiency of the storage system was about 35% and the gained heat energy in the house was equivalent to the electrical energy of 203J.

Several researches have have been done on the performance and efficiency of rock bed use to thermal storage systems. This includes that of Al-Nimr *et al*., (1996), Dincer *et al*., (1997), Spiga *et al*., (1981), Chen and Liu, (2004) and Sanderson and Cunningham (1995). No study has been reported on applying genetic algorithms to come up with an optimal strategy to the mathematical model applied to rock storage systems.

The application and efficiency of genetic algorithm has been studied by many researchers. In 2007, Chang presented an application of genetic algorithm to the optimal-chilled water supply temperature calculation of air-conditioning systems for saving energy. The results showed that genetic algorithm is an effective method which not only solves problem of Lagrangian method but also produces results with high accuracy within a rapid time frame.

Huang and Lam in 1997 used genetic algorithms to optimize proportional, integral and derivative (PID) controller parameters for Heating, Ventilating and Air Conditioning (HVAC) systems to achieve optimal performance and indicated that genetic algorithm is very useful for automatic tuning of proportional, integral and derivative controllers in HVAC systems. In 1998, Chung and Hwang made a study on the application of a genetic algorithm to process optimal design in non-isothermal metal forming. It was shown that the approach (genetic algorithm) was effective in finding the optimal values of diverse process parameters in various design situations.

Wang and Xu in 2006 developed a simplified model of the building thermal load on heat transfer of building internal mass. The parameters of the building thermal network models for building envelope are determined by frequency analysis; the parameters of thermal network models for lumped internal mass are identified with genetic algorithm.

The work by Xie *et al.*, (2008) used genetic algorithm optimization method to search, combine and optimize structure sizes of the compact heat exchange. The results revealed that, it is effective to use genetic algorithm technique to search and combine optimal parameters for heat exchangers under different requirements. It was concluded that the genetic algorithm can provide a strong ability of auto-search and combined optimization in the optimization design of heat exchangers compared to the traditional method, since there is always the possibility that the results from the latter process are not optimal.

In 1997, Coello *et al.*, used a simple genetic algorithm for the design of reinforced concrete beams. The results revealed that, the method led to very practical designs of the concrete beam.

Gosselin *et al.*, in 2009 made some reviews of the previous researches on utilization of genetic algorithms (GAs) in heat transfer problems and did a quantitative analysis of GAs. Three main families of heat transfer problems using GAs were identified: Thermal systems design problems, Inverse heat transfer problems and, Development of heat transfer correlation. The study also presented the main features of the problems solved using genetic algorithms including the modelling, number of variables and genetic algorithm settings.

There is therefore a need to take advantage of the increased knowledge of genetic algorithm to optimize model parameters applied to rock storage systems for thermal cooling. The major task for this study is to use genetic algorithm to optimize the system parameters.

CHAPTER THREE

MODEL FORMULATION AND ANALYSIS

3.1 Introduction

This section gives a review of Schumann model which is the most important models for thermal energy storage in packed beds (Schmidt and Willmont, 1981). It is the first known model for thermal energy storage in packed beds. The other models are modifications in one way or another. It is for this reason that this benchmark model is presented here.

3.1.1 The Benchmark Model (Schumann)

The benchmark model for the thermal energy storage in packed beds was done by Schumann in 1928 (Schmidt and Willmont, 1981). The following assumptions were made to derive the energy balance equations for both the storage material and the energy transporting fluid

- Dispersion effects and intra-particle conduction are negligible.
- Thermal conductivity in the transverse direction is infinite and hence there is no temperature variation in this direction.
- There is zero thermal conductivity in the direction of flow.
- Wall containers are perfectly insulated.
- Physical and thermal properties are constant. This is valid for small temperature ranges.
- The convective heat transfer coefficient h_c is uniform.

- Fluid flow is one-dimensional and velocity of the fluid is constant.
- The bed is initially at constant temperature.
- Radiation effects are negligible. This is reasonable for packed beds operating under moderate temperature conditions.
- Rate of accumulation of energy by the fluid in the bed is negligible. This is true for most practical purposes.
- There is no internal heat generation.
- There is no mass transfer. What flows into the bed flows out of it. Generally, mass transfer tends to increase the thermal storage capacity of the solid material. However, there is experimental evidence that the absorbing nature of solid materials like gravel does not significantly improve the performance of the packed bed system hence mass transfer is neglected (Close, 1976)

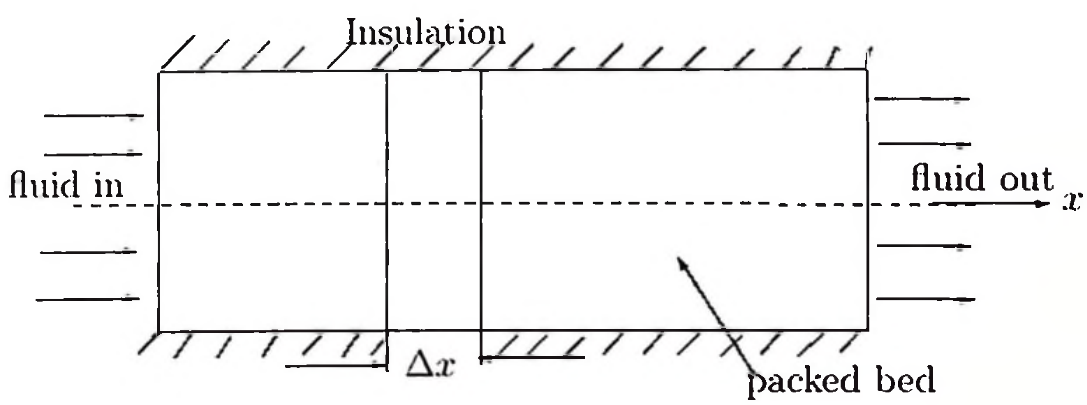

Figure 3.1: Volume control

By doing an energy balance on a control volume across the bed (see Figure 3.1), the following equations can be derived for the fluid and the solid material respectively (Schmidt and Willmont, 1981) for $0 \le x \le L$ and $t > 0$.

at $\xi = 0,\ \theta_f = 1$

and the initial condition is

at $\tau = 0,\ \theta_m = 0.$

It follows from these two conditions and the energy equation for the bed material that,

at $\xi = 0,\ \theta_m = 1 - e^{\tau}$

3.2 Two-Phase Models

3.2.1 Intra-particle conduction and dispersion model

In this model both the effect of intra-particle conduction and dispersion on the performance of the packed bed are taken into account. Provided the thermal capacity of the fluid is negligible compared to that of the solid, the conservation equations for the packed bed of spherical particles and the energy transporting fluid are as follows (Schmidt and Willmont, 1981)

Fluid:

$$0 = -\dot{m}_f c_f \frac{\partial T_f}{\partial x} + k_f S_{fr} \varepsilon \frac{\partial^2 T_f}{\partial x^2} + \frac{h_c A}{L}\left(T_{ms} - T_f\right)$$

Solid:

$$\rho_m c_m \frac{\partial T_m}{\partial t} = k_m \frac{1}{r^2} \frac{\partial}{\partial r}\left(r^2 \frac{\partial T_m}{\partial r}\right) \qquad (3.3)$$

With convective heat transfer boundary condition on the surface of the sphere and an additional boundary condition at the centre (zero first order derivative of the solid material temperature):

$$-k_m \frac{\partial T_m}{\partial r} = h_c\left(T_{ms} - T_f\right) \text{ when } r = R.$$

$$\frac{\partial T_m}{\partial r} = 0, \text{ when } r = 0.$$

where

$$T_{ms}(x,t) = T_m(r = R, x, t) \text{ and } `T_f = T_f(x,t).$$

3.3 The Mathematical Model

3.3.1 Assumptions

The underlying assumptions for the mathematical model are basically the same as for the Schumann model with the following differences.

- There is a step-wise change in the fluid flow rate. Fans blowing air through the bed either on or off at given times of the day. It is during each of these periods that the fluid flow rate is constant: $0\,\mathrm{m}^3/\mathrm{s}$ for no flow and $0.6\ \mathrm{m}^3/\mathrm{s}$ otherwise.

- Each rock is a sphere of same radius R.

- Thermal conduction between neighbouring rocks is neglected. This is reasonable since the area of contact is much smaller than the surface area of a typical rock.

- The model includes the effect of fluid dispersion (axial conduction), intra-particle conduction and heat loss to the ground (environment). Since the ground could provide a significant amount of thermal mass and hence contribute a significant amount of thermal storage to a neighbouring packed bed unit, it is reasonable to take thermal interaction with the ground (ground coupling) into account.

This study consists of two-phase one dimensional mathematical model which uses the fundamental equations similar to those of Schumann model (equations (3.3)), which describes the rock bed which includes heat dispersion in a fluid and heat loss to the environment. A number of researches done on the efficiency of rock bed use to thermal storage system have no information on how important thermal storage unit parameters such as, dimensions of the rock stone, timing, radius of the solid particles, convective heat transfer coefficient, mass flow rate etc. which have an influence on the performance of the cooling system should be chosen. Therefore, this study intends to optimize the thermal cooling parameters applied to rock storage to have a suitable mathematical model for the cooling system.

The problem considered is a mathematical representation of heat transfer in the packed bed unit. It predicts the response of the unit to the time dependent fluid inlet temperature. The rock bed thermal storage unit under investigation is shown diagrammatically in Figure 1.1 in chapter one. The rocks are contained in a wire cage set against the sides of a brick underground as shown in figure 1.2 in chapter one. The bed is used as a thermal storage to regulate temperature in the room space environment for a typical building. The energy transporting fluid is air, and energy transporting materials are rocks.

Figure 1.3 in chapter one shows the path taken by the air as it is drawn from outside. It is blown by fans, one for each packed unit via ducts which are surrounded by concrete walls. It enters a packed bed unit on one end and leaves at the other end before it enters a room as part of a displacement ventilation system. The method of solving the mathematical model uses a finite difference approximation for discretizing space in solid problem domain. A finite element approximation is used in the fluid problem domain and time stepping is done by semi-analytic method.

In the model, the air flow is assumed to be evenly spread in cross-section. This assumption implies that the air (fluid) temperature varies with x and t, i.e. it is given by a variable:

$$T_f(x, t), \qquad 0 \leq x \leq L, \; t \geq 0$$

where the subscript f stands for fluid (air). The rocks at a cross-section are assumed to have the same temperature distribution. In practice the rocks are slightly of varying shape and size, so that in the model an average rock is considered. For the sake of ease of analysing the temperature distribution within the rock, the shape is assumed to be spherical. The temperature in the rocks is given by the variable:

$$T_m(r, x, t), \qquad 0 \leq r \leq R, \quad 0 \leq x \leq L, \quad t \geq 0$$

where R is the radius of the average rock and the subscript m stands for material (rocks). Thus, for the mathematical model the bed is assumed to be evenly packed with spherical rocks of equal radius (that is, we assume the bed contains the same mass and size of rock with uniform cross-section area), with a fluid (air) spread uniformly in cross-section, flowing through the bed starting from the initial time $(t = 0)$.

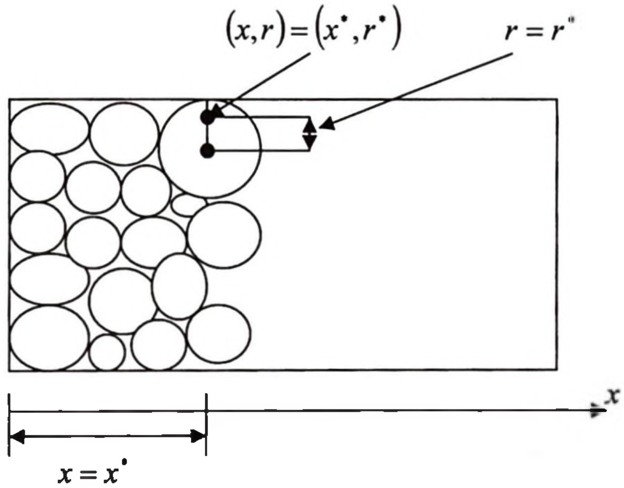

Figure 3.2: Temperature $T_m(x^*,r^*,t)$ at point $(x,r)=(x^*,r^*)$ at any time t

The temperature of the rocks satisfies the heat diffusion equation. The energy equation for the fluid contains diffusion and heat transport terms. Coupling of the solid (rock) and fluid phases is through heat convection between the rock surface and the fluid, which is represented by a term in the equation of each phase. The boundary conditions for the fluid are that the initial temperature is known, and at the outlet end the fluid is assumed not to lose heat significantly to the duct, i.e.

$$\frac{\partial T_f}{\partial x}(x = L, t) = 0, \qquad t \geq 0$$

An additional term in the fluid equation allows for heat loss to the environment. This takes the form of convection to the surrounding earth or bricks which are at a known constant temperature.

3.4 Problem Description

The bed material temperature $T_m(x,r,t)$, satisfies the one-dimensional parabolic equation (3.4) for $0 \le x \le L$.

$$\rho_m c_m \frac{\partial T_m}{\partial t} = k_m \frac{1}{r^2}\frac{\partial}{\partial r}\left(r^2 \frac{\partial T_m}{\partial r}\right), \quad 0 < r < R, \quad 0 \le x \le L, \quad t > 0, \quad (3.4)$$

with boundary conditions:

$$-k_m \frac{\partial T_m}{\partial r}(r = R, x, t) = h_c\left(T_{ms}(x,t) - T_f(x,t)\right), \quad (3.5)$$

$$\frac{\partial T_m}{\partial r}(r = 0, x, t) = 0, \qquad t > 0, \quad (3.6)$$

and initial condition:

$$T_m(r, x, t = 0) = T_0, \qquad 0 \le r \le R, \quad 0 \le x \le L. \quad (3.7)$$

Also the fluid temperature, $T_f(x,t)$ satisfies

$$\dot{m}_a c_f L \frac{\partial T_f}{\partial x} = k_f S_{fr} \varepsilon L \frac{\partial^2 T_f}{\partial x^2} + h_c A\left(T_{ms} - T_f\right) + UPL\left(T_{env} - T_f\right), \ t > 0, \quad (3.8)$$

subject to the boundary conditions:

$$T_f(x = 0, t) = T_{fi}(t), \quad t \ge 0, \quad (3.9)$$

$$\frac{\partial T_f}{\partial x}(x = L, t) = 0, \quad t > 0, \quad (3.10)$$

and initial condition:

$$T_f(x,t=0)=T_0, \qquad 0 \le x \le L, \tag{3.11}$$

where, A is the area of convective heat transfer, c is the specific heat capacity, ε is the bed void fraction (which is defined as the volume of gas per unit volume of rock-bed), h_c is the convective heat transfer coefficient, k is the thermal conductivity, L is the bed length, P is the bed perimeter, r is the radial distance, ρ is the density, R is the radius of the average solid particles (rocks), S_{fr} is the surface frontal area, T is the temperature, t is time, U is the heat loss coefficient from bed to surrounding, x is the distance in the direction of fluid flow, and $\dot{m}_a$ is the mass flow rate of heat transfer fluid . For subscripts: f stands for fluid, fi is fluid inlet, m is bed material and s stands for surface of a rock.

The problem variable $T_m(r,x,t)$ is defined for any x in the range $0 \le x \le L$, although the spheres occur in random discrete positions in the bed. Thus T_m represents the temperature in an average sphere at position x as it varies with time. Similarly $T_f(x,t)$ is the fluid temperature at position x varying with time t. The term on the left hand side of equation (3.8) represents an energy rate associated with the motion of the fluid through the bed. On the right hand side, the first term represents fluid heat dispersion and, the second and third terms represent convective heat transfer on the fluid-solid interface and, thermal interaction with the environment, respectively. The time derivative is not present because the fluid responds very quickly compared with the rocks, that is, a 1 °C change at the inlet is transferred in the fluid in 1 or 2 seconds whereas the rock response is in minutes.

3.5 Methods of Solution

3.5.1 Finite Difference Approximation of the Solid Equation (3.4)

In order to develop a numerical method which uses either finite differences or finite elements, nodes are introduced for the space dimension along the bed and along the radius of the spheres. Consider the following discretization in space for fixed time t.

$$r = i\Delta r, \qquad i = 0,1,2,\ldots,M-1,$$

$$x = j\Delta x, \qquad j = 0,1,2,\ldots,N-1,$$

where $\Delta r = R/(M-1)$ and $\Delta x = L/(N-1)$ are node spacing and M, N are the number of node points used in discretization of the sphere and bed respectively. Consider approximating the space derivatives with finite differences. Equation (3.4) is equivalent to

$$\frac{\partial T_m}{\partial t} = \alpha\left(\frac{\partial^2 T_m}{\partial r^2} + \frac{2}{r}\frac{\partial T_m}{\partial r}\right), \quad 0 < r < R, \quad t > 0, \tag{3.12}$$

where $\alpha = \dfrac{k_m}{\rho_m c_m}$ and satisfies the boundary condition $\dfrac{\partial T_m}{\partial r}(r = 0, x, t) = 0$.

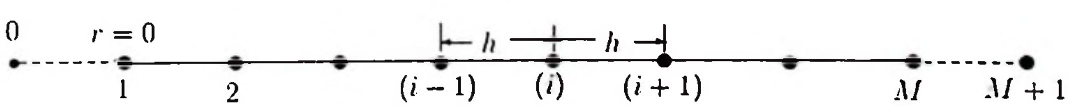

Figure 3.3: Problem domain

A consideration of the symmetry of the solution shows that $\frac{\partial T_m}{\partial r} = 0$ at the origin.

Now keeping t constant, we treat T_m as a function of r only and expand in a Taylor series around $r = 0$, giving

$$T_m(r) = T_m(0) + r\frac{\partial T_m}{\partial r}(0) + \frac{r^2}{2}\frac{\partial^2 T_m}{\partial r^2}(0) + \cdots$$

$$= T_m(0) + \frac{r^2}{2}\frac{\partial^2 T_m}{\partial r^2}(0) + \cdots \tag{3.13}$$

Since $\frac{\partial T_m}{\partial r}(0) = 0$, then

$$\frac{1}{r^2}\frac{\partial}{\partial r}\left(r^2\frac{\partial T_m}{\partial r}\right) = \frac{1}{r^2}\frac{\partial}{\partial r}\left[r^2\left(\frac{\partial T_m}{\partial r}(0) + r\frac{\partial^2 T_m}{\partial r^2}(0) + \cdots\right)\right]$$

$$= \frac{1}{r^2}\frac{\partial}{\partial r}\left(r^3\frac{\partial^2 T_m}{\partial r^2}(0) + \cdots\right)$$

$$= \frac{1}{r^2}\left(3r^2\frac{\partial^2 T_m}{\partial r^2}(0) + r^3\frac{\partial^3 T_m}{\partial r^3}(0) + \cdots\right)$$

$$= 3\frac{\partial^2 T_m}{\partial r^2}(0) + r\frac{\partial^3 T_m}{\partial r^3}(0) + \cdots$$

By neglecting higher order terms, we have

$$\approx 3\frac{\partial^2 T_m}{\partial r^2}(0) \tag{3.14}$$

This approximation transforms equation (3.12) to

$$\frac{\partial T_m}{\partial t} = 3\alpha\frac{\partial^2 T_m}{\partial r^2} \tag{3.15}$$

Therefore, at the first node, we have

$$\frac{dT_m^{(1,j)}}{dt} = 3\alpha\frac{\partial^2 T_m^{(1,j)}}{\partial r^2}, \tag{3.16}$$

Upon replacing $\frac{\partial^2 T_m^{(1,j)}}{\partial r^2}$ with a central difference quotient, equation (3.16) becomes

$$\frac{dT_m^{(1,j)}}{dt} = 3\alpha\left(\frac{T_m^{(0,j)} - 2T_m^{(1,j)} + T_m^{(2,j)}}{(\Delta r)^2}\right)$$

$$= 3\alpha\left(\frac{-2T_m^{(1,j)} + 2T_m^{(2,j)}}{(\Delta r)^2}\right) \tag{3.17}$$

since $T_m^{(0,j)} = T_m^{(2,j)}$ and this follows from boundary condition (3.6). For the middle nodes the discrete form of equation (3.4) is

$$\frac{dT_m^{(i,j)}}{\partial t} = \alpha\left(\frac{T_m^{(i-1,j)} - 2T_m^{(i,j)} + T_m^{(i+1,j)}}{(\Delta r)^2} + \left(\frac{2}{r_i}\right)\frac{T_m^{(i+1,j)} - T_m^{(i-1,j)}}{2\Delta r}\right) \tag{3.18}$$

and at node M :

$$\frac{dT_m^{(M,j)}}{dt} = \alpha\left(\frac{T_m^{(M-1,j)} - 2T_m^{(M,j)} + T_m^{(M+1,j)}}{(\Delta r)^2} + \left(\frac{2}{R}\right)\frac{T_m^{(M+1,j)} - T_m^{(M-1,j)}}{2\Delta r}\right) \tag{3.19}$$

We note that the number of nodes in the solid particles is M and the numbering of the nodes ends at $M-1$. In order to retain the tridiagonal nature of the finite difference equations, it is best to use the method of artificial nodes. In this method a hypothetical node $M+1$ outside the medium is introduced as indicated in the sketch of figure 3.3. Using central difference quotient for the first derivative for the surface boundary condition equation (3.5) we obtain,

$$\frac{T_m^{(M+1,j)} - T_m^{(M-1,j)}}{2\Delta r} = \sigma\left(T_{ms}^{j} - T_f\right), \qquad \sigma = -\frac{h_c}{k_m} . \tag{3.20}$$

Hence,

$$T_m^{(M+1,j)} = 2\sigma\,\Delta r\left(T_{ms}^j - T_f\right) + T_m^{(M-1,j)} \ . \tag{3.21}$$

By substituting this result into equation (3.19) we obtain

$$\frac{dT_m^{(M,j)}}{dt} = \alpha\left(\frac{T_m^{(M-1,j)} - 2T_m^{(M,j)} + 2\sigma\,\Delta r T_m^{(M,j)} - 2\sigma\,\Delta r T_f + T_m^{(M-1,j)}}{(\Delta r)^2}\right.$$

$$\left. + \left(\frac{1}{R}\right)\frac{2\sigma\Delta r T_m^{(M,j)} - 2\sigma\Delta r T_f}{\Delta r}\right)$$

$$= \alpha\left(\frac{2T_m^{(M-1,j)} + (2\sigma\Delta r - 2)T_m^{(M,j)} - 2\sigma\Delta r T_f}{(\Delta r)^2} + \frac{2\sigma T_m^{(M,j)} - 2\sigma T_f}{R}\right)$$

$$= \alpha\left(\frac{2}{(\Delta r)^2}T_m^{(M-1,j)} + \left(\frac{2\sigma\Delta r - 2}{(\Delta r)^2} + \frac{2\sigma}{R}\right)T_m^{(M,j)} - 2\sigma\left(\frac{1}{\Delta r} + \frac{1}{R}\right)T_f\right) \tag{3.22}$$

where $T_{ms}^j = T_m^{(M,j)}$ is the interface rock temperature.

3.5.2 Solid Energy Equation in Matrix form

The system of equations for the thermal energy material (solid) may be written in full as follows:

$$\frac{dT_m^{(1,j)}}{dt} = \frac{3\alpha}{(\Delta r)^2}\left(-2T_m^{(1,j)} + 2T_m^{(2,j)}\right),$$

$$\frac{dT_m^{(2,j)}}{dt} = \alpha\left(\left(\frac{1}{(\Delta r)^2} - \frac{1}{(\Delta r)r_2}\right)T_m^{(1,j)} - \frac{2}{(\Delta r)^2}T_m^{(2,j)} + \left(\frac{1}{(\Delta r)^2} + \frac{1}{(\Delta r)r_2}\right)T_m^{(3,j)}\right),$$

$$\frac{dT_m^{(3,j)}}{dt} = \alpha\left(\left(\frac{1}{(\Delta r)^2} - \frac{1}{(\Delta r)r_3}\right)T_m^{(2,j)} - \frac{2}{(\Delta r)^2}T_m^{(3,j)} + \left(\frac{1}{(\Delta r)^2} + \frac{1}{(\Delta r)r_3}\right)T_m^{(4,j)}\right),$$

$$\vdots$$

$$\frac{dT_m^{(i,j)}}{dt}=\alpha\left(\left(\frac{1}{(\Delta r)^2}-\frac{1}{(\Delta r)r_i}\right)T_m^{(i-1,j)}-\frac{2}{(\Delta r)^2}T_m^{(i,j)}+\left(\frac{1}{(\Delta r)^2}+\frac{1}{(\Delta r)r_i}\right)T_m^{(i+1,j)}\right),$$

$$\frac{dT_m^{(M-1,j)}}{dt}=\alpha\left(\left(\frac{1}{(\Delta r)^2}-\frac{1}{(\Delta r)r_{M-1}}\right)T_m^{(M-2,j)}-\frac{2}{(\Delta r)^2}T_m^{(M-1,j)}\right.$$

$$\left.+\left(\frac{1}{(\Delta r)^2}+\frac{1}{(\Delta r)r_{M-1}}\right)T_m^{(M,j)}\right),$$

$$\frac{dT_m^{(M,j)}}{dt}=\alpha\left(\frac{2}{(\Delta r)^2}T_m^{(M-1,j)}+\left(\frac{2\sigma\Delta r-2}{(\Delta r)^2}+\frac{2\sigma}{R}\right)T_m^{(M,j)}-2\sigma\left(\frac{1}{\Delta r}+\frac{1}{R}\right)T_f\right)$$

which may be written in matrix form as:

$$\dot{\mathbf{T}}_m(t)=B\mathbf{T}_m(t)-T_f(t)\mathbf{b} \tag{3.23}$$

where,

$$\dot{\mathbf{T}}_m(t)=\left(\dot{T}_m^{(1,1)},\dot{T}_m^{(2,1)},\ldots,\dot{T}_m^{(M,1)},\dot{T}_m^{(1,2)},\dot{T}_m^{(2,2)},\ldots,\dot{T}_m^{(M,2)},\dot{T}_m^{(1,N)},\dot{T}_m^{(2,N)},\ldots,\dot{T}_m^{(M,N)}\right)^T,$$

$$\mathbf{T}_m(t)=\left(T_m^{(1,1)},T_m^{(2,1)},\ldots,T_m^{(M,1)},T_m^{(1,2)},T_m^{(2,2)},\ldots,T_m^{(M,2)},T_m^{(1,N)},T_m^{(2,N)},\ldots,T_m^{(M,N)}\right)^T,$$

$$\mathbf{b}=\left(0,0,0,\ldots,-2\alpha\sigma\left(\frac{1}{\Delta r}+\frac{1}{R}\right)\right)^T.$$

$\mathbf{b}$ is the constant vector from the convection boundary condition and B is an $MN\times MN$ matrix shown below:

$$\mathbf{B}=\alpha\begin{pmatrix} -2\delta & 2\delta & & & & & & \\ a_{t2} & b_t & c_{t2} & & & & & \\ & a_{t3} & b_t & c_{t3}\cdots & & & & \\ & \vdots & & \ddots & & & & \\ & & & a_{ti} & b_t & c_{ti}\cdots & & \\ & & & \vdots & & \ddots & & \\ & & & & & a_{t(M-1)} & b_t & c_{t(M-1)} \\ & & & & & & -b_t & \varphi \end{pmatrix}, \tag{3.24}$$

where,

$$\delta=\frac{3}{(\Delta r)^2},\quad b\ =-\frac{2}{(\Delta r)^2},$$

$$a_{ti}=\left(\frac{1}{(\Delta r)^2}-\frac{1}{(\Delta r)r_i}\right),\quad i=2,3,\ldots,M-1,$$

$$c_{ti}=\left(\frac{1}{(\Delta r)^2}+\frac{1}{(\Delta r)r_i}\right),\quad i=2,3,\ldots,M-1,$$

$$\phi=\left(\frac{2\sigma\,\Delta r-2}{(\Delta r)^2}+\frac{2\sigma}{R}\right).$$

ϕ may be written in terms of b_t and c_t as:

$$\phi=\left(\frac{2\sigma\,\Delta r-2}{(\Delta r)^2}+\frac{2\sigma}{R}\right),$$

$$=\left(\frac{2\sigma}{\Delta r}-\frac{2}{(\Delta r)^2}+\frac{2\sigma}{R}\right),$$

$$=\left(-\frac{2h_c}{k_m\Delta r}-\frac{2}{(\Delta r)^2}-\frac{2h_c}{k_mR}\right),\ \text{since } \sigma=-\frac{h_c}{k_m},$$

$$=-\frac{2}{(\Delta r)^2}-\frac{2h_c}{k_m}\left(\frac{1}{\Delta r}+\frac{1}{R}\right),$$

$$= b_t - qc_t,\ \text{where}\ q = \frac{2\Delta r h_c}{k_m}$$

The system of equations (3.23) is consistent and consists of MN equations in MN unknowns for the solid which are

$$T_m^{(1,j)}, T_m^{(2,j)}, \ldots, T_m^{(M-1,j)}, T_m^{(M,j)} \qquad j = 1, 2, 3, \ldots, N.$$

3.5.3 Semi-Analytic Method for Solution in Time

Let us assume that the rock and fluid temperatures are known at a particular time t_1, and that we needed to find the rock temperatures at $t_2 = t_1 + \Delta t$. The fluid temperatures are known at t_2 from the given inlet temperature. We assume that the fluid temperature T_f varies linearly between times t_1 and t_2, and that, the fluid temperature responds very quickly to a change in input temperature because of the flow speed. This contrasts with the change of temperature in the rocks. That is,

$$T_f(t) = T_{f1} + \frac{t - t_1}{\Delta t}\left(T_{f2} - T_{f1}\right) \tag{3.25}$$

Then equation (3.23) becomes

$$\frac{d\mathbf{T}_m(t)}{dt} = B\mathbf{T}_m(t) - \mathbf{b}\left[T_{f1} + \left(T_{f2} - T_{f1}\right)\left(\frac{t - t_1}{\Delta t}\right)\right] \tag{3.26}$$

for $t_1 \le t \le t_2$ with $\mathbf{T}_m(t_1) = \mathbf{T}_{m1}$ known and $\Delta t = t_2 - t_1$. Setting $P = -\mathbf{b}T_{f1}$ and $Q = -\mathbf{b}\left(\frac{T_{f2} - T_{f1}}{\Delta t}\right)$, equation (3.26) becomes

$$\dot{\mathbf{T}}_m(t) = B\mathbf{T}_m(t) + P + Q(t - t_1) \qquad t_1 \le t \le t_2 \tag{3.27}$$

Let $\mathbf{T}_a(\tau)=\mathbf{T}_m(t)-\mathbf{T}_{m1}$, where the subscript a stands for "additional" and $\tau=t-t_1$ see Figure 3.3. Then, equation (3.27) changes to

$$\dot{\mathbf{T}}_a(t)=B\mathbf{T}_a(\tau)+B\mathbf{T}_{m1}+P+Q\tau\ ,\quad \mathbf{T}_a(0)=0 \tag{3.28}$$

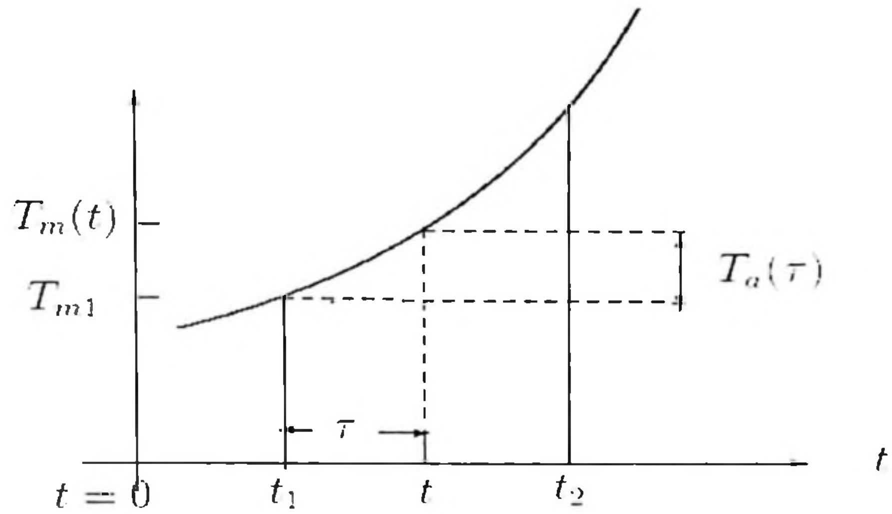

Figure 3.4: The change of variables in solving solid energy analytically

The differential equation (3.28) has both a particular and complementary solutions. The particular solution is called the steady-state solution and the complementary solution is called the transient solution.

Suppose X is a matrix that diagonalizes B , then

$$\mathbf{X}^{-1}\mathbf{B}\mathbf{X}=\mathbf{D}=\begin{pmatrix} \lambda_1 & & & & \\ & \lambda_2 & & & \\ & & \ddots & & \\ & & & \lambda_{M-1} & \\ & & & & \lambda_M \end{pmatrix} \tag{3.29}$$

is a diagonal matrix, where $\lambda_1, \lambda_2, \cdots, \lambda_{M-1}, \lambda_M$ are eigenvalues of B and columns $\mathbf{x}_1, \mathbf{x}_2, \ldots, \mathbf{x}_{M-1}, \mathbf{x}_M$ of X are corresponding eigenvectors.

Pre multiplying each term of equation (3.28) by XX^{-1} we get

$$XX^{-1}\dot{\mathbf{T}}_a(\tau) = BXX^{-1}\mathbf{T}_a(\tau) + XX^{-1}(B\mathbf{T}_{m1} + P) + XX^{-1}Q\tau \qquad (3.30)$$

writing $\mathbf{z}(\tau) = X^{-1}\mathbf{T}_a(\tau)$, it follows that $\dot{\mathbf{z}}(\tau) = X^{-1}\dot{\mathbf{T}}_a(\tau)$, $\mathbf{z}(0) = X^{-1}0 = 0$ and since $BX = XD$ then equation (3.30) becomes

$$X\dot{\mathbf{z}}(\tau) = XD\mathbf{z}(\tau) + XX^{-1}(B\mathbf{T}_{m1} + P) + XX^{-1}Q\tau$$

or

$$\dot{\mathbf{z}}(\tau) = D\mathbf{z}(\tau) + X^{-1}(B\mathbf{T}_{m1} + P) + X^{-1}Q\tau \qquad (3.31)$$

Letting $H = X^{-1}(B\mathbf{T}_{m1} + P)$ and $S = X^{-1}Q$ equation (3.31) can be written as

$$\dot{\mathbf{z}}(\tau) = D\mathbf{z}(\tau) + H + S\tau, \qquad \mathbf{z}(0) = \mathbf{0}, \qquad (3.32)$$

This is a set of uncoupled ordinary differential equations for the temperature at each x along the rock cage. In matrix form we have,

$$\begin{pmatrix} \dot{z}_1 \\ \dot{z}_2 \\ \dot{z}_3 \\ \vdots \\ \dot{z}_{n-1} \\ \dot{z}_n \end{pmatrix} = \begin{pmatrix} \lambda_1 & 0 & 0 & 0 & \ldots & 0 \\ 0 & \lambda_2 & 0 & 0 & \ldots & 0 \\ 0 & 0 & \lambda_3 & 0 & \ldots & 0 \\ \vdots & & & \ddots & & \vdots \\ 0 & 0 & \ldots & & \lambda_{n-1} & 0 \\ 0 & 0 & \ldots & & 0 & \lambda_n \end{pmatrix} \begin{pmatrix} z_1 \\ z_2 \\ z_3 \\ \vdots \\ z_{n-1} \\ z_n \end{pmatrix} + H + S\tau \qquad (3.33)$$

The general equation of uncoupled system is

$$\dot{z}_j = \lambda_j z_j + H + S\tau \qquad (3.34)$$

Equation (3.34) is a first order differential equation and can be solved using the usual methods. The complementary solution of the equation (3.34) is given by

$$z_c = Ae^{\lambda\tau}$$

and the particular solution is

$$z_p = \alpha + \beta\tau$$

This is a solution if

$$\beta - \lambda(\alpha + \beta\tau) = R + S\tau$$

Comparing the coefficients of τ we find that

$$\beta = -\lambda^{-1}S$$

Solving for α, we obtain

$$\alpha = \lambda^{-1}(\beta - R)$$

Therefore, the general solution is

$$z(\tau) = Ae^{\lambda\tau} + \alpha + \beta\tau \tag{3.35}$$

To obtain A:

$$z(0) = 0 = A + \alpha, \quad \Rightarrow A = -\alpha$$

Thus, A, α, β are known and equation (3.35) becomes

$$z_j(\tau) = -\alpha_j e^{\lambda_j\tau} + \alpha_j + \beta_j\tau \tag{3.36}$$

For each row of the system (3.33) the solution is, at $\tau = \Delta t$, we have

$$z_j = \alpha_j(1 - \exp(\lambda_j\Delta t)) + \beta_j\,\Delta t, \quad i = 1, 2, \ldots, M$$

In general, we have

$$\mathbf{z}(\Delta t) = \alpha(1 - \exp(\Delta t D)) + \beta\Delta t, \tag{3.37}$$

and

$$\mathbf{T}_a(\Delta t) = X\,\mathbf{z}$$

$$\mathbf{T}_{m2} = \mathbf{T}_{m1} + \mathbf{T}_a$$

3.5.4 Finite Element Solution of the Fluid Equation (3.8)

The finite element method is a technique used for solving partial differential equations by first discretizing the space domain into small elements. The discretization is carried out locally over small regions of simple but arbitrary shape; the finite elements. This results in corresponding systems of linear equations relating the input at specified points in the elements (nodes) to the output at these same points. In order to solve the equations over a large region, the systems for the sub-regions called elements are formed. The matrix for an individual element is called an element stiffness matrix. The element stiffness matrices are usually summed element by element resulting in a larger matrix called the global stiffness matrix. The solution of the global system of equations is the approximate solution of the differential equation (Logan, 2007). In this section we introduce the iso-parametric formulation of the element stiffness matrices with the fluid temperature approximated by linear variation on each element. This has been chosen because the temperature along the bed does not vary sharply.

3.5.5 Iso-parametric Formulation

The term **iso-parametric** is derived from the use of shape functions (or interpolation functions) $[N]$ to define the element's geometric shape as are used to define displacements within the element. Thus, when the shape function is

$$u = a_1 + a_2 p$$

for the displacement, we use

$$x = a_1 + a_2 p$$

for the description of the nodal coordinate of a point on the rock bed element and, hence the physical shape of the element. Iso-parametric element equations are formulated using a natural coordinate system p that is defined by the element geometry and not by the element orientation in the global-coordinate system. There is a relationship (called a transformation mapping) between the natural coordinate systems and the global system x for each element of a specific structure and this relationship must be used in the element equation formulations (Logan, 2007).

3.5.6 Finite Element Formulation steps

The following are the steps involved in finite element formulation of the fluid equation (3.8).

Step 1: Selection of Element type

The basic element with two nodes 1 and 2 is chosen as shown in figure 3.4.

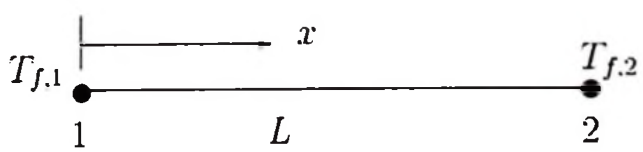

Figure 3.5: (a) Basic one-dimensional temperature element

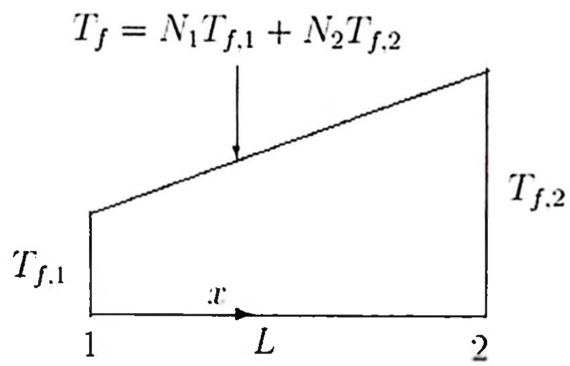

Figure 3.5: (b) Temperature variation along length of element

Step 2: Temperature Function

We choose the temperature function T_f (Figure 3.4 (b)) within each element similar to the displacement function as

$$T_f(x) = N_1T_{f,1} + N_2T_{f,2} \tag{3.38}$$

where $T_{f,1}$ and $T_{f,2}$ are the nodal temperatures to be determined and

$$N_1 = 1 - \frac{x}{L}, \quad N_2 = \frac{x}{L} \tag{3.39}$$

and again with the same shape functions. The $[N]$ matrix is then given by

$$[N] = \left[1 - \frac{x}{L}, \ \frac{x}{L}\right] \tag{3.40}$$

and the nodal temperature matrix is

$$\{\hat{T}\} = \begin{Bmatrix} T_{f,1} \\ T_{f,2} \end{Bmatrix} \tag{3.41}$$

In matrix form, we express equation (3.38) as

$$\{T_f\} = [N]\{\hat{T}\} \tag{3.42}$$

Step 3: Temperature Gradient

The temperature gradient matrix $\{G\}$ is given by

$$\{G\}=\left\{\frac{\partial T_f}{\partial x}\right\}=[B]\{\hat{T}\} \tag{3.43}$$

where $[B]$ is obtained by substituting equation (3.38) for $T_f(x)$ in (3.43) and differentiating with respect to x, that is

$$[B]=\left[\frac{dN_1}{dx},\ \frac{dN_2}{dx}\right]$$

3.5.7 Finite Element Formulation of the Fluid Equation by Galerkin's Method

At an instant in time the fluid temperature satisfies

$$-\gamma\frac{\partial^2 T_f}{\partial x^2}+b\frac{\partial T_f}{\partial x}+\mu T_f(x)=g(x) \tag{3.44}$$

where

$\gamma=k_f S_{f_r}\varepsilon L$,

$b=\dot{m}_f c_f L$,,

$\mu=h_c A+UPL$

$g(x)=h_c A T_{ms}+UPL\,T_{env}$.

From the fluid temperature equation (3.44), the residual is

$$R(x)=-\gamma\frac{\partial^2 T_f}{\partial x^2}+b\frac{\partial T_f}{\partial x}+\mu T_f(x)-g(x)\ . \tag{3.45}$$

Lemma 1: [Fundamental Lemma of variational calculus] (Logan, 2007). The lemma states that "If a residual function $R(x)$ is continuous and

$$\int_a^b R(x)v(x)dx = 0 \tag{3.46}$$

for all continuous test functions $v(x): v(a) = v(b) = 0$, then $R(x) = 0$ for $a < x < b$.

By selecting a suitable test function $v(x)$ and from the fundamental lemma of variational calculus (1), the fluid temperature problem is converted into its variational form and it becomes: Find $T_f(x): T_f(0) = T_f^0$ such that

$$\int_0^L \left(-\gamma \frac{\partial^2 T_f}{\partial x^2} + b \frac{\partial T_f}{\partial x} + \mu T_f(x) - g(x) \right) v(x) dx = 0 \tag{3.47}$$

for all $v(x)$ with $v(0) = 0 = v(L)$.

Applying Galerkin's criterion i.e. we choose the interpolation function, in terms of N_i shape functions for the independent variable in the differential equation such that for each i, we have

$$\int_0^L R(x) N_i \, dx = 0 \qquad \text{for} \qquad i = 1, 2, \ldots, n \tag{3.48}$$

From equation (3.48, equation (3.47) now takes the form

$$\int_0^L \left(-\gamma \frac{\partial^2 T_f}{\partial x^2} + b \frac{\partial T_f}{\partial x} + \mu T_f(x) - g(x) \right) N_i \, dx = 0, \quad (i = 1, 2) \tag{3.49}$$

where the shape functions N_i are defined by equations (3.39). Applying integration by parts to the first term of equation (3.49), we obtain

$$u = N_i, \qquad du = \frac{dN_i}{dx} \cdot dx,$$

$$dv = -\gamma \frac{d^2 T_f}{dx^2} \cdot dx, \quad \Rightarrow \quad v = -\gamma \frac{dT_f}{dx}, \tag{3.50}$$

Using equations (3.50) in the general formula for integration by parts we obtain

$$\int_0^L \left(-\gamma \frac{d^2 T_f}{dx^2} \right) N_i dx = -\gamma \frac{dT_f}{dx} N_i \Bigg|_0^L + \gamma \int_0^L \frac{dT_f}{dx} \frac{dN_i}{dx} dx \tag{3.51}$$

Substituting equation (3.51) into equation (3.49), we obtain

$$\int_0^L \left(\gamma \frac{dT_f}{dx} \frac{dN_i}{dx} \right) dx + \int_0^L \left(\gamma \frac{dT_f}{dx} + \mu T_f - g(x) \right) N_i dx = -\gamma \frac{dT_f}{dx} N_i \Bigg|_0^L \tag{3.52}$$

Using equation (3.39) and (3.38) for T_f, we obtain

$$\frac{dT_f}{dx} = -\frac{T_{f,1}}{L} + \frac{T_{f,2}}{L} \tag{3.53}$$

From equation (3.39), we have

$$\frac{dN_1}{dx} = -\frac{1}{L}, \qquad \frac{dN_2}{dx} = \frac{1}{L} \tag{3.54}$$

By letting $N_i = N_1 = 1 - \frac{x}{L}$ and substituting equations (3.53) and (3.54) into equation (3.52), along with equation (3.48) for T_f we obtain the first finite element equation

$$\int_0^L \gamma \left(-\frac{T_{f,1}}{L} + \frac{T_{f,2}}{L} \right) \left(-\frac{1}{L} \right) dx + \int_0^L b \left(-\frac{T_{f,1}}{L} + \frac{T_{f,2}}{L} \right) \left(1 - \frac{x}{L} \right) dx$$

$$+ \mu \int_0^L \left[\left(1 - \frac{x}{L} \right) T_{f,1} + \left(\frac{x}{L} \right) T_{f,2} - g(x) \right] \left(1 - \frac{x}{L} \right) dx = Q_{x1}^{*} \tag{3.55}$$

where Q_x is the heat conducted at the surface edge x. Equation (3.55) has a boundary condition $Q^{\bullet}_{x1}$ at $x=0$ only because $N_1 = 1$ at $x=0$ and $N_1 = 0$ at $x = L$.

Integrating equation (3.55) with respect to x we obtain

$$-\frac{\gamma}{L}\left(-T_{f,1}+T_{f,2}\right)+b\left(-\frac{T_{f,1}}{2}+\frac{T_{f,2}}{2}\right)+\frac{\mu L}{3}T_{f,1}+\frac{\mu L}{6}T_{f,2}=Q^{\bullet}_{x1}+\frac{\beta T_{env}L}{2}+\frac{\delta T_{ms}L}{2} \quad (3.56)$$

Upon rearranging, equation (3.56) becomes

$$\left(\frac{\gamma}{L}-\frac{b}{2}+\frac{\mu L}{3}\right)T_{f,1}+\left(-\frac{\gamma}{L}+\frac{b}{2}+\frac{\mu L}{6}\right)T_{f,2}=Q^{\bullet}_{x1}+\frac{\beta T_{env}L}{2}+\frac{\delta T_{ms}L}{2} \quad (3.57)$$

To obtain the second finite element equation, we let $N_i = N_2 = \frac{x}{L}$ in equation (3.52) and use equations (3.53), (3.54) and (3.38) in equation (3.52) to obtain

$$\int_0^L \gamma\left(-\frac{T_{f,1}}{L}+\frac{T_{f,2}}{L}\right)\left(\frac{1}{L}\right)dx+\int_0^L b\left(-\frac{T_{f,1}}{L}+\frac{T_{f,2}}{L}\right)\left(\frac{x}{L}\right)dx$$

$$+\mu\int_0^L\left[\left(1-\frac{x}{L}\right)T_{f,1}+\left(\frac{x}{L}\right)T_{f,2}\right]\left(\frac{x}{L}\right)dx=Q^{\bullet}_{x2}+\beta T_{env}\int_0^L\frac{x}{L}dx+\delta T_{ms}\int_0^L\frac{x}{L}dx \quad (3.58)$$

Integrating equation (3.58) with respect to x we obtain

$$\frac{\gamma}{L}\left(-T_{f,1}+T_{f,2}\right)+b\left(-\frac{T_{f,1}}{2}+\frac{T_{f,2}}{2}\right)+\frac{\mu L}{6}T_{f,1}+\frac{\mu L}{3}T_{f,2}=Q^{\bullet}_{x2}+\frac{\beta T_{env}L}{2}+\frac{\delta T_{ms}L}{2} \quad (3.59)$$

Upon rearranging, equation (3.59) becomes

$$\left(-\frac{\gamma}{L}-\frac{b}{2}+\frac{\mu L}{6}\right)T_{f,1}+\left(\frac{\gamma}{L}+\frac{b}{2}+\frac{\mu L}{3}\right)T_{f,2}=Q^{\bullet}_{x2}+\frac{\beta T_{env}L}{2}+\frac{\delta T_{ms}L}{2} \quad (3.60)$$

free ends of the system modelled by the element. When the element stiffness matrices assembled, the heat fluxes $Q^{\bullet}_{x1}$ and $Q^{\bullet}_{x2}$ are usually equal and opposite at the node common to two elements, unless there is an internal concentrated heat flux in the system. Furthermore, for insulated ends $Q^{\bullet}_{x}$'s are also zero (Logan, 2007). In this case, the nodal force matrix becomes

$$\{f\} = \frac{\beta T_{env} L}{2}\begin{pmatrix}1\\1\end{pmatrix} + \frac{\delta T_{ms}}{2}\begin{pmatrix}1\\1\end{pmatrix} \tag{3.68}$$

Thus, the equations for fluid without boundary conditions becomes

$$\mathbf{K}\begin{pmatrix}T_{f1}\\T_{f2}\\T_{f3}\\\vdots\\T_{fN}\end{pmatrix} = \mathbf{f} \tag{3.69}$$

or,

$$\mathbf{K}\,\mathbf{T}_f = \mathbf{f} \tag{3.70}$$

The stiffness matrix $\mathbf{K}$ comes from the terms involving the fluid temperatures, and the element nodal force matrix $\mathbf{f}$ from the convection and environmental terms. The condition that $T_{f1} = T_{fi}$ has to be imposed, that is, we set $\mathbf{K}(1,1) = 1$ and zero for the rest of the rows and $\mathbf{f}(1) = T_{fi}$. If equation (3.70) is multiplied by $\mathbf{K}^{-1}$ and the derivative boundary condition is incorporated the resulting equation has the form:

$$\mathbf{T}_f = K^{-1}\mathbf{f} + T_{fi}\mathbf{g} \tag{3.71}$$

where $\mathbf{g} = [1\ 0\ 0\ \ldots\ 0]^T$.

3.6 Model Predictions

3.6.1 Introduction

In this section, numerical predictions are presented based on the mathematical model for heat transfer in the packed beds that was developed in Section 3.3. A Matlab code is written for the numerical computations. The mathematical model is validated against measured data. Tests are carried out to find how sensitive the model is to small changes in some parameters such as convective heat transfer coefficient h_c, mass flow rate $\dot{m}_a$, length of the packed bed L, and radius of rocks R.

3.6.2 Numerical Solution

Presented here is the transient response of a packed bed to a step change in the inlet fluid temperature in the absence of thermal interaction with the surroundings of the bed for morning unit. The trend is similar for the afternoon packed bed unit. The bed is initially at a constant temperature T_{m0}, taken as $20\ ^{\circ}\mathrm{C}$ and then experiences a sudden change in fluid inlet temperature T_{fi}, of $30\ ^{\circ}\mathrm{C}$. The fluid inlet temperature is maintained at T_{fi}, a constant temperature at all times $t \geq 0$ from the occurrence of the step change. The fluid outlet temperature $T_f(x = L, t)$ is observed as it rises asymptotically with time toward the maximum possible value $T_{fi} = 30\ ^{\circ}\mathrm{C}$. To calculate values of the temperature using the Matlab code, 8 finite difference mesh points were used for each sphere and 3 linear finite elements are used for the fluid problem domain.

The solution in time is analytic and an iterative process is used to solve the uncoupled fluid and solid energy equations uncoupled. For each time step t_1 to t_2, the solution follows three main steps:

1. Estimate $\mathbf{T}_f(t_2)$, the fluid temperatures at time t_2, using $\mathbf{T}_m(t_1)$, the solid temperatures at time t_1, $T_{fi}(t_2)$ the fluid inlet temperatures at time t_2 and the energy equation. That is

$$\mathbf{T}_f(t_2) = K^{-1}\mathbf{T}_m(t_1) + \mathbf{T}_{fi}(t_2)\mathbf{g}$$

2. Solve the solid energy equations analytically in time

$$\dot{\mathbf{T}}_m(t) = B\mathbf{T}_m(t) + \mathbf{T}_f(t)\mathbf{v}$$

   assuming a linear variation (linear variation is sufficient because of fluid speed) in the fluid temperatures in the interval $t_1 < t < t_2$, that is

$$\mathbf{T}_f(t) = \mathbf{T}_f(t_2) + \frac{t - t_1}{t_2 - t_1}\left(\mathbf{T}_f(t_2) - \mathbf{T}_f(t_1)\right)$$

   and compute an estimate of $\mathbf{T}_m(t_2)$.

3. Repeat stages 1 and 2 using $\mathbf{T}_m(t_2)$ instead of $\mathbf{T}_m(t_1)$.

Figure 3.6 shows the variations of the fluid outlet temperature. The figure shows that, the fluid outlet temperature increases asymptotically to the maximum possible inlet temperature value $T_{fi} = 30\ ^\circ\mathrm{C}$. At the outlet, temperature will be highest at the beginning before it starts spreading to the surrounding.

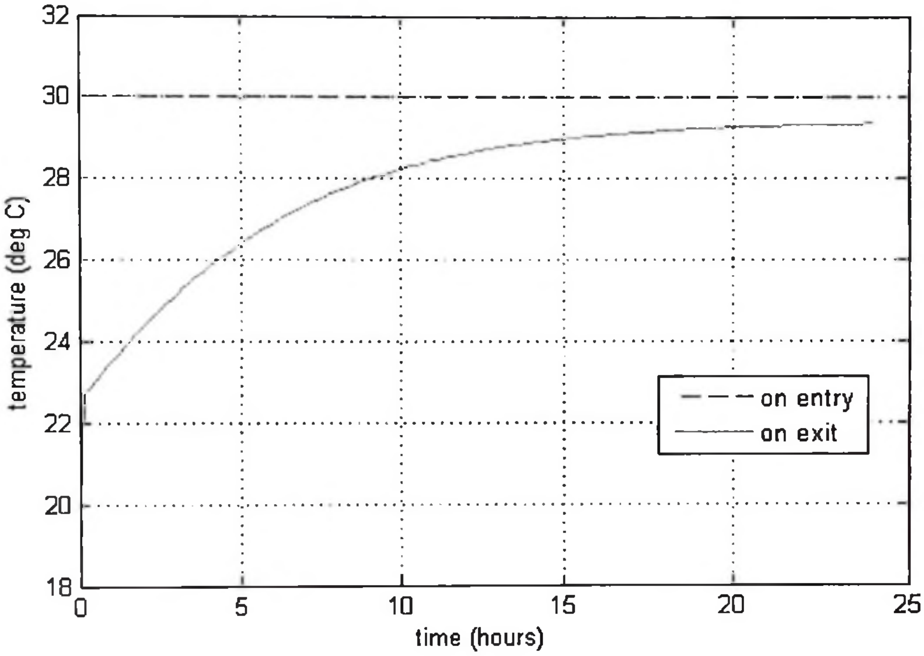

Figure 3.6: Fluid outlet temperature at constant T_{fi}

Table 3.1 shows values used for the basic parameters to generate the results presented.

Table 3.1: Input Parameters

Rocks	$c_m = 800$ J/kg °C $\rho_m = 2700$ kg/m^3 $k_m = 2.1$ W/m °C $R = 0.1$ m
Air	$c_f = 1007$ J/kg °C $\rho_f = 1.106$ kg/m^3 $k_f = 0.25$ W/m °C
Other parameters	$h_c = 6$ W/m^2 °C $\varepsilon = 0.5$ $L = 2$ m $S_{fr} = 5.4\,\text{m}^2$ $A = 3\frac{(1-\varepsilon)}{R} S_{fr} L$ m^2

Figure 3.7 shows the variation of the fluid temperature along the length of the rock bed at fixed time. From the Figure we see that the air temperature decreases asymptotically along the bed length (x-direction) toward the outlet. It is important to note that for a long rock-bed thermal cooling system, the temperature variations in the inlet are smoothed.

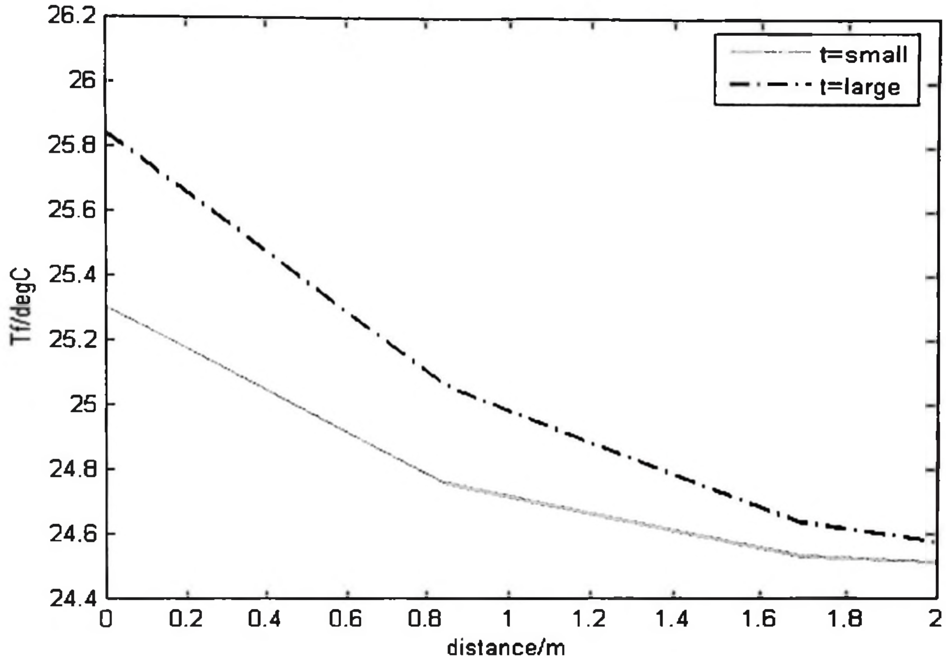

Figure 3.7: Variation of the air temperature along the bed length (x-direction) at fixed time

3.6.3 Temperature Gain and Phase Change

To measure the temperature gain in the fluid outlet temperature and the associated phase change (time lag), the transient response of the bed to the sinusoidal variation in the fluid inlet temperature were considered. Figure 3.8 presents the numerical predictions made for a time scale of 48 hours for the morning packed bed unit. The trend is also similar for the afternoon packed bed unit. The difference between the temperature at the second peak of the fluid inlet and outlet gives the temperature gain. Similarly, the difference between the corresponding times gives the phase change. The results shown in Figure 3.8 indicate that the estimate of the temperature gain between the inlet and outlet temperature is approximately $3.750\,^{\circ}C$ and the corresponding phase change (time lag) is 2.60 hours.

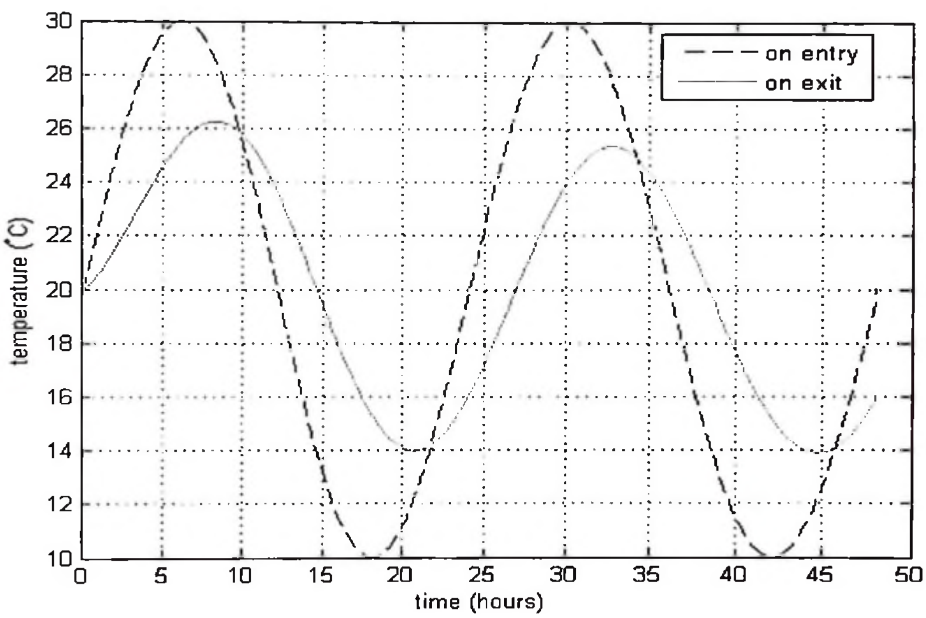

Figure 3.8: Fluid temperature gain and phase change for morning packed bed unit

The Figure also clearly shows that there is time delay in the peaking of the fluid outlet temperature relative to fluid inlet temperature. This means that there must be a pre-defined level of comfort for the occupants in the building. Since the phase lag delays the peak temperature between the inlet and outlet temperature, it may be arranged to improve room comfort in the building. For example, suppose the peak temperature for the ambient air occurs at 14:00 hrs, it might be possible to control the system in order to delay the peak indoor temperature so that the room temperature becomes hottest when the occupants of the office rooms are off from work, say at 16:00 hrs.

3.6.5 Comparing Measured and Predicted Fluid outlet Temperatures

The rock-store compartment is comprised of two halves and a packed bed unit is one of the two halves. One is the *morning unit*, supplying cooling in the morning and the other the *afternoon unit*, which the same for the afternoon, but they both supplies cooling during the night from 22.00 hrs till 6.00 hrs. Air is forced by the morning (*am*) or afternoon (*pm*) fan, which are wind driven fans that are mounted on the roofs of the buildings, (See Figure 3.9). Each fan is switched on and off depending on the time of the day, and with different regimes for weekdays and the weekend.

Figure 3.9: Aerial view of Harare International School

During the week both fans are switched on at 22.00 hrs at night till 6.00 hrs in the morning when they are both switched off for the next 2 hours. At 8.00 hrs, the *am* fan is switched on and it runs till 12 noon when it is switched off, and at the same time the *pm* fan is switched on and runs till 15:30 hrs.

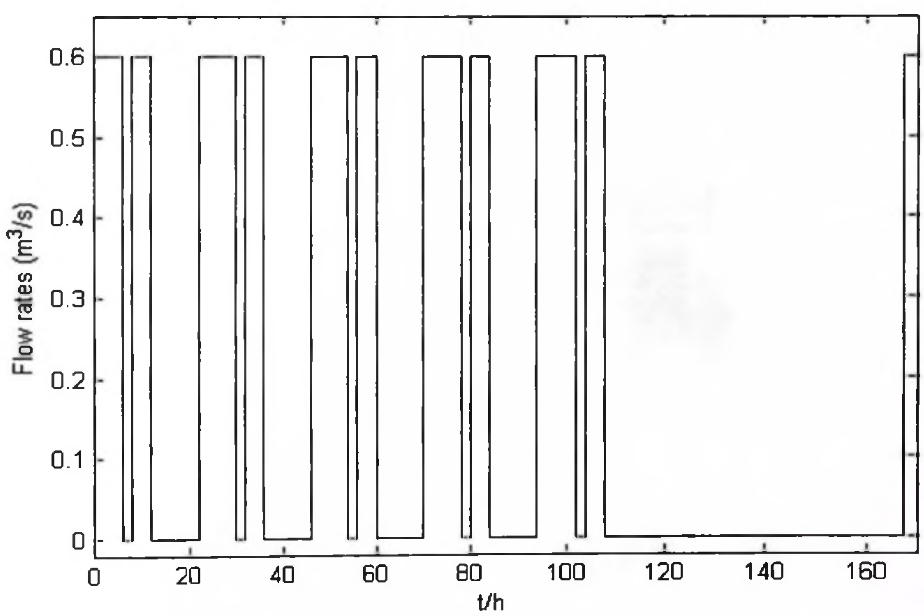

Figure 3.10: The flow rates for the *am* fan

Both fans then remain switched off till 22.00 hrs and the cycle is repeated for the week. However, the weekend is an exception. Both fans are not switched on at 22.00 hrs on Friday. They stay off throughout Saturday, Sunday morning and afternoon and, both of them are only switched on Sunday at 22.00 hrs for the next weekly cycle.

The mathematical model results are compared with measured data for both the morning and afternoon units. The measured fluid inlet temperature is used as the force for the model, and the outlet fluid temperature is both measured and the model results. The readings were taken off a data logger connected to sensors which measure the air temperature at various positions in the air flow path. Two different sensors are used to measure the fluid inlet temperature for each of the morning and the afternoon units. Consequently, a different fluid inlet temperature is used depending on which unit (morning or afternoon) is being considered.

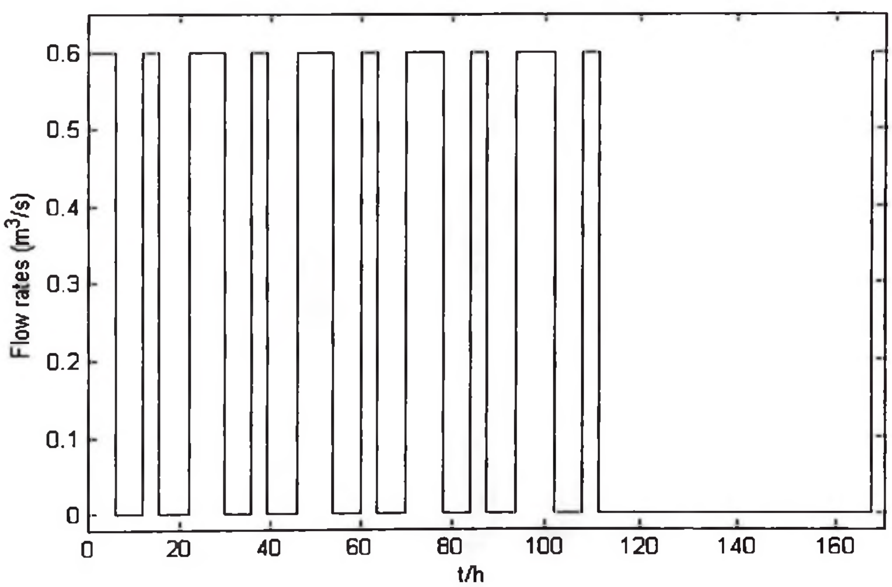

Figure 3.11: Mass flow rates for the *pm* fan

Figure 3.10 and 3.11 show the fluid flow rates used for the *am* and *pm* fans. The time scale used is one week beginning on Monday. The figures are clearly indicating when the fans are off for the weekend.

3.6.6 Performance of the Morning Unit

In this section, a comparison is shown in Figure 3.12 between the predicted and the measured outlet fluid temperature for the morning packed bed unit. A constant convective heat transfer coefficient $h_c = 6$ W/m^2 °C is assumed as was suggested by engineer at the Harare International School. The value for h_c and other parameters used are given in Table 3.1. Shown in Figure 3.12 is the transient response of the morning packed bed unit to ambient air temperature. A time scale of two weeks is chosen to make sure that the numerical system has settled down since it was assumed that the packed bed unit is initially at a constant temperature throughout.

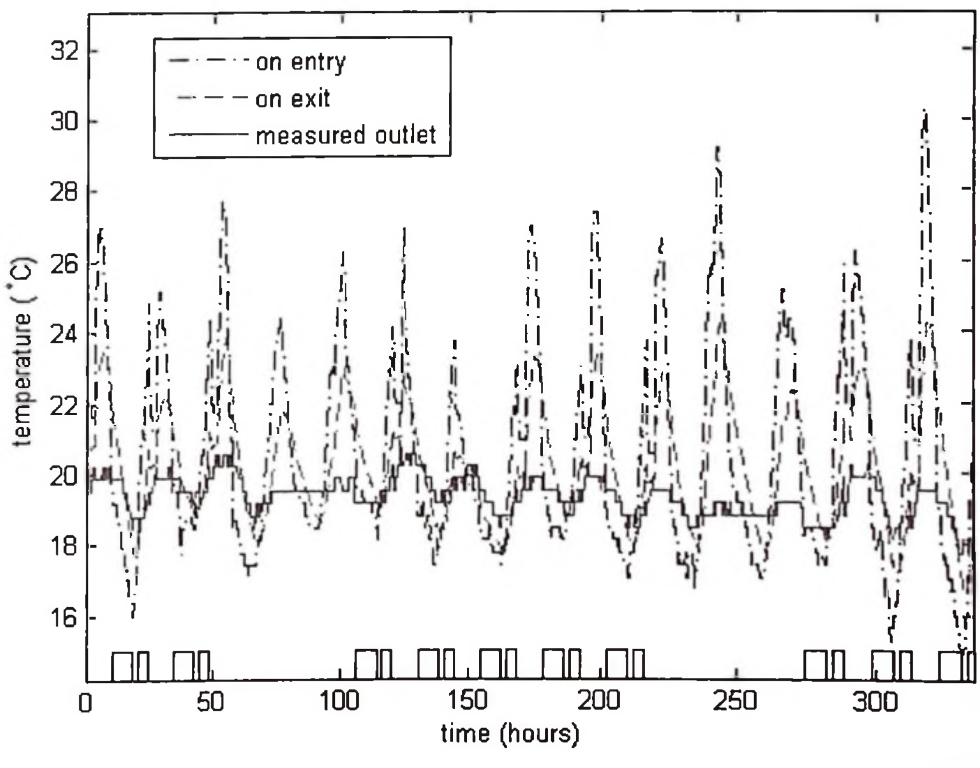

Figure 3.12: Performance of morning unit, over a 2-week period

The predicted and measured fluid outlet temperatures are shown in the figure. At the bottom of the plot the variation of the fluid volume flow rate $\dot{m}_a$ is shown to indicate how the fluid outlet temperature is affected by changes in the fluid flow rate.

Generally, the agreement between predicted and measured fluid outlet temperatures is satisfactory especially for the night cooling periods. However, the morning cooling is underestimated. This may be due to an assumed value for either h_c or $\dot{m}_a$. Tests are carried out later to see how the agreement is sensitive to slight changes in the values of h_c and $\dot{m}_a$. During the weekend there is prolonged absence of forced fluid flow. The agreement between predicted and measured results is better for the second week since the numerical system has by then settled down.

3.6.7 Performance of the Afternoon Unit

Figure 3.13 shows a comparison between the predicted and measured fluid outlet temperature for the afternoon unit responding to a measured fluid inlet temperature and a given fluid flow variation over a period of two weeks. The material and fluid parameters used are the same as in the previous section and they are shown in Table 3.1.

The fluid volume flow rate varies as shown in the measured fluid outlet temperature, but the model predictions are uniformly higher, even for the weekend. The possible explanations for this difference are: the two different sensors measure the fluid inlet temperature for each of the morning and afternoon packed bed unit. They may not have been uniformly calibrated nor equally shielded from thermal radiation. Also they are located at different positions and this could affect the readings.

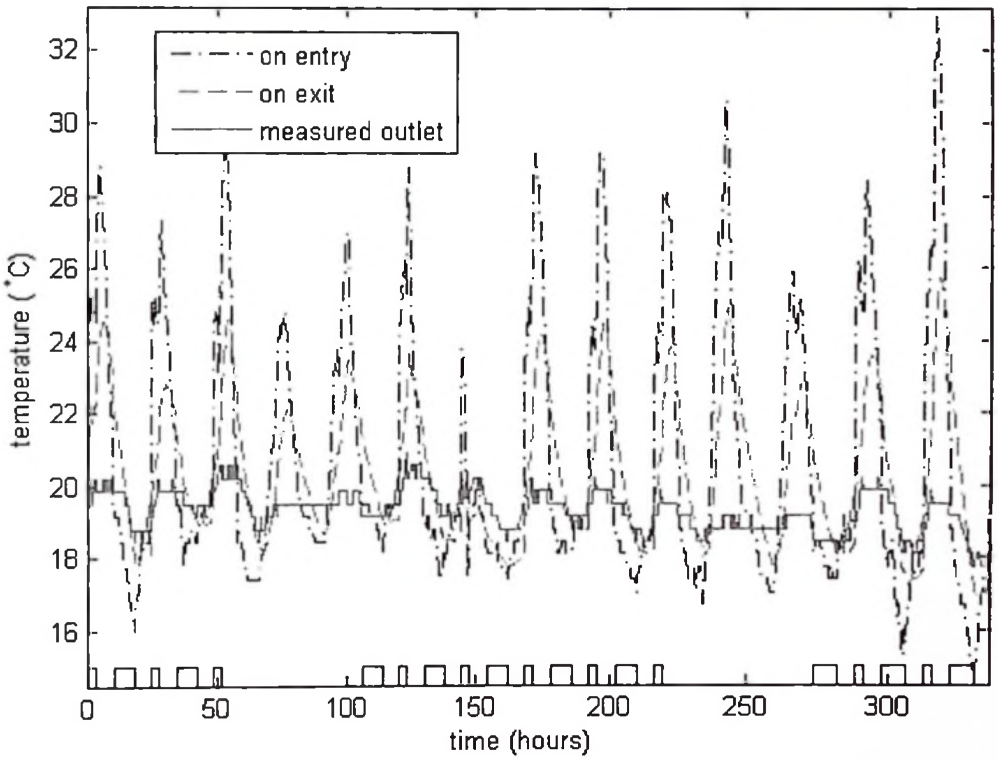

Figure 3.13: Performance of afternoon unit, over a 2-week period

The possible reasons for differences between measured and computed results which are valid for both the morning and the afternoon units include the following:

- The thermal mass between the fans and bed inlet along the air flow path is not included in the model. The walls surrounding these channels are made up of concrete. This will add to the thermal capacity of the bed and delay its reaction to changes in the ambient air temperature.

- The uncertainties in the values of the physical properties for both the bed material and the air flowing through it, and the amount of storage material in the bed.

3.7 Sensitivity Analysis

Sensitivity analysis techniques have been used to estimate the error in the simulation results as a consequence of input uncertainties. Basically such techniques consist of varying the inputs and monitoring the consequent variation of the outputs, and thereby identify those inputs that cause significant variation in the outputs or what parameters are more significant in a specific simulation tool (Westphal and Lamberts, 2005). In this section a sensitivity study is described to show the potential of the model as a design tool for packed beds. Here the study investigates the effect of the:

- Convective heat transfer coefficient, h_c,
- Fluid mass flow rate, $\dot{m}_a$,
- Length of the bed, L, and
- Radius of the sphere, R,

on the amount of heat stored in the bed after a fixed time of operation.

3.7.1 Variation of the Convective Heat Transfer Coefficients

Figure 3.14 shows the transient response of the packed unit for different peak values of the convective heat transfer coefficient. Calculation of the fluid temperature leaving the rock bed for various values of convective heat transfer coefficient (h_c)

shows that this parameter has significant influence on the thermal performance of the system as shown in Figure 3.14. A period of 18 hrs is chosen to allow closer look at the behaviour rather than show the whole fortnight. This covers two periods of fan operation from 12.00 noon to 15:30 hrs, and 22.00 hrs to 6.00 hrs of the Tuesday in the second week for the afternoon unit.

Figure 3.14 shows that the effect of increasing the convective heat transfer coefficient h_c is to dampen the response of the fluid outlet temperature. This is because the interaction between the rocks and the air is enhanced.

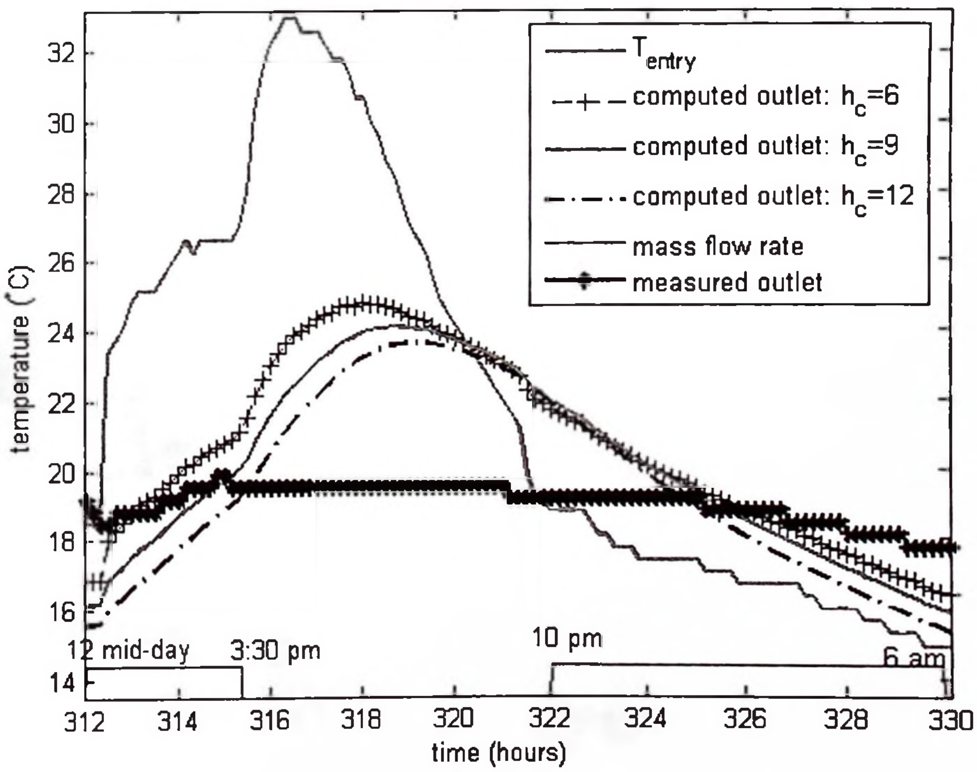

Figure 3.14: Effect of varying convective heat transfer coefficient h_c

The bigger the convective heat transfer coefficient the greater the gain in the fluid temperature and this brings the predicted temperature closer to the measured value. For the period 12.00 noon to 15:30 hrs, increasing heat transfer on the rock-air interface results in lowering the outlet temperature. During the period 22.00 hrs to 6.00 hrs, the rocks are being cooled so that with the greater interaction the temperature of the air rises. For the period 15:30 hrs to 22.00 hrs both fans are off and the heat transfer on the rock-air interface is facilitated by free convection. Similar behaviour is also exhibited by the morning unit.

In practice, mechanical ventilation is required to achieve reasonable values of convective heat transfer coefficient. However the actual values of convective heat transfer coefficient depend not only on the air flow rate but also on the level of turbulence created in the air flow in the channels, which is a function of surface roughness and obstructions in the air flow path (Isanska-Cwiek, 2005).

The mathematical model assumes a constant convective heat transfer coefficient h_c throughout the entire period. Generally, h_c values, for example 6 W/m^2 °C, are valid for the free convection and higher values for forced convection. In the period of free convection a flow, a rate of 0 m^3/s is assumed. The flow rate of $\dot{m}_a = 0.6\,\mathrm{m^3/s}$ is used for forced convection. Several correlations between h_c have been published for example, by Schmidt and Willmont (1981) and Duffie and Beckman (1980). However, some of these correlations have been indicated to be not entirely satisfactory in predicting the measured performance of their experimental packed bed. They apply for bed materials with different physical properties and size and not for the granite used.

3.7.2 Variation of the Air Flow Rates

This section investigates the effect of the air flow rate $\dot{m}_a$ by simulating low rates of $0.4\,m^3/s$, $0.6\,m^3/s$ and $0.8\,m^3/s$ and observing the agreement between predicted and measured fluid outlet temperature. Figure 3.15 shows the transient response of the morning unit for different peak values of $\dot{m}_a$ denoted by m_a in the figure. The temperatures shown in the figure are for the Tuesday of the second week but the trend is the same over the 2-week period for both the morning and afternoon unit.

For each of the three air flow rates, the convective heat transfer coefficient h_c is assumed to be constant at $6\ W/m^2\ ^\circ C$ and the other parameters are as given in Table 3.1. Since air flow rate has significant impact on the value of the heat transfer coefficient value, the results are comparable to those of previous part. This shows that the air flow rate parameter has a strong dependence on the thermal performance of the system. From Figure 3.15 it can be seen that using the lower flow rate of $0.4\,m^3/s$ is to dampen the fluid outlet temperature. The greater temperature gain achieved with a lower flow rate may be due to the air being given more time to be in contact with the rocks.

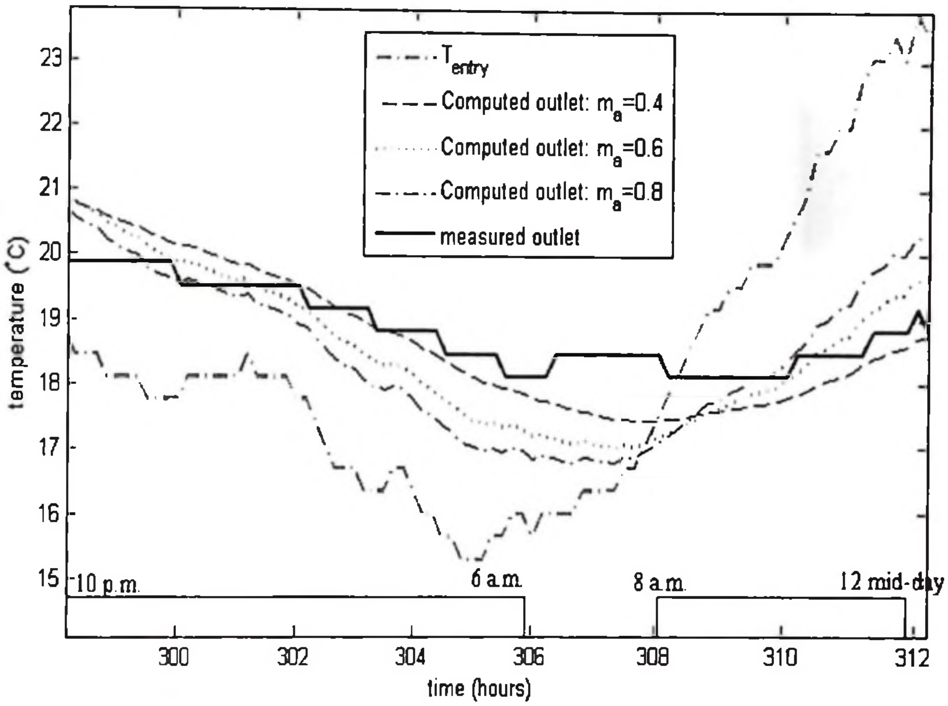

Figure 3.15: Effect of varying air flow rate $\dot{m}_a$

The situation is complicated if it is assumed that convection is linked to air flow rate; then lowering the air flow rate in itself increases the peak damping, but the related result of decreasing the convective heat transfer coefficient reverses the effect. Also, the measured average value of $0.6\,m^3/s$ recommended for use in the modelling is not a correct value. The fluid must be well mixed before taking a measurement otherwise the reading is not a true representative of the fluid flow rate.

3.7.3 Variation of Length of the Packed Bed

Figure 3.16 compares the outlet air temperature from packed beds of the different lengths. The figure indicates that the effect of increasing the bed length L is increases the peak damping of the fluid outlet temperature. That is, the temperature difference is greater as the bed length increases.

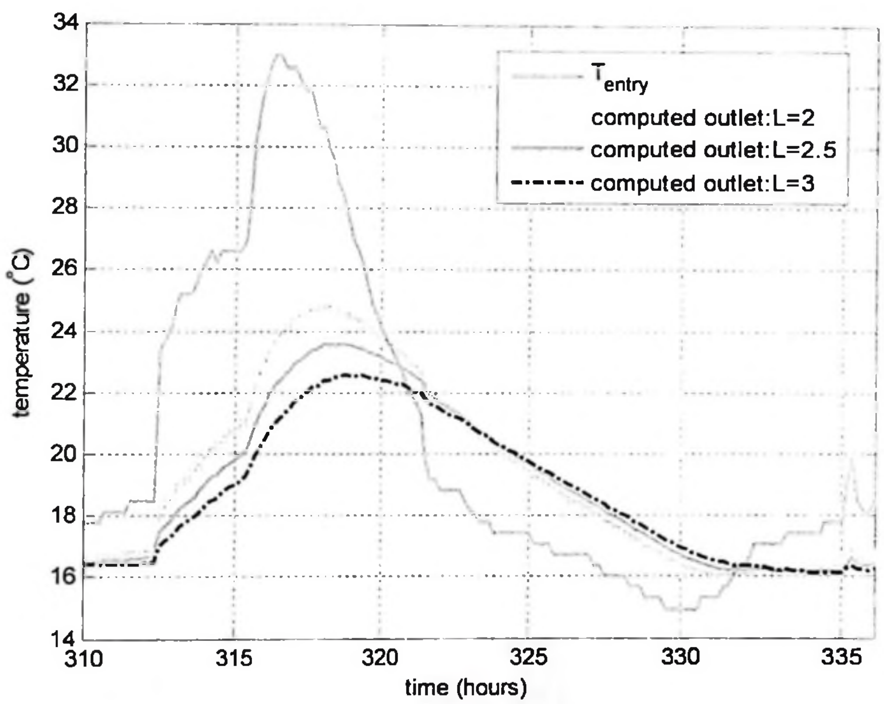

Figure 3.16: Effect of varying length of the packed bed

3.7.4 Variation of Rock sizes

Figure 3.17 compares the outlet air temperature from packed beds of the different rock sizes. The Figure indicates that lowering the radius of the rocks increases the peak damping of the fluid outlet temperature. Hence, for efficient operation, smaller rocks allow for more efficient storage of energy than large rocks.

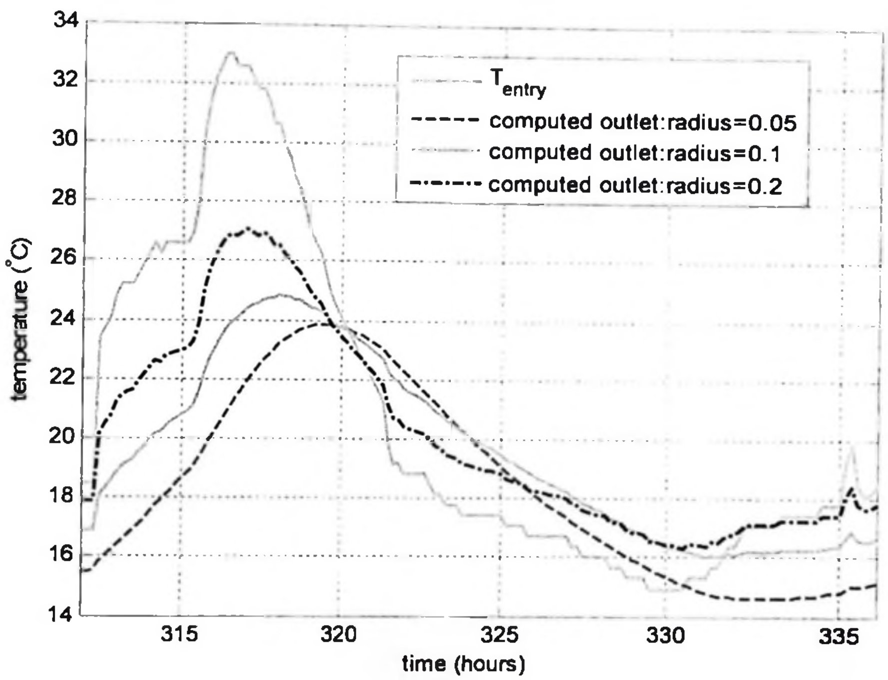

Figure 3.17: Effect of varying rock sizes

3.8 Parametric Study

A parametric study can be used to optimize the design of a packed bed and to come up with optimal operational parameters such as the optimal fluid mass flow rate. In this section one such study is carried out by investigating the effect of

- length of bed L,
- fluid mass flow rate $\dot{m}_a$, and
- type of bed material,

on the amount of heat stored in the bed after a fixed time of operation. A similar analysis is carried out on the fraction of maximum possible heat stored in the bed. A packed bed operating in single-blow mode is considered with three different types of bed materials. These are granite rocks, concrete rubble and brick rubble and their physical properties are shown in Table 3.3. The solid particles for all the three types of material are all modelled as spheres of radius $0.1\,\mathrm{m}$. The period of heat storage is chosen to be $t = 8$ hours, this duration was chosen to match the duration of storage of cooling for the Harare International School. This begins at 22.00 hrs and ends at 6.00 hrs the following morning. The inlet fluid temperature T_{fi} and the initial temperature throughout the bed T_{m0} were assumed to be 20 °C and 0 °C respectively.

Table 3.3: Physical properties for the three materials used in parametric study

Brick rubble	$c_m = 800$ J/kg °C $\rho_m = 1700$ kg/m^3 $k_m = 0.73$ W/m °C
Concrete rubble	$c_m = 878$ J/kg °C $\rho_m = 2100$ kg/m^3 $k_m = 1.1$ W/m °C
Granite rubble	$c_m = 800$ J/kg °C $\rho_m = 2700$ kg/m^3 $k_m = 2.1$ W/m °C

3.9 Amount of Energy Stored in a Packed Bed

The amount of energy stored in the packed bed can be obtained by determining the average temperature of the bed

$$Q = S_{fr}(1-\varepsilon)\rho_m c_m (T_{fi} - T_0) \int_0^L T_m \, dx \tag{3.72}$$

The energy stored in the bed after time t may also be determined by using the temperature of the fluid leaving the unit. The appropriate expression is

$$Q(t) = \dot{m}_f c_f \int_0^t \left(T_{fi} - T_{f0}(\tau)\right) d\tau \tag{3.73}$$

Equation (3.73) can be estimated numerically. Tables 3.4 through 3.6 show the effect of L and $\dot{m}_a$ on the amount of energy stored in the bed after 8 hours for the three different types of storage material. The integral (3.73) was used to determine the results in Tables 3.4 through 3.6. The results indicate that: much less amount of heat energy is stored by increasing $\dot{m}_a$ than by increasing L and the amount of heat energy stored is higher in the order: brick rubble, concrete rubble and granite rocks. This suggests that of the three different types of material, granite is the best storage material.

Table 3.4: Heat stored (KJ): brick rubble

$L(\text{m}) \backslash \dot{m}_a(\text{m}^3/\text{s})$	0.2	0.4	0.6	0.8	1.0	1.2
0.5	10.340	11.010	11.231	11.338	11.399	11.438
1.0	18.095	20.693	21.584	22.029	22.294	22.468
1.5	23.582	29.068	31.044	32.045	32.646	33.045
2.0	27.318	36.202	39.631	41.394	42.460	43.173
2.5	29.825	42.194	47.373	50.089	51.744	52.854
3.0	31.511	47.173	54.306	58.143	60.503	62.093

Table 3.5: Heat stored (KJ): concrete rubble

$L(\text{m})\backslash \dot{m}_a(\text{m}^3/\text{s})$	0.2	0.4	0.6	0.8	1.0	1.2
0.5	12.171	13.183	13.523	13.690	13.788	13.851
1.0	20.596	20.358	25.698	26.376	26.783	27.054
1.5	26.064	33.636	36.542	38.045	38.957	39.567
2.0	29.497	41.204	46.120	48.725	50.325	51.402
2.5	31.638	47.291	54.511	58.455	60.908	62.572
3.0	32.986	52.138	61.810	67.279	70.730	73.090

Table 3.6: Heat stored (KJ): granite rubble

$L(\text{m})\backslash \dot{m}_a(\text{m}^3/\text{s})$	0.2	0.4	0.6	0.8	1.0	1.2
0.5	13.451	14.776	15.232	15.459	15.593	15.680
1.0	22.198	26.921	28.667	29.564	30.108	30.472
1.5	27.538	36.689	40.386	42.339	43.540	44.350
2.0	30.708	44.410	50.521	53.851	55.927	57.340
2.5	32.589	50.431	59.214	64.173	67.315	69.473
3.0	33.720	55.086	66.619	73.386	77.751	80.779

Figure 3.18 shows the typical mass flow rate heat stored profiles at different bed lengths. The difference between mass flow rate heats stored increases with increasing bed length. Figure 3.19 typical bed length heat stored profiles at different mass flow rates. The difference between bed length heats stored increases with increasing mass

flow rates. In this case, the increase of bed length show high increase of the quantity of heat storage stored at different mass flow rate.

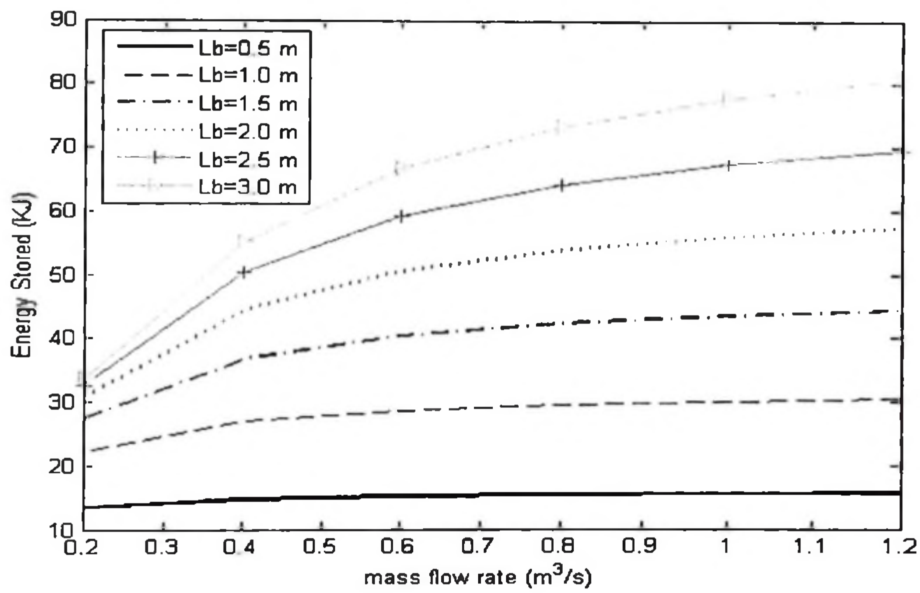

Figure 3.18: The change in heat storage with mass flow rate for constant bed length

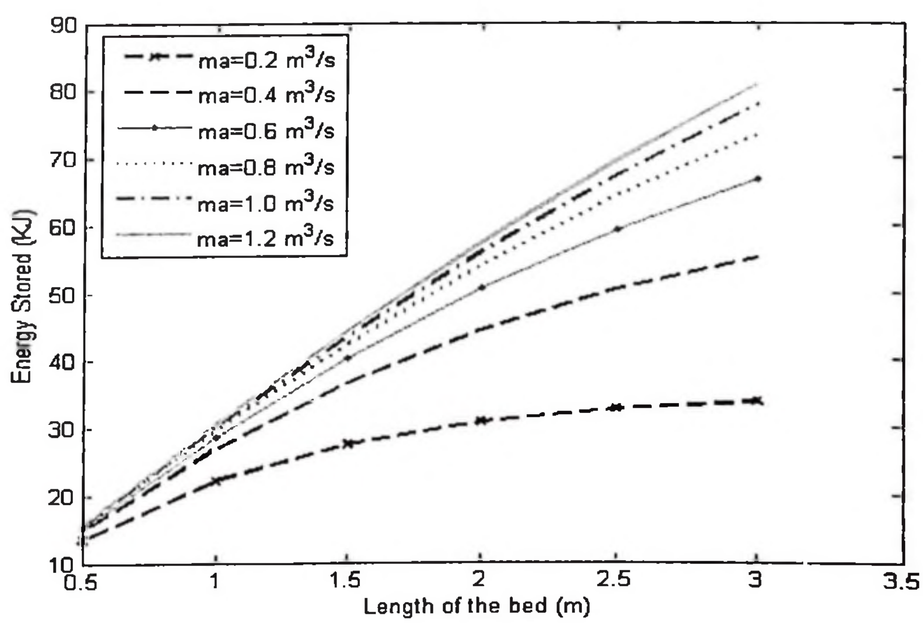

Figure 3.19: The change in total heat storage with bed length for constant mass flow rate

3.10 The Fraction of Maximum Possible Energy Stored in the Bed

The fraction of maximum possible heat stored in the bed after time t is defined in terms of the outlet fluid temperature $T_{f0}(t)$ by equation (3.74).

$$Q^{+}(t)=\frac{Q}{Q_{\max}}=\frac{\dot{m}_f c_f \int_0^t \left(T_{fi}-T_{f0}(\tau)\right)d\tau}{\rho_m S_{fr} L(1-\varepsilon)c_m\left(T_{fi}-T_0\right)} \tag{3.74}$$

where the denominator in equation (3.74) stands for the maximum possible heat stored in the packed bed $Q_{\max}$. The maximum possible heat stored in a packed bed $Q_{\max}$ will be obtained when the temperature of the packed bed is uniform and is equal to the temperature of the fluid entering the unit. Tables 3.7 through 3.9 show the effect of L and $\dot{m}_a$ on the fraction of maximum possible heat stored in the bed after 8 hours for the three different types of storage material. The results indicate that:

- The fraction of maximum possible heat stored increases with flow rate for each bed material. However, increasing mass flow rate is subject to the constraint of a maximum allowable pressure drop for the fans. More fan power is required to blow air through the bed at higher flow rates.
- The fraction of maximum possible heat stored decreases with length of bed. The longer the bed the less efficient it is as not all storage material is utilized. This is because heat can only penetrate to a certain depth of storage material.
- Higher fraction of maximum possible heat is stored for granite, concrete rubble and brick rubble in that order.

Table 3.7: Absolute heat stored ($\times 10^{-4}$): brick rubble

$L(\mathrm{m}) \backslash \dot{m}_a(\mathrm{m}^3/\mathrm{s})$	0.2	0.4	0.6	0.8	1.0	1.2
0.5	2.708	2.865	2.917	2.943	2.958	2.969
1.0	2.396	2.710	2.815	2.866	2.897	2.918
1.5	2.098	2.553	2.711	2.789	2.836	2.867
2.0	1.833	2.397	2.606	2.711	2.774	2.815
2.5	1.607	2.245	2.501	2.632	2.711	2.763
3.0	1.419	2.099	2.397	2.554	2.648	2.711

Table 3.8: Absolute heat stored ($\times 10^{-4}$): concrete rubble

$L(\mathrm{m}) \backslash \dot{m}_a(\mathrm{m}^3/\mathrm{s})$	0.2	0.4	0.6	0.8	1.0	1.2
0.5	2.446	2.652	2.722	2.757	2.778	2.793
1.0	2.069	2.448	2.584	2.653	2.694	2.722
1.5	1.746	2.253	2.449	2.549	2.611	2.653
2.0	1.482	2.070	2.317	2.449	2.529	2.584
2.5	1.271	1.901	2.191	2.350	2.449	2.516
3.0	1.105	1.746	2.070	2.254	2.369	2.449

Table 3.9: Absolute heat stored ($\times 10^{-4}$): granite rubble

$L(\mathrm{m}) \backslash \dot{m}_a(\mathrm{m}^3/\mathrm{s})$	**0.2**	**0.4**	**0.6**	**0.8**	**1.0**	**1.2**
0.5	2.308	2.537	2.616	2.657	2.681	2.697
1.0	1.904	2.309	2.460	2.538	2.585	2.617
1.5	1.574	2.098	2.310	2.422	2.491	2.538
2.0	1.317	1.904	2.167	2.310	2.399	2.460
2.5	1.118	1.730	2.032	2.202	2.310	2.384
3.0	0.964	1.575	1.905	2.098	2.223	2.310

3.11 Ground Coupling

In this section, we consider the effect of thermal interaction between the packed bed unit and the surrounding ground, for a bed that is subjected to a step change in its fluid inlet temperature. The bed is initially at a uniform temperature $T_{m0} = 0$ °C. Suddenly, the fluid inlet temperature experiences a step change to a constant value $T_{fi} = 20$ °C while the environment temperature is maintained at a constant temperature $T_{env} = 15$ °C. The time scale of interest is 30 hours. The basic parameters are as given in Table 3.1 together with the following additional parameters: $U = 2\ \mathrm{W/m^2}$ °C, $P = 26.8\ \mathrm{m}$, $T_{env} = 15$ °C, where U is the heat loss coefficient from bed to surrounding, P is the perimeter of the packed bed and T_{env} is the environment temperature.

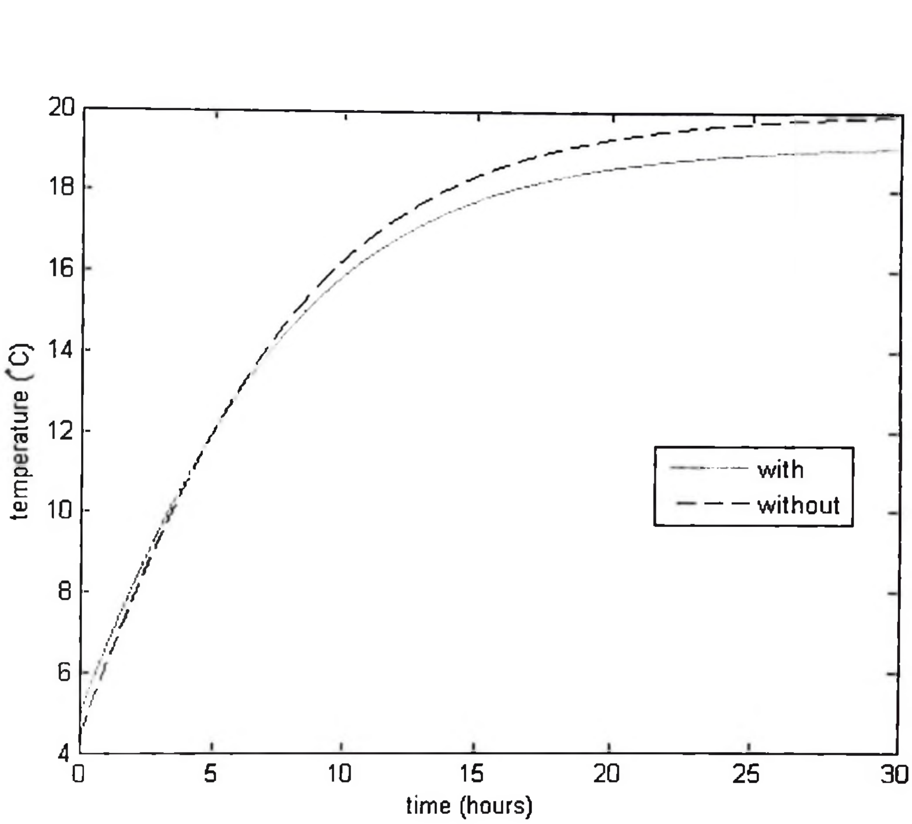

Figure 3.20: Effect of ground coupling on the fluid outlet temperature for the morning and afternoon units

The value of 15 °C used for the ground temperature is an annual estimate. Figure 3.20 shows the effect of ground coupling on the fluid outlet temperature for the afternoon packed bed unit and similar behaviour is obtained using the morning packed bed unit. The fluid outlet temperature is plotted for the case when there is no thermal interaction with the ground surrounding the packed unit. On the same graph, the fluid outlet temperature is plotted for the case when ground coupling is taken into account. The figure indicates that the fluid outlet temperature in the presence of ground coupling is initially higher because of the extra heat gained from the ground. The opposite is true when heat transfer between the ground and the bed reverses its direction of flow.

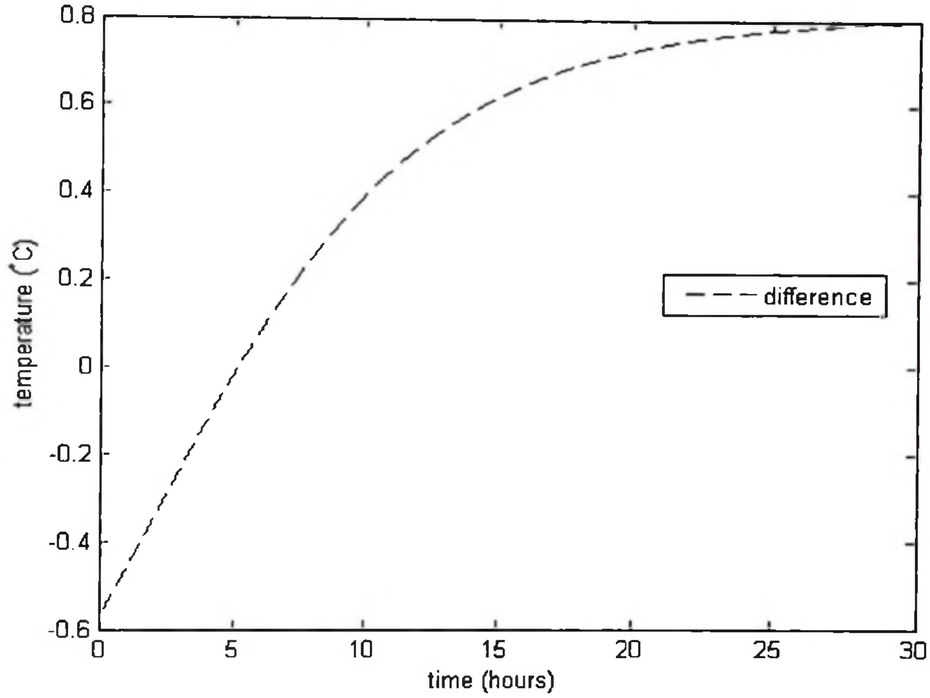

Figure 3.21: Difference in fluid outlet temperature with or without ground coupling

The effect of adding ground coupling is to increase the thermal capacity of the bed and hence delay the time it takes for the fluid outlet temperature to reach its maximum possible value of 20 °C. For the parameters given in Table 3.1, the overall effect is not great; the presence of the earth reduces the temperature by about 0.8 °C after 30 hours. Figure 3.21 shows the difference between fluid outlet temperature without ground coupling and fluid temperature with ground coupling. It displays the difference caused by coupling, that is, outlet temperature without coupling minus outlet temperature with coupling.

CHAPTER FOUR

OPTIMIZATION OF THERMAL COOLING PARAMETERS USING GENETIC ALGORITHM

This chapter aims at optimizing the thermal cooling parameters of the rock storage systems of the mathematical model introduced in chapter 3 by using a natural optimization method, the genetic algorithm, which generates new points in the search space by applying operators to current points and statistically moving them towards more optimal places in the search space. Before doing that, it is important to define what is generally meant by optimization, why it is important to differentiate between discrete, continuous and mixed-variable optimization, and why the genetic algorithm is used for tackling these types of problems.

4.1 Need for the Optimization Algorithms

In the equations of the mathematical model of thermal cooling system described previously, some parameters are unknown and some of them are difficult to derive from physics or engineering principles or to be obtained through experimental tests. Therefore the identification of the model unknown parameters becomes an important part for the study. Parameter optimization is an optimization process that finds optimal parameters that will enable the simulation results to show good agreement to the results acquired by experimental tests. The optimization process for this study is to maximize the objective function which is defined as the difference between the simulated and experimental results at each time. The set of parameters to achieve the maximum value of the objective function is considered to be the fittest set.

It needs to point that the objective here is to optimize the parameters of a model with an already known structure. To concentrate on the objective, the thesis focuses on optimization algorithms for parameter optimization.

4.2 Optimization Problems and Algorithms

4.2.1 Optimization Problems

Optimization is a procedure or procedures used to make a system or design as effective or functional or as possible. From a mathematical point of view, optimization is a process of finding the global minimum or maximum value of an objective function, or cost function, by adjusting some variables or some parameters within a given set.

An optimization problem begins with a set of independent variables (parameters) and a scalar measure of "goodness" termed the objective function which in a way depends on the variables. Besides the objective function there are also conditions or restrictions (termed the constraints of the problem) that define acceptable values of the variables (More *et al.*, 1980). The solution of an optimization problem is the set of allowed values of the variables for which the objective function assumes an "optimal" value. A single objective optimization problem can be defined as follows (Boyd and Vandenberghe, 2004):

Definition 4.1: Given a function $f : \mathbf{D} \to \mathbf{R}$, find $\mathbf{x}^* \in \mathbf{S} : \forall \mathbf{x} \in \mathbf{D}, f(\mathbf{x}^*) \leq f(\mathbf{x})$ (minimization) or $f(\mathbf{x}^*) \geq f(\mathbf{x})$ (maximization) subject to a set Ω of constraints $c_1, \ldots, c_m$, defined by $h_i : \mathbf{S} \to \mathbf{D}$ and $h_i \leq c_i$, for $i = 1, 2, \ldots, m$.

The n-dimensional real-valued function f is called an *objective function*, *energy function*, or *cost function*. Its domain $\mathbf{D}$ is called the *search (or solution) space* and the elements of $\mathbf{S}$ are called *candidate* or *feasible solutions*. A feasible solution $\mathbf{x}^* \in \mathbf{S}$ is a vector of optimization variables $\mathbf{x}^* = \{x_1, x_2, \ldots, x_n\} \in \mathbf{R}^n$ which satisfies all the constraints. If the set Ω of constraints is empty, the problem is called an *unconstrained problem*, otherwise it is said to be constrained.

In global optimization, it is a convention in which optimization problems are most often defined as minimizations and if an objective function f is subject to maximization, we simply minimize its negation $-f$. The optimization algorithm searches for a solution in a search space, $\mathbf{D}$ of candidate solutions. In the case of constrained problems, a solution is found in a feasible space $\mathbf{F} \subseteq \mathbf{D}$, called the *feasible region*.

Definition 4.2: The solution, $\mathbf{x}^* \in \mathbf{N} \subseteq \mathbf{F}$ is a strong local minimum of f if

$$f(\mathbf{x}^*) < f(\mathbf{x}), \ \forall \mathbf{x} \in \mathbf{N} \tag{4.1}$$

where $\mathbf{N} \subseteq \mathbf{F}$ is a set of feasible points in the neighbourhood of $\mathbf{x}^*$.

Definition 4.3: The solution $\mathbf{x}^* \in \mathbf{F}$, is a strict global optimum of the objective function, f, if

$$f(\mathbf{x}^*) < f(\mathbf{x}),\ \forall \mathbf{x} \in \mathbf{F} \tag{4.2}$$

That is, the global optimum is the best possible solution to a problem.

The ultimate goal of an optimization method is to find the globally optimal solution $\mathbf{x}^*$ and the corresponding optimal value of the objective function $f^* = f(\mathbf{x}^*)$. Although there are several strong local maxima or minima, there is at most one strict global maximum or minimum. Optimization problems can be classified into various families based on a number of characteristics such as the type of variables, the number of variables, the number of optimization criteria. In this thesis, we use the classification based on the type of variables, that is, on how the optimization problems differ in the definition of their search space. Optimization problems can be classified into three types based on the type of variables:

- *Discrete optimization problems* – problems in which all the optimization variables x_i, $i = 1, 2, \ldots, n$ are discrete, that is, x_i belong to a countable set D_i, $i = 1, 2, \ldots, n$.
- *Continuous optimization problems* – problems in which all the optimization variables are continuous, that is, $x_i \in \mathbf{R}$ for each $i = 1, 2, \ldots, n$.
- *Mixed-variable optimization problems* – problems that have both discrete-valued and continuous-valued variables, that is, p out of $n = p + q$

variables are discrete, $x_i \in D_i$ for $i = 1, 2, \ldots, p$, and q are continuous $x_i \in \mathbf{R}$ for each $i = p+1, \ldots, p+q$.

Solving these three different classes of optimization problems poses different difficulties and often requires different methods. While some methods work well on discrete optimization problems, they may not be appropriate for continuous optimization problems, and vice versa (Nkansah-Gyenke, 2010). In the thesis we shall focus on continuous optimization since there are many problems of this type, and several algorithms have been proposed to deal with such continuous problems.

Definition 4.4: A model $P = (\mathbf{D}, \Omega, f)$ of a continuous optimization problem consists of:

- a search (or solution) space, $\mathbf{D}$, of a finite set of continuous decision variables x_i, $i = 1, 2, \ldots, n$;
- a set Ω of constraints, and
- an objective function f to be minimized or maximized, where $f : \mathbf{D} \to \mathbf{R}$.

The search space of a continuous optimization problem is not finite as each of the continuous decision variables x_i may assume an infinite number of values in its respective domain $\mathbf{D}$.

4.2.2 Optimization Algorithms

Optimization algorithms are search methods, where the goal is to find a solution to an optimization problem, such that a given quantity is optimized, possibly subject to a set of constraints. Optimization algorithms can be classified as deterministic or stochastic. Algorithms with stochastic components are often referred to as ***heuristic***.

Heuristic methods are approximate methods that produce solutions close to the optimum however the majority of them are specifically designed for a given problem. In recent years a new kind of approximate algorithm, called a *metaheuristic algorithm*, has emerged which basically they do combine basic heuristic methods in higher level frameworks aimed at efficiently and effectively exploring a search space (Nkansah-Gyenke, 2010).

The algorithms for solving continuous optimization problems are divided into two classes: the *exact* and *approximate* algorithms. Exact algorithms for the solution of continuous optimization problems include analytical approach, numerical methods based on gradient descent, and direct search methods. Approximate algorithms for solving continuous optimization problems are metaheuristics. While some metaheuristics were developed with the continuous optimization in mind, most of them have been adopted to continuous optimization based on their counterparts initially developed for combinatorial optimization. Metaheuristics for continuous optimization are often hybridized with local search methods to allow them to focus on global optimization, while the local search methods, such as direct search or gradient-based methods, help them in finding local optimums.

In this thesis, an optimal solution to the mathematical model cannot be found in polynomial time using simple deterministic algorithms. Stochastic heuristics such as the GA offer better alternatives. These methods, which aim at finding near-optimal solutions in polynomial time, have proved to be very successful when applied to problems in various fields such as industrial management, financial services, and graph theory.

Natural optimization algorithms, including the GA rely upon an intelligent search in a large but finite solution space using statistical methods. They represent processes in nature that are remarkably successful at optimizing natural phenomena (Öztürk and Çelik, 2011).

4.3 An Overview of the Genetic Algorithm

The genetic algorithm models natural selection and evolution and relies upon an intelligent search of a large but finite solution space using statistical methods. It does not require taking objective function derivatives and can therefore deal with discrete parameters and discontinuous objective functions. The GA has been formalized into a meta-heuristic for combinatorial optimization problems. The goal of heuristic methods is to quickly produce good approximate solutions, without necessarily providing any guarantee of solution quality. Typically, the core of heuristic methods is an iterative principle that includes stochastic elements in generating new candidate solutions and/or in deciding whether these replace their predecessors – while still incorporating some mechanism that prefers and encourages improvements (Mitchell, 1996; Koza, 1992). Heuristic methods have several advantages over traditional deterministic methods:

- Their randomness allows escaping local optima;
- They are typically suitable for a general purpose and can therefore deal with a vast array of different functional forms and constraints; and
- They are reasonably efficient compared to other widely used methods when traditional optimization fails.

Disadvantages of Heuristic algorithm are:

- Cannot easily incorporate problem specification information.
- Do not guarantee an optimal solution.
- Require large number of response (fitness) function evaluations.
- Need problem specific parameters.

In this thesis, we explore the use of the GA for solving the optimization problem of maximizing the performance of the thermal cooling system described by a mathematical model in Chapter 3.

4.4 The Genetic Algorithm

4.4.1 Introduction to Genetic Algorithm

The Genetic Algorithm is a search method for solving both constrained and unconstrained optimization problems. It is based on the mechanics of natural selection and genetics in Darwin's theory, with the original aim of designing autonomous learning and decision-making systems (Mitchell, 1996; Beasley *et al.*, 1993). It is applicable to a variety of optimization problems that are not well suited for standard optimization algorithms, including problems in which the objective function is discontinuous, non-differentiable, stochastic, or highly nonlinear. Koza (1992), stated that the GA is a highly parallel mathematical algorithm that transforms a set (population) of individual mathematical objects (typically fixed-length character strings patterned after chromosomes strings), each with associated fitness value, into a new population (i.e. the next generation) using operation patterned after the Darwinian principle of reproduction and survival of the fittest and after naturally occurring genetic operations (notably sexual recombination).

Genetic Algorithms manipulate a population of potential solutions to an optimization (or search) problem. Specifically, they operate on encoded representations of the solutions and not directly on the solutions themselves. The GA encodes the decision variables of a search problem into finite-length strings of alphabets of certain cardinality (Mitchell, 1996; Sastry *et al.*, 2005). The strings which are candidate solutions to the search problem are referred to as *chromosomes*, the alphabets are referred to as *genes* and the values of genes are referred to as *alleles*. In contrast to traditional optimization techniques, the GA works with coding of parameters rather than the parameters themselves. Each solution is associated with a fitness measure that reflects how good it is, compared to other solutions in the population. The measure could be an objective function (either a single objective function in single-objective optimization or a multi-objective function in multi-objective optimization) that is a mathematical model or a computer simulation, or it can be a subjective function where people intuitively choose better solutions over worse ones (Grefenstette, 1986; Beasley *et al.*, 1993).

Along with the coding scheme used, the fitness function is the most crucial aspect of any GA. Ideally the fitness function must be smooth and regular, so that chromosomes with reasonable fitness are close, in the parameter space, to chromosomes with slightly better fitness. Although it is not guaranteed for all problems, but one must strive to construct a fitness function which does not have too many local maxima, or a very isolated global maximum. The general rule is that a fitness function should reflect the value of the chromosome in some "real" way (Beasley *et al.*, 1993; Haupt, R.L and Haupt, S.E., 2004).

According to Arunasalam *et al.*, (2005), the fitness function should be a simple expression that can represent the quality of a solution to a problem. Also, a fitness function does not need information beyond the required representation of the solution to the problem because an over representation of the fitness function can hamper the search space of the GA.

Unlike traditional search methods, the GA relies on a population of candidate solutions. The population size, which is usually a user-specified parameter, is an important factor that affects the scalability and performance of genetic algorithms (Mitchell, 1996). Small population sizes may lead to premature convergence and yield substandard solutions, while large population sizes lead to unnecessary expenditure of valuable computational time.

The GA begins with and repeatedly modifies a randomly generated population of individual solutions modelled on gene combinations in biological reproduction and not a single trajectory evolving from a unique initial solution. At each step, the GA selects individuals at random according to their fitness from the current population to be parents and uses them to produce the children for the next generation. The algorithm repeatedly applies selection, crossover, mutation and replacement operators at each step to create the next generation from the current population until a satisfactory solution is found or a maximum number of iterations are reached. The population evolves toward an optimal solution over successive generations. In the following, we assume a function maximization problem. Hence, a good solution is one that has the highest relative fitness.

4.4.2 The Genetic Algorithm Scheme

Having encoded a problem in a chromosomal manner and having devised a means of discriminating good solutions from bad ones, we can use a GA to evolve solutions to the problem by the following steps (Sivanandam and Deepa, 2008):

Step 1: *Initialization.* The algorithm begins by creating a random initial population of individuals.

Step 2: The algorithm then creates a sequence of new populations. At each step, the algorithm uses the individuals in the current generation to create the next population. To create the new population, the algorithm iteratively performs the following steps:

a) *Evaluation.* The objective function values of the candidate solutions in the current population are computed.

b) *Fitness Assignment.* The algorithm uses the objective function values to determine fitness values of the candidate solutions.

c) *Selection.* The algorithm selects members, called parents, based on their fitness. The main idea of selection is to prefer better solutions to worse ones, and many selection procedures have been proposed to accomplish this, including roulette- wheel selection, ranking selection, stochastic universal selection, and tournament selection.

d) *Elitism.* Some of the individuals in the current population that have low fitness are chosen as elite individuals and are passed on to the next population as children.

e) *Crossover (Recombination).* Crossover combines the vector entries or genes of two parents to form potentially better solutions (offspring) for the next generation. The crossover is controlled by the crossover probability p_c which is typically in the range [0.7 – 0.95]. That is, a uniform random number r is generated and if $r \le p_c$, the two randomly selected parents undergo recombination. Common crossover operators are k-point crossover and uniform crossover.

f) *Mutation.* Mutation applies random changes to one or more genes of an individual parent to form children. Mutation adds to the diversity of a population. It is performed with a low probability p_m typically in the range [0.01 – 0.2].

g) *Replacement.* The current population is replaced with the children created by selection, crossover, and mutation to form the next generation.

Step 3: The algorithm stops when one of the stopping criteria is met. Two types of stopping criteria are used. These are: number of generations and threshold value.

4.4.3 Main Features of Genetic Algorithms

A genetic algorithm for a particular problem must have the following five basic components (Michalewicz, 1996):

a) A genetic representation for potential solutions to the problem.
b) A way to create an initial population of potential solutions.
c) An evaluation function to rate the solutions in terms of their fitness.
d) Genetic operators that alter the genetic composition of children during reproduction.
e) Values for all parameters of the Genetic Algorithms must be defined (population size, probabilities of applying genetic operators, etc.).

The above listed main features of the GAs are discussed in more detail below.

Representation

Fundamental to the GA structure is the encoding mechanism to represent the decision variables of the optimization problem into finite-length strings of alphabets of certain cardinality. The strings which are candidate solutions to the search problem are referred to as chromosomes, the alphabets are referred to as genes and the values of genes are referred to as alleles. The encoding scheme depends on the nature of the problem variables. The classical representation scheme for GAs is binary vectors of fixed length for binary-valued, nominal-valued, and continuous-valued variables. GAs have also been developed that use integer or real-valued representations and order-based representations where the order of variables in a chromosome plays an important role.

Initial Population

As a preparation to start the optimization process, a GA requires a group of initial population (solutions) as the first generation. There are several strategies to generate the initial population. The standard way of generating an initial population is to assign a random value from the allowed domain to each of the genes of each chromosome. The goal of random selection is to ensure that the initial population is a uniform representation of the entire search space. The size of the initial population has consequences for scalability and performance in terms of computational complexity and exploration abilities. A large initial population of individuals increases the diversity, thereby improving the exploration abilities of the population. However, there is a high computational complexity per generation for a large population. On the other hand, small population sizes may lead to premature convergence and yield substandard solutions. A population of between twenty and one hundred chromosomes is normally sufficient for most applications (Fleming *et al.*, 1994).

Selection Methods

Selection models nature's survival-of-the-fittest mechanism by allocating more copies of those solutions with higher fitness values. The main idea of selection is to prefer better solutions to worse ones, and many selection procedures have been proposed to accomplish this, including roulette-wheel selection, ranking selection, stochastic universal selection, and tournament selection. Selection operators are characterized by their *selection pressure*, which is defined as the speed at which the best solution will occupy the entire population by repeated application of the selection operator alone. An operator with a high selection pressure decreases diversity in the population more rapidly than operators with a low selection pressure. The most frequently used selection methods (Goldberg and Deb, 1991) are fitness proportionate selection methods, such as, roulette-wheel selection and ordinal selection methods, such as, tournament selection and truncation selection, rank-based selection, stochastic remainder technique, and elitism.

Crossover Operators

Crossover (or recombination) is a genetic operator that combines the traits of two or more parental solutions to create new, hopefully better offspring. The offspring under crossover will not be identical to any particular parent and will instead combine parental traits in a novel manner (Grefenstette, 1986; Goldberg, 2002). The two main attributes of crossover that can be varied are the type of crossover that are implemented and the probability of their occurrence. In most crossover operators, two individuals are randomly selected and are recombined with a crossover probability p_c which is typically in the range $[0.7-0.95]$. That is, a uniform random number r is generated and if $r \leq p_c$, then the two randomly selected parents undergo recombination. If crossover is not applied, offspring are produced by duplicating the parents. This gives each individual a chance of passing on its genes without the disruption of crossover. Common crossover operators are *k-point crossover* and *uniform crossover* (Syswerda, 1989).

The two main ways of performing crossover are called single-point and two-point crossover. When a single-point crossover scheme is used, a position of the chromosome is randomly selected as crossover point as indicated in Figure 4.1. When a two-point crossover scheme is used, two positions of the chromosome are randomly selected as indicated in Figure 4.2. Let $x_1 = 1010:001110$, $x_2 = 0011:010010$ and suppose that the crossover point has been chosen as indicated, we have the following (Grefenstette, 1986)

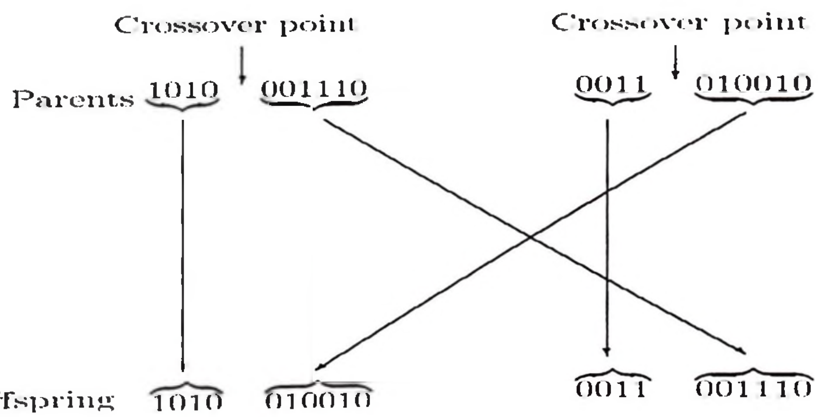

Figure 4.1: Use of a single-point crossover between two chromosomes

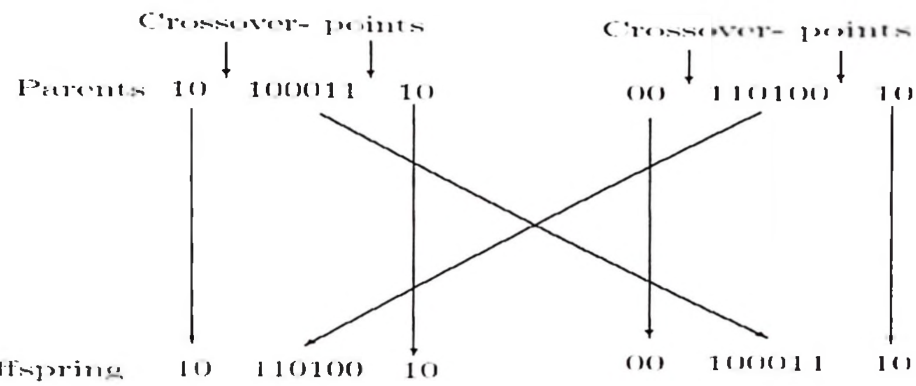

Figure 4.2: Use of two-point crossover between two chromosomes

Mutation Operators

Mutation is the process of randomly changing the values of genes in a chromosome. Mutation stochastically flips bits in each generation. It applies random changes to one or more genes of an individual parent to form children. The aim of mutation is to introduce new genetic material into an existing individual, that is, to add to the diversity of the genetic material of the population. It thereby enlarges the search space and delays the convergence of the GA. The mutation rate greatly affects the performance of the GA. Too much mutation badly affects the results. It is performed with a low probability p_m typically in the range $[0.01-0.2]$(Beasley *et al.*, 1993).

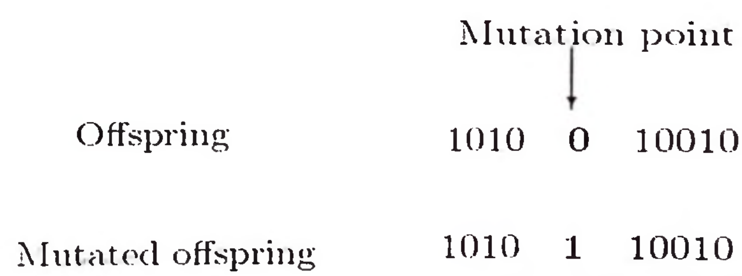

Figure 4.3: Use of a single mutation between two chromosomes

Figure 4.3 shows the fifth gene of the chromosome being mutated. It has been noted that crossover is more important of the two techniques for rapidly exploring a search space. Mutation provides a small amount of random search, and helps insure that no point in search space has a zero probability of being examined.

Replacement

The current population is replaced with the children created by selection, crossover, and mutation to form the next generation. Some of the common replacement techniques are (Sastry *et al.*, 2005):

- Delete-all. This technique deletes all the members of the current population and replaces them with the same number of chromosomes that have just been created.
- Steady-state. This technique deletes *n* old members and replaces them with *n* new members.
- Steady-state-no-duplicates. This is the same as the steady-state technique but the algorithm checks that no duplicate chromosomes are added to the population.

4.5 Real Parameter Genetic Algorithm

In the present study real parameter genetic algorithm is implemented instead of binary-coded GAs. There are some difficulties in binary-coded GAs, including inability to solve the problem where the values of variables have continuous search space or when the required precision is high. According to Deb (2001) hamming cliffs related to certain strings (01111 or 11110) is one of the difficulties where altering to near neighbor string requires changes in many genes. He also clams necessity of large strings (chromosomes with many genes) in order to fulfill a necessary precision which consequently increases the size of population, as another struggle for binary GAs. Therefore, in most problems using floating point numbers to represent the variables is more logical and requires less storage than binary coded strings. In addition, since there is no need for decoding the chromosomes before evaluation of the objective function in the selection phase, the real parameter GA (in some literature called continuous GA) is inherently faster than binary GA (Haupt *et al.*, 2004).

4.6 Genetic Algorithm Optimization of the Cooling System Parameters

The mathematical model described in Chapter 3 is a nonlinear problem. In this section we explore the use of GAs for finding the optimal parameters of the model in order to maximize the performance of the rock storage cooling system.

The major steps for using the GA as may be recalled from section 4.4.2 as follows

Step 1 *Initialization*: generate a random initial population of candidate solutions

Step 2 *Evaluation*: the objective function values of the candidate solutions in the current population are evaluated

Step3 *Fitness assignment*: Use the objective function value to determine the fitness values of the candidate solutions in the current population.

Step 4 *Selection*: select members; called parents, based on their fitness.

Step 4 *Reproduction*: reproduce the children created by selection, crossover, and mutation to form the next generation.

Step 6 *Go to step2*, until stopping criteria is met.

4.6.1 Estimation of Optimal Parameters of the Model using GA

Finding the best values of the parameters of the mathematical model (equations 3.4-3.11) of the thermal cooling system applied to rock storage is a non linear optimization process. There are many methods of optimizing problems and among them a GA is a better optimization method, especially when an optimal problem is not perfectly smooth and unimodal (Mitchell, 1997). It can quickly find a sufficiently good solution (i.e. near optimal solution) and also can be utilized to search for optimal parameters of the cooling model. The algorithm has been used to search for global optimal solutions in air conditioning fields (Wang and Jin, 2000).

In this thesis, a GA is utilized to search for the optimal values of individual radius of sphere (R), convective heat transfer coefficient (h_c), mass flow rate ($\dot{m}_a$) and the length of the packed bed (L). The use of GA improves the values of the control parameters. The improved "corrected" parameters are used for re-simulation of the model. The Genetic Algorithm Toolbox developed by Mathworks Inc. (2007) is employed to identify the parameters of the cooling system.The process is shown in Figure 4.4.

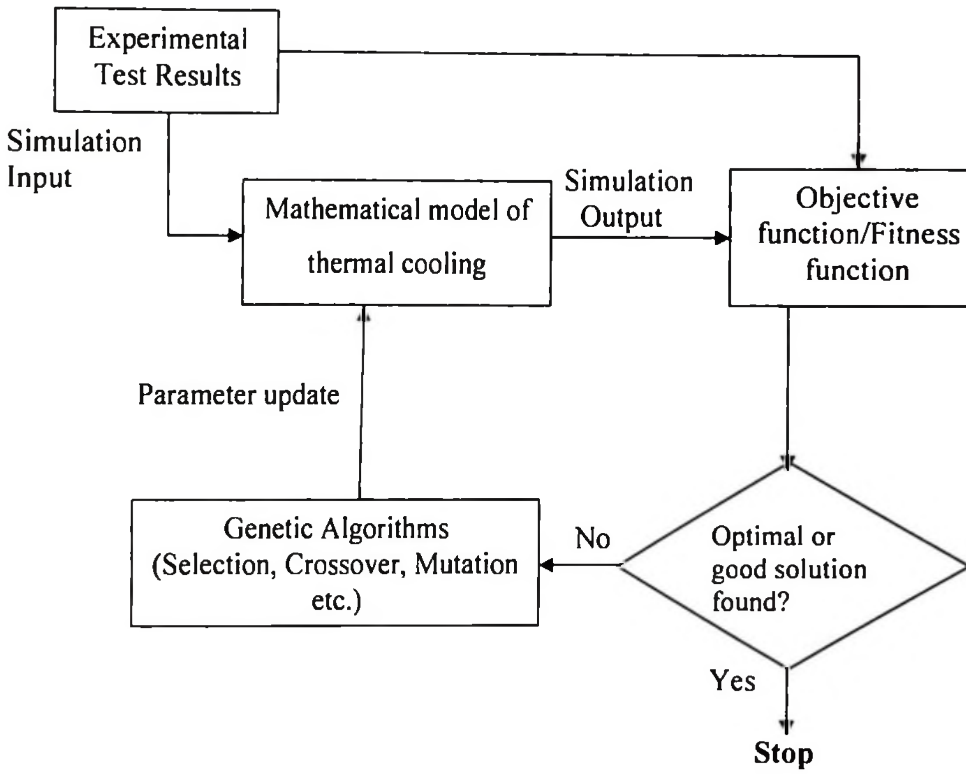

Figure 4.4: Progress of Parameter Optimization

4.6.2 Objective Function of Optimization

The simulated air temperatures from the mathematical model equations (3.4)-(3.11) are used to compare with the measured temperature. The parameters being optimized are radius of the sphere(R), convective heat transfer coefficient (h_c), mass flow rate $(\dot{m}_a)$ and the length of the packed bed (L) of the model which give the best fitting with the operation data. The estimate of the parameters is carried through GAs with the purpose of maximizing an objective function J that considers the error between the air inlet temperature and the model output vector (outlet air temperature) defined in equation (4.3), so that a reliable adjusted model can be determined to be used to design and operational strategies development.

$$J(R,\, h_c,\, \dot{m}_a,\, L) = \max_{\mathbf{x}} f_n(\mathbf{x}) \tag{4.3}$$

Subject to

$$\mathbf{x}_l \le \mathbf{x} \le \mathbf{x}_u$$

where

$$f_n(\mathbf{x}) = T^{in,\,n} - T^{out,\,n} \tag{4.4}$$

n - represents the number of experimental points,

T^{in} -the measurement of the inlet air temperature [$^{\circ}$C],

T^{out} -the measurement of the outlet air temperature [$^{\circ}$C],

$\mathbf{x}$ -Vector of unknown parameters,

$\mathbf{x}_l$ - is the lower bound of unknown parameters,

$\mathbf{x}_u$ - is the upper bound of unknown parameters.

To tackle the optimization problem of maximizing the objective function (4.3) by using a GA, we assume a function minimization problem. Hence, a good solution is one that has low relative fitness. Since the GA algorithm performs minimization of the objective function J, maximization of the objective function (4.3) is achieved by supplying $-J$ to the routine because the point at which $-J$ has a minimum is the same as the point at which J has maximum value. Therefore, in this study, the fitness of each chromosome in the population is calculated using a “fitness function” that characterizes how well each particular member solves the given problem. The fitness function is designed to be the minus of the objective function as equation (4.3). The fitness of each chromosome in the population is calculated by using equation (4.5).

$$f = f(R, h_c, \dot{m}_a, L) = \min_{\mathbf{x}}(-J) = \min_{\mathbf{x}}(-f_n(\mathbf{x})) \qquad (4.5)$$

Figure 4.5 shows schematically the GA flow chart developed for parameter optimization. It starts with the initial estimates of the individual radius of the sphere (rocks), convective heat transfer coefficient, mass flow rate, and length of the packed bed within assumed ranges. In the genetic algorithm, the four parameters (R, h_c, $\dot{m}_a$, L) constitute the chromosome of an individual; the assumed ranges of these parameters are the search space for these parameters. Initializing the four parameters produces the initial population to start a GA run.

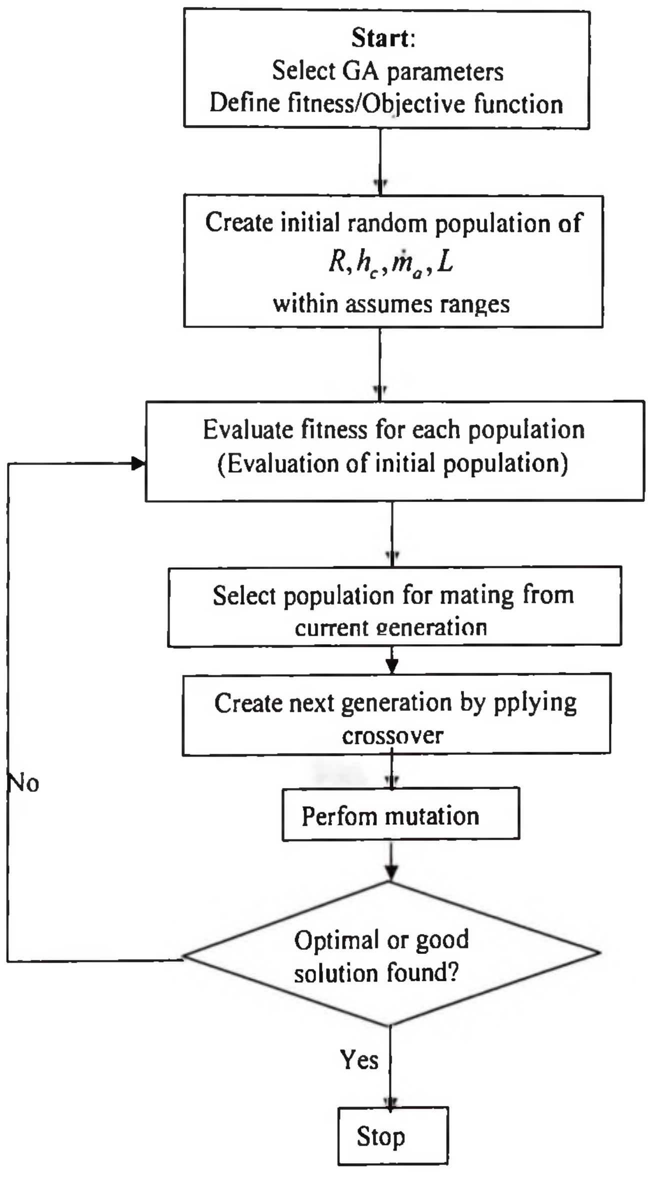

Figure 4.5: Flow chart of the GA for parameter estimation

In order to achieve good results in using a GA, one may have to experiment with different GA operators (selection, crossover, and mutation operators) and different GA parameters (population size, crossover probability, and mutation probability).

Population size specifies how many individuals are in each generation. With a large population size, the genetic algorithm searches the solution space more thoroughly, and gives more possibility to return the global minimum. The number of generations specifies the maximum number of iterations for the genetic algorithm to perform. If the number is too low, the genetic algorithm will not converge to the global solution. On the other hand a large population size or a large number of generations can cause the algorithm to run more slowly. The crossover rate and mutation rate are properties that control the crossover and mutation operator. High rate of these values means that the genetic algorithm has a high expectation of producing new offspring, but it can be easy to miss the current best solution if these values are too big.

4.6.3 Determined Parameters of the Thermal Cooling System

The sensitivity tests which were carried out in sections 3.6 show how parameters affect the prediction of the model and, thus indicating the need to come up with optimal operational parameters. Since some of the parameters are physical parameters which should be bounded in certain ranges, the lower and upper bounds are based on their assumed initial ranges. The search space of the parameters were chosen following on how the parameter showed the effect on the prediction of the model during the sensitivity tests. The membership values (lower bound lb, upper bound ub) for the four parameters are summarized in Table 4.1:

Table 4.1: Parameters for performance evaluation

Parameters	Value (lb, ub)
Length of the bed (L)	[2.00, 3.00] m
Heat transfer coefficient (h_c)	[6.00,9.00] $\mathrm{W/m^2\,^\circ C}$
Mass flow rate ($\dot{m}_a$)	[0.40, 0.60] $\mathrm{m^3/s}$
Radius of rocks (R)	[0.05, 0.10] m

The GA optimization experiments were performed by the roulette wheel selection rule that lays out a line in which each parent corresponds to a section of the line of length proportional to its scaled value, and used the control parameter options: population size $npop = 50$, elite count$=2$, single-point crossover type with $p_c = 0.75$ and mutation probability $p_m = 0.02$. These parameters are listed in Table 4.2. The initial population starts off with a set of feasible and non-feasible solutions are dropped during reproduction. The solutions obtained using the GA with the MATLAB GA Toolbox developed by Mathworks Inc. are summarized in Table 4.3.

Table 4.2: The property settings for GA

Name of the GA properties	Value of the GA properties
Number of generations	100
Population size	50
Fitness assignment	Rank-base fitness assignment
Elite count	2
Crossover type	Single-point
Crossover probability	0.75
Mutation function	Uniform mutation
Mutation probability	0.02
Selection method	Roulette Wheel Selection

Table 4.3: Parameters identified by GA

Parameter	Optimal Value
Radius of sphere (R)	0.096 m
Heat transfer coefficient (h_c)	7.900 W/m^{2}C
Mass flow rate ($\dot{m}_a$)	0.589 m^3/s
Length of the bed (L)	2.900 m

Figure 4.6 shows the best fitness function value and the average distance between individuals for the four parameters obtained using MATLAB Genetic Algorithm

Toolbox. The Figure shows that the population converges slowly to the best solution for the control parameter settings indicated above.

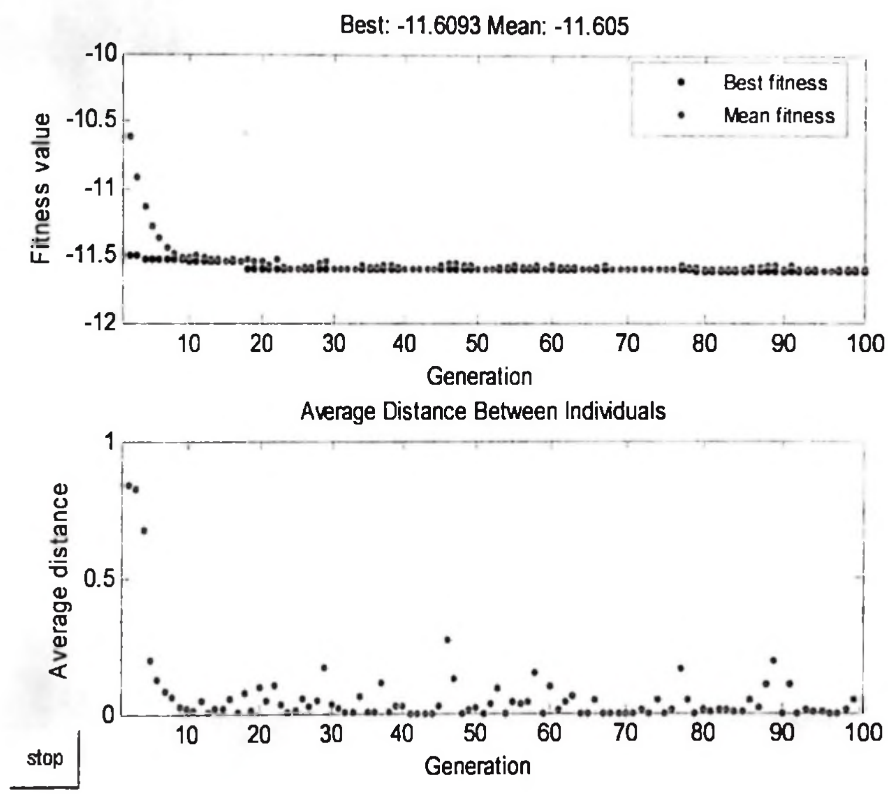

Figure 4.6: Genetic Algorithm Performance (Fitness function)

4.7 Numerical results of the model after parameter optimization

The optimal parameters of the mathematical model of the thermal cooling system were determined using Genetic Algorithm Toolbox provided by Mathworks Inc. and the predicted model with the identified parameters responses are compared with the simulated results. Figure 4.7 shows the variation of the fluid outlet temperature with the identified parameters of the mathematical model. The figure shows that, the fluid outlet temperature of the predicted model increases asymptotically with a delay time to the maximum possible value $30\,^{\circ}C$.

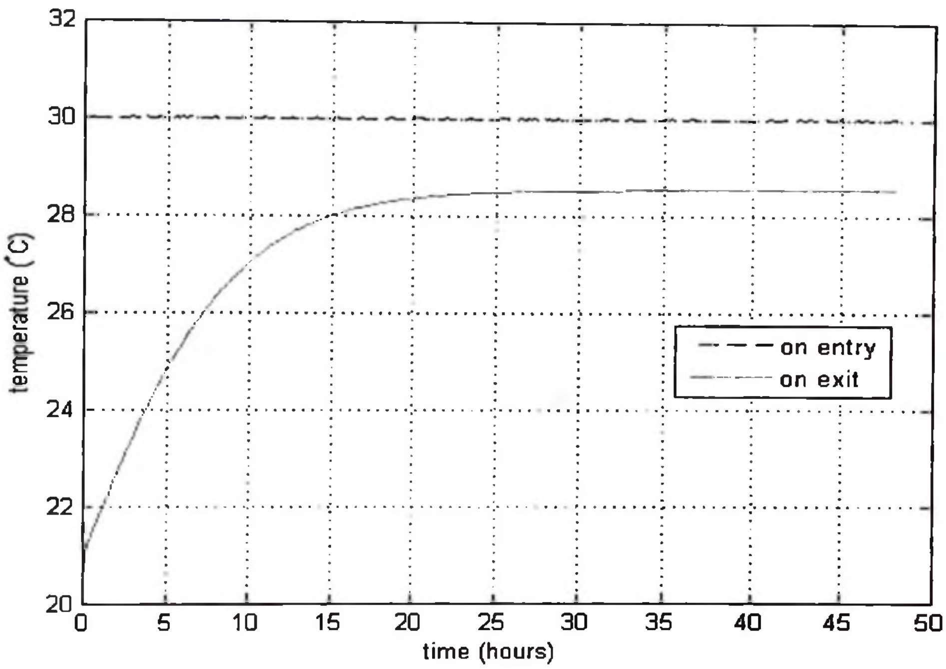

Figure 4.7: Fluid outlet temperature at constant T_{fi} after parameter optimization

4.7.1 Temperature gain and Phase lag after parameter optimization

Figure 4.8 shows the numerical prediction made for a time scale of 48 hours for the morning unit using improved thermal cooling system model after parameter optimization. The Figure shows the peak reduction by applying optimal parameters. The Figure also shows that the temperature gain and phase lag of the thermal cooling model with parameter optimization have increased compared to those without parameter optimization. From the figure, the estimates of the temperature gain between the inlet and outlet fluid without and with parameter optimization are 3.75 °C and 5.42 °C respectively.

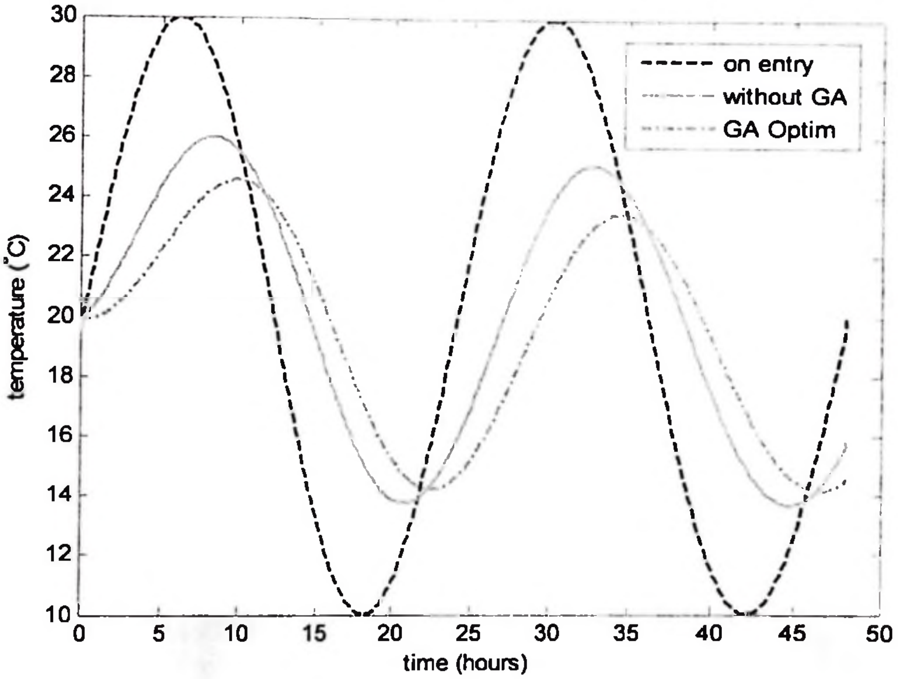

Figure 4.8: Fluid temperature gain and phase change after parameter optimization

The corresponding phase lags of the model before and after parameter optimization are 2.6 hours and 3.17 hours, respectively. It can be seen that the peak reduction has increased. Figure 4.8 also indicates that the time delay of the peaking of the temperature between the inlet and outlet temperature with parameter optimization has increased.

From these results, the phase lag delays the peaking of temperature between the inlet and outlet temperature for approximately 3hrs. This means that there must be a pre-defined level of comfort for the occupants in the building. For example, suppose the peak temperature for the ambient air occurs at 1:00 pm, it might be possible to control the system in order to delay the peak indoor temperature so that the room temperature becomes hottest when the occupants of the office are off from work, say at 4:00 pm.

4.7.2 Ground Coupling after Parameter Optimization

Figure 4.9 shows the effect of ground coupling on the fluid outlet temperature after parameter optimization for the afternoon unit. The fluid outlet temperature for parameter optimization when there is no thermal interaction with the ground surrounding the packed bed unit is plotted on the same graph with fluid outlet temperature for the case when ground coupling is taken into account.

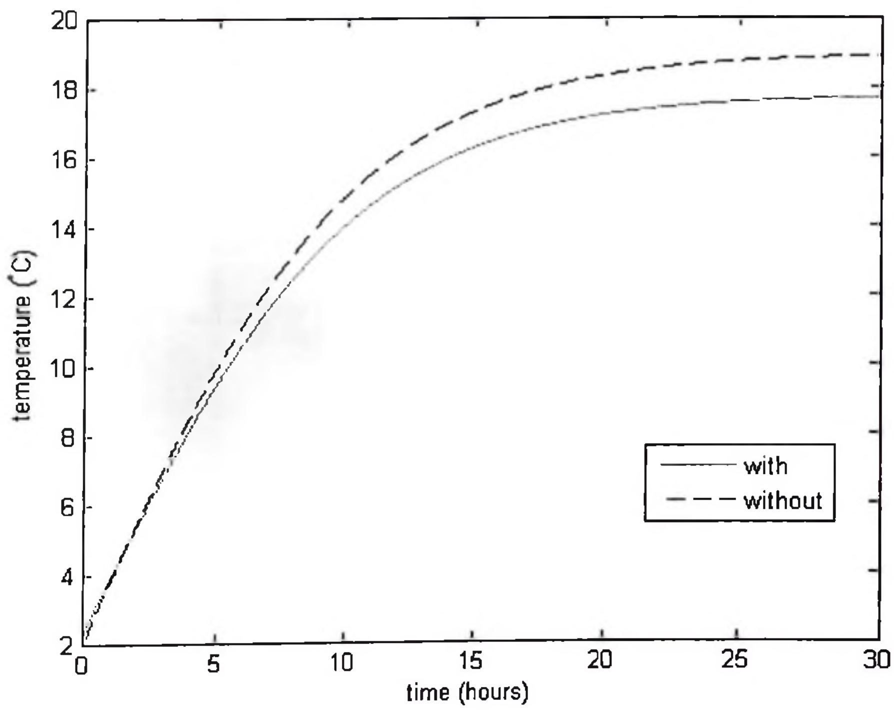

Figure 4.9: Effect of ground coupling on the fluid outlet temperature after parameter optimization

The effect of ground coupling for the optimal parameters has reduced the air outlet temperature by 0.95 C more. The delay time it takes to reach the maximum temperature of 20 °C has increased compared to the situation before parameter optimization. It can be seen in Figure 4.10 that, after 30 hours the maximum fluid outlet temperature for the case when ground coupling is taken into account after parameter optimization is approximately 17.8 °C, but before parameter optimization it was 19 °C. From the figure we see that for the improved parameters, the overall effect in the presence of the ground coupling reduces the temperature to about 1.2 °C after 30 hours.

Figure 4.10 shows the difference in fluid outlet temperature with and without ground coupling with parameter optimization for the afternoon unit. From the figure we see that for optimized parameters, the overall effect of adding ground coupling has increased from 0.8 to 1.2 after 30 hours.

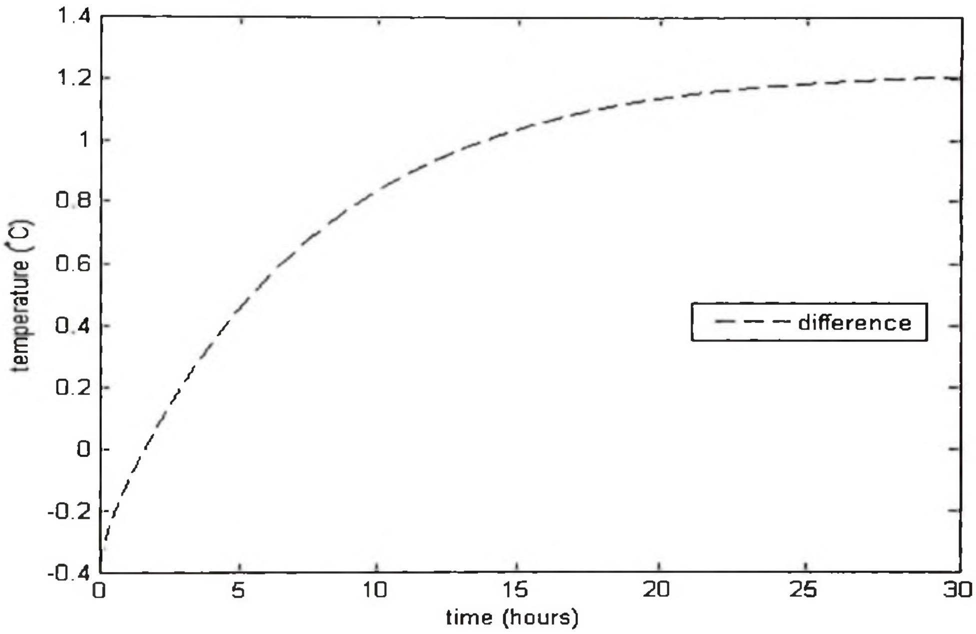

Figure 4.10: Difference in fluid outlet temperature with or without ground coupling after parameter optimization

4.7.3 Application of an Improved Model for Dar es Salaam Weather Condition

The temperature of Dar es Salaam ranges from 18 °C in August to 32 °C in December, January, February and March. The annual average temperature in Dar es Salaam is hot at 26 °C. January is the hottest month of the year for Dar es Salaam with an average temperature 28 °C. This weather condition causes large-scale demand of air-conditioning and causes higher power consumption during peak hours, whereby air-conditioning takes up much of the power consumption. Our attention is limited to efficiency assessment of rock-bed thermal energy storage system in January. The data from climatemps.com website are presented in Table 4.4 below,

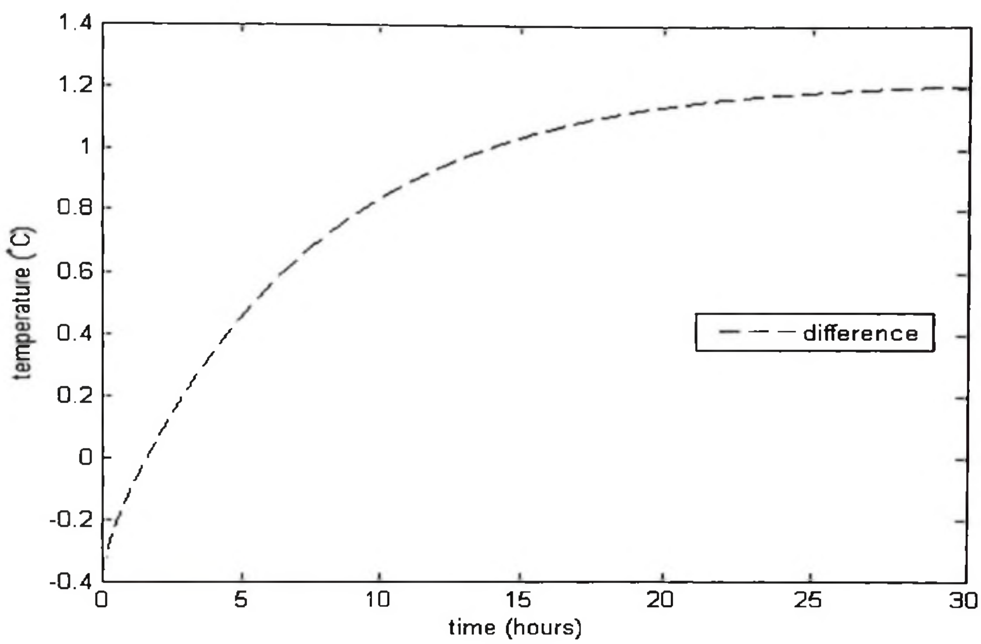

Figure 4.10: Difference in fluid outlet temperature with or without ground coupling after parameter optimization

4.7.3 Application of an Improved Model for Dar es Salaam Weather Condition

The temperature of Dar es Salaam ranges from 18 °C in August to 32 °C in December, January, February and March. The annual average temperature in Dar es Salaam is hot at 26 °C. January is the hottest month of the year for Dar es Salaam with an average temperature 28 °C. This weather condition causes large-scale demand of air-conditioning and causes higher power consumption during peak hours, whereby air-conditioning takes up much of the power consumption. Our attention is limited to efficiency assessment of rock-bed thermal energy storage system in January. The data from climatemps.com website are presented in Table 4.4 below, which presents important climate metrics average throughout the hours of daytime and night time of a typical January.

Table 4.4: Average weather conditions throughout a typical January for Dar es Salaam city. From www.climatemps.com visited on 20th December, 2013

Average hours of sunlight	7.45 hrs
Average daily mean temperature	28 °C
Average temperature during the daytime	32 °C
Average temperature during the nighttime	24 °C

The proposed model and numerical methods (see Chapter 3) are used to simulate a rock-bed thermal cooling system with the improved parameters using GA that is relevant to residential and commercial buildings to Dar es Salaam geographical condition. The system was assumed to be an isotropic homogenous bed of closely-packed rocks (porosity =0.5, radius of rocks =0.096 m, length of bed =2.90 m). The improved rock bed thermal cooling system parameters presented in Table 4.3 together with the data in Table 4.4 are used to show the efficiency performance of the rock-bed thermal cooling to the climate condition of Dar es Salaam. The properties of both rocks and the working fluid (air) are considered to be constant at the value of the average temperature in the rock-bed thermal cooling system. The rock-bed thermal cooling system performance as well as temperature profiles along the length of the rock-bed (axial direction of flow) are presented and analyzed at the end of each charging/discharging cycle during the initial daily-averaged simulations, as well as at the end of each hourly-updated simulation.

The purpose of the cooling system is to make the temperature in the room to be comfortable for the occupants. So for a hot day, the system should reduce the input temperature as much as possible at the time when the temperature is hottest. In this test, an investigation is carried out on heat transfer between the rock-bed and air with $T_f(t)$ (air temperature) varying sinusoidally with time i.e. $T_f(t) = T_{av} + A\sin\omega t$. The equation takes into account the average daily ambient temperature for a specific period of the year T_{av} (average daily temperature, as presented in Table 4.5), the amplitude of temperature swing A, the angular frequency $\omega = \frac{2\pi}{T}$, and the period of oscillation T. To demonstrate the potential of the rock bed cooling storage system to store thermal energy for Dar es Salaam climate condition, the simplified model was used as a means of comparison since no reliable measured data for a typical building could be obtained for validation.

In Figure 4.11, the fluid temperature varies sinusoidally about the mean of $28^\circ C$ to $38\ ^\circ C$ and the rock bed temperature varies about the mean temperature which rises from $28^\circ C$ to $32.8\ ^\circ C$. From the figure, one can see that the bed temperature has less swing than the fluid temperature. This happens because rocks are slow in gaining and loosing heat. Also we see clearly that there is time delay in the peaking of the rock bed temperature relative to fluid temperature which is about 2.7 hrs.

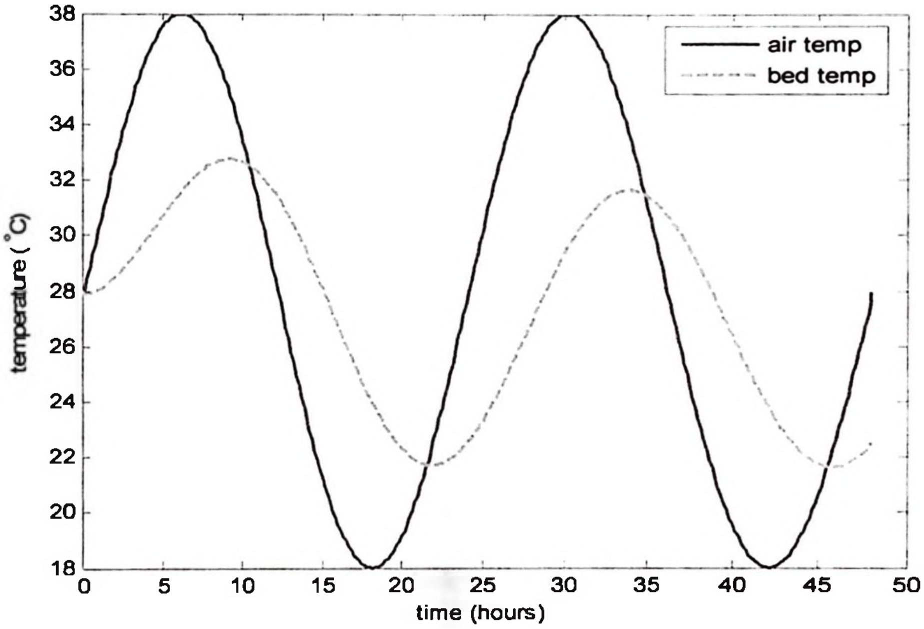

Figure 4.11: Sinusoidal Variation of temperature in the rock bed when $T_{av} = 28$ °C (mean daily temperature for Dar es Salaam) using improved parameters

From Figure 4.11, the temperature difference supplied between fluid temperature and rock bed peak is about 5 °C. Therefore, using these results, it is evident that if the rock-bed thermal cooling storage system is installed to residential/commercial buildings in Dar es Salaam city could reduce the energy consumption to occupants and hence reduce the energy cost. From the results, the improved model using optimized parameters has shown robustness in predicting the thermal performance under different operation condition. Therefore, the model can be used to predict building thermal performance for practical applications with acceptable accuracy and good reliability.

CHAPTER FIVE

DISCUSSION, CONCLUSION AND RECOMMENDATIONS

5.1 Discussion

In this thesis, a mathematical model for thermal energy storage in low energy buildings is proposed and analyzed. The cooling system which uses rock bed for storing night cooling to be used later for daytime air conditioning is presented. A two-phase one-dimensional mathematical model is used to describe the thermal behaviour of the rock bed which includes heat dispersion in a fluid and heat loss to the environment. The partial differential equations that govern the flow and heat transfer for both the air and the solid, constituting the bed and their boundary conditions are presented.

In chapter three, a numerical study of the model has been conducted to describe the thermal behaviour of the rock bed. The temperature field for the air and the solid are obtained. The results are compared with measured data at the outlet of the bed both using the measured inlet temperature and good agreement of trend is observed.

A numerical study of the model is also used to investigate the influence of certain key parameters on the performance of the thermal energy storage system. It is observed that, an increase in either heat transfer coefficient or length of the bed leads to damping the response of the fluid outlet temperature and this brings the model predicted fluid outlet temperature closer to the measured fluid outlet temperature value. On the other hand, lowering either mass flow rate or rock sizes leads to damping the response fluid outlet temperature.

A parametric study has been conducted to optimize the design of a packed bed to come up with optimal operational parameters such as the optimal fluid mass flow rate. An investigation was conducted on the impact of length of bed, fluid mass flow rate and the type of bed materials on the amount of heat stored in the bed after a fixed time of operation. A packed bed operating in single-blow mode was considered with different type of bed materials, these are granite rocks, concrete rubble and brick rubble. It is observed that, much less amount of energy is stored by increasing mass flow rate than by increasing the length of bed. It is also noted that, the amount of energy stored is higher in the order: brick rubble, concrete rubble and granite rocks. The results suggest that, of the three different types of material, granite is the best storage material. A similar analysis was carried out on the fraction of maximum possible heat stored in a bed. It was observed that, the fraction of maximum possible heat stored increases with flow rate for each bed material and decreases with bed length. Higher fraction of maximum possible heat is stored for granite, concrete rubble and brick rubble in that order.

A numerical study of the model was also used to investigate the effect of ground coupling on the fluid outlet temperature. The results indicate that, the effect of adding ground coupling is to increase the thermal capacity of the bed and hence delay the time it takes for the fluid outlet temperature to reach its maximum possible value. It was observed that, the presence of the ground coupling reduces the fluid outlet temperature by about 0.8 °C.

In chapter four, an optimization of thermal cooling system parameters was conducted. A genetic algorithm (GA) was used as a tool to optimize the thermal cooling system parameters related to the mathematical model, including the rock sizes (radius of the sphere), mass flow rate, heat transfer coefficient and length of the packed bed. The outcomes of the optimization process show the ability of the algorithm in maintaining solutions in the entire search region. The use of GA improves the values of the parameters and the improved "corrected" parameters were used for re-simulation of the model. Results with respect to optimal values are produced and showed robustness in predicting the thermal performance under different operation condition.

5.2 Conclusion and Recommendations

In this research, a two-phase one-dimensional mathematical model is proposed and analyzed to study the thermal behaviour of the rock bed cooling system. The model includes heat dispersion in a fluid and heat loss to the environment. When modelling the thermal cooling using rock-bed thermal energy storage system, special difficulties arise in choice of several parameters, for example, coefficient of heat transfer, mass flow rate, length of bed, specific heat, etc. In chapter 3, a mathematical model was analyzed to predict the temperature of air as it leaves the cooling system. The model was tested against measured data and good agreement in trend is observed. Sensitivity analysis was conducted to investigate the influence of certain key parameters on the performance of the thermal energy storage system such as, convective heat transfer coefficient, mass flow rate, rock sizes and length of bed. The analysis shows how parameters can be modified to move the model predicted fluid outlet temperatures closer to the measured fluid outlet temperature values.

The work uses a method for optimization of the model parameters based on the mechanics of natural selection and genetics in Darwin's theory. The procedure to estimate the cooling system parameters with genetic algorithm has been presented in the study and can be effectively used to optimize the parameters using operation data. An optimization of the parameters was studied to aid the future design of buildings using rock beds for cooling or heating. The most concern was to see when the hottest temperature occurs and use parameters to see how they affect it. In itself it means which time of the year, particularly for Dar es Salaam is of most concern. The study has generally shown the efficiency of the model and is recommended that the model could be useful to designers of similar cooling systems in future buildings designs, particularly in Dar es Salaam where due to its climate conditions, there is a great need for saving on energy consumption and for the use of sustainable energy technologies.

It is also recommended that, the application of computation intelligence methods, combined with the knowledge of the manufacturing technology products should enable efficient selection of parameters of mathematical model and thus, allow a more precise control of the process of cooling/heating to ensure the required quality or desired level of comfort for the building occupants. In general, the model with optimal parameters has shown good robustness to predict the performance of the cooling system by reducing the input (air) temperature as much as possible at the time when the temperature is hottest.

Further research is needed to develop a control algorithm that minimizes the total cooling energy cost when the demand charge is included in the cost function.

REFERENCES

Al-Nimr MA, Abu-Qudais MK and Mashaqi MD 1996 *Dynamic Behaviour of Packed Bed Energy Storage System.* Energy Conversion and Management **37(1)**: 23-30.

Adebiyi GA, Hodge BK, Nsofor EC, Steele WG and Jalaalzadeh-Azar A 1996 *Computer Simulation of a high-Temperature Thermal Energy Storage System Employing Multiple Families of Phase Change Storage Materials.* Trans. ASME J. Energy Resources Tech. **118**:102-111.

Aly SL and El-Sharkawy AL 1990 *Effect of Storage Medium on Thermal Properties of Packed Bed.* Heat Recovery System CHP **10(5/6)**: 509-519.

Arkar C, Vidrih B and Medved, S 2007 *Efficiency of Free Cooling using Latent Heat Storage Integrated into the ventilation System of a Low Energy Building.* Int. Journal of Refrigeration **30**: 134-143.

Arunasalam P, Seetharamu K N and Abdul Aziz I 2005 *Determination of Thermal Compact Model via Evolutionary Genetic Optimization Method.* IEEE transactions on components and packaging technologies **28**: No. 2.

Ataer OE 2006 *Storage of Thermal Energy, in Energy Storage Systems, in Encyclopedia of Life Support Systems (EOLSS)*, Eolss Publishers, Oxford ,UK.

Athienitis AK 1997 *Investigation of Thermal Performance of a Passive Solar Building with Floor Radiant Heating.* Solar Energy **61(5)**: 337-345.

Balaras CA 1996 *The role of Thermal Mass on the Cooling load of Buildings. An Overview of Computational Methods.* Energy and Buildings **24**: 1-10.

Athienitis AK and Chen Y 2000 *The effect of Solar Radiation on Dynamic Thermal Performance of Floor Heating Systems*. Solar energy **69(3):** 229-237.

Barnard N 2006 *Hybrid Cooling Solutions: Night Cooling and Mechanical Refrigeration*. In Proc. of Institute of Refrigeration, 7th December, 2006, London South Bank University, London SEI.

Beasley DE and Clack JA 1984 *Transient Response of a Packed Bed for Thermal Energy Storage*. International Journal of Heat Mass Transfer **27(9)**: 1659-1669.

Beasley D, Bull DR and Martin RR 1993 *An Overview of Genetic Algorithms*: Part 1, Fundamentals, University Computing **25(2)**: 58-69.

Beasley D, Bull DR and Martin RR 1993 An *Overview of Genetic Algorithms*: Part 2, Research Topics, University Computing **25(4)**: 170-181.

Bhardwaj SJ, Kaushik SC and Garg HP 1991 *Sensible Thermal Storage in Rock Beds for Space Conditioning: A State of the Art Study*. International Journal of Ambient Energy **20(4)**: 211-219.

Boyd S and Vandenberghe L 2004 *Convex Optimization*, Cambridge University Press

Duffe JA and Beckman WA 1980 *Solar Engineering of Thermal Processes*, Wiley.

Deb K 2001 *Multi-Objective Optimization Using Evolutionary Algorithms*. John Wiley & Sons Ltd, The Atrium, Southern Gate, Chichester, West Sussex PO19 8SQ, England.

Chang YC 2007 *Application of Genetic Algorithm to the Chilled water Supply Temperature Calculation of Air-conditioning Systems for Serving Energy*. Int. J. Energy Res.**31**: 796-810.

Chang YC 2007 *Optimal Chiller Loading by Evolution Strategy for Saving Energy.* Energy and Building **39**: 437-444.

Chen W and Liu W 2004 *Numerical and Experimental Analysis of Convection Heat Transfer in Passive Solar Heating Room with Greenhouse and Heat Storage.* Solar Energy **76**: 623-633.

Close DJ 1976 *Design and Performance of a Thermal Storage Air-conditioning System.* ASME Transactions Journal of Heat Transfer, **98:**336-338.

Fleming PJ, Chipperfield AJ and Fonseca CM 1994 *Genetic Algorithm Tools for Control Systems Engineering.* Adaptive Computing in Engineering Design and Control. Plymouth, UK.

Chung JS and Hwang SM 1998 *Application of a Genetic Algorithm to Process Optimal Design in Non-isothermal Metal Forming.* Journal of Material Processing Technology **80-81**: 136-143.

Coello Coello CA, Christiansen AD and Santos Hernandez F 1997 *A simple Genetic Algorithm for the Design of Reinforced Concrete Beams.* Journal of Engineering with Computers **13**: 185-196.

Coutier JP and Farber EA 1982 *Two Applications of a Numerical Approach of Heat Transfer Process within Rock beds.* Solar Energy **29(6):** 451-462.

Crandall DM and Thacher EF 2004 *Segmented Thermal Storage.* Solar Energy **77**: 435-440.

Danok SH, Abbas IF and Weis MM 2011 *Theoretical Study of Thermal Performance of Rock Bed Storage.* Tikrit Journal of Engineering Sciences **18(2)**: 20-28.

Dincer I, Dost S and Li X 1997 *Performance Analysis of Sensible Heat Storage Systems for Thermal Applications.* Int. J. Energy Research **21**: 1157-1171.

Goldberg DE 2002 *Design of Innovation: Lessons from and for Competent Genetic Algorithms*, Kluwer Academic Publishers, Boston, Massachusetts.

Goldberg DE and Deb K 1991 *A Comparative Analysis of Selection Schemes Used in Genetic Algorithms*. In Foundations of Genetic Algorithms, G. J. E. Rawlins (Ed.), Morgan Kaufmann, 1991: 69-93.

Gosselin L, Tye GM and Mathieu PF 2009 *Review of Utilization of Genetic Algorithms in Heat Transfer Problems*. Int. J. Heat and Mass Transfer **52**: 2169-2188.

Grefenstette JJ 1986 *Optimization of Control Parameters for Genetic Algorithm*. IEEE Transactions on Systems, Man, and Cybernetics **SMC-16**, No. 1.

Haupt RL and Haupt SE 2004 *Practical Genetic Algorithms*, 2nd edition, John Wiley and Sons, Inc.

Hessari FA, Parsa S and Khashechi AK 2004 *Behaviour of Packed Bed Thermal Storage*. IJE Transactions A: Basics **16(2)**: 181-192.

Huang W and Lam HN 1997 *Using Genetic Algorithms to Optimize Controller Parameters for HVAC Systems*. Energy and Buildings **26**: 277-282.

Hui SCM and Cheung KP 1998 *Application of Building Energy Simulation to Air-Conditioning Design*. In Proc. of the Mainland-Hong Kong HVAC Seminar 98, 23-35 March 1998, Beijing: 12-20.

Isanska-Cwiek A 2005 *Experimental and CFD research on the thermal performance on the air cooled slab system*. Building Simulation, Ninth International IBPSA conference.

Koza JR 1992 *Genetic programming: On the Programming of Computers by Means of Natural Selection*. MIT Press, Cambridge, MA, USA.

Logan DL 2007 *A First course in the Finite Element Method*, 4^{th} edition, Rahul Print O pack, Delhi-20.

Manohar K and Adeyanju AA 2009 *Comparison of Thermal Energy Storage Techniques*. Journal of Engineering and Applied Sciences **4(3)**: 221-231.

Marewo GT 2005 *Mathematical Modelling of Passive Cooling in Buildings*. PhD thesis, Department of Mathematics, University of Zimbabwe.

Marewo GT and Henwood DJ 2006 *A Mathematical Model for Supplying Air-Cooling for a Building Using a Packed Bed*. Building Service Eng. Res. Tech. **27(1)**: 11-26.

Michalewicz Z 1996 *Genetic Algorithms + Data Structures = Evolution Programs*, 3rd. rev and extended edition.Springer-Verlag, Berlin.

Mitchell M 1996 *An Introduction to Genetic Algorithms*, MIT Press.

More JJ, Tapia RA and Wright MH 1980 "*Optimization*", ACM SIGNUM Newsletter **15**, Issue 4, December 1980: 16-26.

Nkansah-Gyenke Y 2010 *An Intelligent Vertical Handoff Decision Algorithm in next Generation Wireless Networks*. PhD Thesis, Department of Computer Science, University of Western Cape

Nsofor EC and Adebiyi GA 2001 *Measurements of the Gas-Particle Convective Heat Transfer Coefficient in a Packed Bed for High-Temperature Energy Storage*. Experimental Thermal and Fluid science **24**: 1-9.

Öztürk N and Çelik E 2011 *Application of Genetic Algorithms to Core Loss Coefficient Extraction*. Progress in Electromagnetics Research M **19**: 133-146.

Pasupathy AP and Velraj R 2006 *Mathematical modelling and Experimental study on building ceiling using Phase Change Material for Energy conservation.* The 2nd Joint International Conference on Sustainable Energy and Environment (SEE 2006) 21-23 November 2006, Bangkok, Thailand.

Phueakphum D and Fuenkajorn K 2010 *A Rock Fills Based Solar Thermal Storage System for Housing.* ScienceAsia **36**:237-243.

Ravikumar M and Srinivasan PSS 2005 *Phase Change Material as a Thermal Energy Storage Material for Cooling of Building.* Journal of Theoretical and Applied Information Technology **4**, No. 6: 503-511.

Ren MJ and Wright JA 1998 *A Ventilated Slab Thermal Storage System Model.* Building and Environment **33**, No. 1: 43-52.

Sanderson TM and Cunningham GT 1995 *Performance and Efficient Design of Packed Bed Thermal Storage Systems. Part I.* Applied Energy **50**: 119-132

Sastry K, Goldberg DE and Kendall G 2005 *"Genetic Algorithms: A Tutorial".* In E. Burke, and G. Kendall (Eds.), Introductory Tutorials in Optimization, Search, and Decision Support Methodologies (Chapter 4, pp. 97-125), Berlin: Springer, 2005.

Schmidt FW and Willmott AJ 1981 *Thermal Energy Storage and Regeneration.* McGraw-Hill.

Singh R, Saini RP and Saini JS 2010 *A Review on Packed bed Solar Energy Storage Systems.* Renewable and Sustainable Energy Reviews **14**: 1059-1069

Singh R, Saini RP and Saini JS 2008 *Simulated Performance of Packed Bed Solar Energy Storage System having Storage material Elements of Large size-Part I.* The Open Fuels and Energy Science Journal **1**: 91-96.

Sivanandam SN and Deep SN 2008 *Introduction to Genetic Algorithms.* Springer Berlin Heidelberg, New York.

Spiga G and Spiga M 1980 *A Rigorous Solution to a Heat Transfer Two Phase Model in Porous Media and Packed Beds.* International Journal of Heat mass transfer **24**: 355-364.

Ståhl F 2009 *Influence of Thermal Mass on the Heating and Cooling Demands of the Building unit.* PhD thesis, Chalmers University of Technology, Göteborg, Sweden.

Syswerda G 1989 *Uniform Crossover in Genetic Algorithms.* In J. D. Schaffer, Ed. Proceedings of the Third International Conference on Genetic Algorithms, San Mateo, CA: Morgan Kaufmann

Wang S and Xu X 2006 *Parameter Estimation of Internal Thermal Mass of Building dynamic Models using Genetic Algorithm.* Energy Conversion and Management **47**: 1927-1941.

Wang SW and Jin XQ 2000 *Model-Based Optimal Control of VAV Air-conditioning using Genetic Algorithm.* Building Environment **35 (6)**: 471-487.

Westphal FS and Lamberts R 2005 *Building Simulation Calibration using Sensitivity Analysis, Building Simulation*, Ninth International IBPSA conference, Montréal, Canada August 15-18, 2005.

Wright JA, Loosemore H A and Farmani R 2002 *Optimization of Building Thermal Design and Control by Multi-Genetic Algorithm.* Energy and Buildings **34**: 959-972.

Xie GN, Sunden B and Wang QW 2008 *Optimization of Compact Heat Exchangers by a Genetic Algorithm.* Applied Thermal Engineering **28**: 895-906.

APPENDIX

Program MATLAB Code

rock_store.m

```
%%%%%%%%%%%%%%%%%%%%%%%%%%%%%%%%%%%%%%%%%%%%
clear
close all
%%%%%%%%%%%%%%%%%%%%%%%%%%%%%%%%%%%%%%%%%%%%
% method data
% nfe : number of fluid elements linear (were previously quadratic)
% nnx : number of nodes in the x-direction = nfe+1
% nnr : number of nodes in each rock
% nnt : number of times at which the initial temperature is recorded this comes from
%       the given or chosen data
nfe = 3;
nnx = nfe+1;
nnr = 8;

%%%%%%%%%%%%%%%%%%%%%%%%%%%%%%%%%%%%%%%%%%%%
% Temperature data on entry to the rock store, Tf(1,t) this may be read from the data
% logger or set analytically i.e. the inlet temperature which drives the storing
% dt   : the time step for computing (from the measured scheme) (secs)
% inte : inlet temperature at discrete times (deg)
% nnt  : number of time steps, which may be computed or read

dt   = 10*60; % every 15 minutes

% setting time over "nd" days with steps of dt seconds and frequency etc
nd   = 14;
af   = (2*pi)/(24*60*60);
stme = 0; % start time
etme = nd*24*60*60; % end time

%%%%%%%%%%% Fuid (air)%%%%%%%%%%%%%%%%%%%%%%%%%
% ma   : mass flow rate (kg/sec)
% rhof : density (kg/m^3)
% cf   : specific heat capacity (J/kgdegC)
% kf   : thermal conductivity (W/mdegC)
% Sfr  : Surface frontal area (Cross sectional area of bed) (m^2)

ma = 0.6;
cf= 1007;  kf  = 0.025;
Wb = 2.7; % Wb - Width of bed (m)
Db = 2; % Db - Depth of bed (m); for future use?
Sfr= Db*Wb; rhof= 1.106;
%
% Environment heat loss parameters
```

```
% U     : heat loss factor (W/m^2degC)
% P     : perimeter of bed (m)
% T_env : environment temperature (degC)
U = 0;
Lb = 2; % Lb - Length of bed (m)
P = 2*(Lb+Wb); % Revisit formula when including loss to environment but not
               % important if U=0

% Data file for the rock store
% A        - Area of convective heat transfer (m^2)
% hc       - convective film coefficient (W/m^2 degC)
% porosity - (void fraction or) porosity of bed = (volume of fluid)/(volume of bed)
% radius   - average sphere radius (m)
% A        - total surface area of convection (m^2)
% rpuv     - rocks per unit volume (/m^3)
hc       = 6;
porosity = 0.5;
radius   = 0.1;
rpuv     = 3*(1-porosity)/(radius); % rocks per unit volume (/m^3)
A        = rpuv*Sfr*Lb;
gamma    = kf*Sfr*porosity*Lb; % gamma=a
%
delta    = hc*A;
beta1    = U*P*Lb;
mu       = delta + beta1;
h        = Lb/(nfe); % length of each element
T_env    = 0; % degree celsius: not wrong but not necessary since U=0

%%%%%%%%%% Data on the rocks %%%%%%%%%%%%%%
% rm : rock density (kg/m^3)
% cm : specific heat capacity (J/kgdegC)
% km : thermal conductivity of rock material (W/mdegC)
%
rm = 1800; cm = 1000; km = 0.96;
% for plotting
nsteps  = round((etme-stme)/(dt)+1); % plot at how many t values?
T_entry = zeros(nsteps,1);
T_exit  = zeros(nsteps,1);
itime   = 1;
% end of data
% setting up the stepping matrices for the fluid and the rocks

%%%%%%%%%%%% ROCKS %%%%%%%%%%%%%%%%%%%%%%%%%%%
nts = nsteps;
Z  = zeros(nnr,nnx);
Z0 = zeros(nnr,1);
B  = zeros(nnr,nnr);
```

```
v   = zeros(nnr,1);
bv  = zeros(nnr,1);
hr  = radius/(nnr-1); % step size in radial direction the general rows
% forming the iteration matrix B of FD equations:
%   dTm/dt=B*Tm-Tf*v                 (1)
for it = 2 : nnr-1
   rp = (it-1)*hr; % distance along radius from centre of rock
   at = (1/hr)*(1/hr-1/rp); % at=lambda_i
   bt = -2/hr/hr; % bt=theta
   ct = (1/hr)*(1/hr+1/rp); % ct=\tilde{lambda}_i
   B(it,it-1:it+1) = [at bt ct];
end

% for the first and last nodes

B(1,1:2)  = (6/hr/hr)*[-1 1];
rp = radius; % last node
% at = (1/hr)*(1/hr-1/rp);
% bt = -2/hr/hr;
% ct = (1/hr)*(1/hr+1/rp);
q  =  2*hr*hc/km; % phi=bt-q*ct
B(nnr,nnr-1:nnr)= [-bt bt-q*ct];
%
B          = (km/(rm*cm))*B; % had factored out alpha
% Eqn (1) transforms, under change of variable Ta=X*z, to
%   dz/dtau=D*z+R+S*tau              (2)
% Matrices X and D are given by
[X,D]   = eig(B); % X diagonalizes B
lamb    = diag(D); % eigenvalues
Omexp  = 1-exp(D*dt); % the solution of eqution (2) is
%     z = alpha*Omexp+beta*dt           (3)
XI      = inv(X); % R=X\(B*Tm1+P)
DI      = inv(D); % inv(D) related to beta
v(nnr)  = (2*hc/(rm*cm))*(1/hr+1/radius); % part of v in equation (1)

% %%%%%%%Semi-analytic solution%%%%%%%%%%%%%%%
% Solve equation (1) on interval [t1,t2] on t-axis, where we assume
% linear variation of Tf(t), i.e Tf(t)=Tf1+(t-t1)*(Tf2-Tf1)/dt
% where
% Tf1 = fluid temperature at time t=t1
% Tf2 = fluid temperature at time t=t2
%  dt = t2-t1

% Similar notation:

% Tm1 = rock temperature at time t=t_1
% Tm2 = rock temperature at time t=t_2
```

```
% Ta    = Tm2-Tm1

% Setting the basic loop: progressing from time t1 to time t2
% with the computation over the time range

Tf1 = 20*ones(1,nnx); %=zeros(1,nnx);
Tf2 = zeros(1,nnx); % is this used?
Tm1 = 20*ones(nnr,nnx); %zeros(nnr,nnx);
Tm2 = zeros(nnr,nnx);
Z   = zeros(nnr,nnx);  Z0  = zeros(nnr,nnx);
Ta  = zeros(nnr,nnx);

% Tf(1) is the inlet and Tf(nnx) the outlet temperatures
% Tm(nnr,:) is the temperature Tm(R,x,t) of the rock face in contact with
% the fluid at any time t and a distance x from entry into bed starting at time t1, with
% zero temperature throughout and then setting in the given input temperature to
% obtain the temperatures at time t2; then recursively.

itme        = 1; % start at time level 1
%
tmes=stme:dt:etme;
measured_99_0217_0303
intes=md_air_in; % inlet temperatures or temperatures at entry
T_entry(itme) = intes(1); % Tf1(1); % initial air temperature at entry
T_exit(itme)  = intes(1); % initial air temperature at exit
tcounter=1;
for tme =tmes  % time stepping
   %inte  = 20 +10*sin(af*tme); %
   inte      = intes(tcounter); tcounter=tcounter+1;
   time(itme) = tme/60/60; % can this be improved later?
   itme      = itme+1; % increase counter for time levels
   %
   % now at time t2
   %
   nup = 10;
   for upgrade = 1:nup
      % compute Tf2
      bc    = zeros(nnx,1); % begin with zeros in bc of K*Tf=bc
      % Tf2(1) = inte; % replaced in (4) below
      % forming the right hand side vector of the fluid equation

      for ia = 1:nnx-1 % assemble bc in K*Tf=bc
         vt    = [ia ia+1];
         be    = ((Tms(ia)+Tms(ia+1))/2)*(delta*h/2)*[1 1]';
         be    = be+T_env*(beta1*h/2)*[1 1]';
         bc(vt) = bc(vt)+be;
      end
```

```
      bc(1)  = inte; % imposing bc T_f(0,t)=T_fi(t) on RHS of K*Tf=bc
      % K changes with time but how? any code that changes K comes here!
%bc  = zeros(nnx,1);
K   = zeros(nnx,nnx);
% Tms = zeros(1,nnx); % Temperature of rock surface in contact with the fluid
t  = 0:0.1666:336; % hours in 2 weeks
%
%%%%%%%AFTERNOON UNIT FLOW RATES%%%%%%
[r,c] = size(t);
ma     = zeros(size(t));%0.6*ones(r,c); % initial flow rate
s     = rem(t,24);
for i=1:max(r,c)
   if ((s(i)>=0 & s(i)<=3.5)|(s(i)>=10 & s(i)<=18)|(s(i)>=24 & s(i)<=27.5))
      ma(i)=0.6; % flow rate when the fan is ON
   end
end
t2=find((t>=51.5 & t<=106)|(t>=219.5 & t<=274));
ma(t2)=0;% flow rate when the fan is OFF

%%%%%MORNING UNIT FLOW RATES %%%%%%
%[r,c] = size(t);% hours in a day
%ma = zeros(size(t)); % initial flow rate
%s = rem(t,24);
%for r=1:max(r,c)
   % if ((s(r)>=10 & s(r)<=18) | (s(r)>=20 & s(r)<=24)|(s(r)>=34& s(r)<=42));
    %  ma(r)=0.6;%flow rate when the fan is OFF
   % end
%t2=find((t>=48 & t<=106)|(t>=216 & t<=274));
%ma(t2)=0;%flow rate when the fan is OFF

Be  = (gamma/h)*[1 -1
           -1  1]; % Be (here)=Kc (in paper)
Re  = (ma(r)*cf*Lb/2)*[-1  1
              -1  1]; % Re (here)=Km (in paper)
Ze  = (mu*h/6)*[2  1
           1  2]; % Ze (here)=Kh (in paper)
Ke  = Be+Re+Ze; % element stiffness matrix
% assembling K and bc in Ku=bc
for ia = 1:nnx-1
    va     = [ia ia+1];
%    be     = ((Tms(ia)+Tms(ia+1))/2)*(delta*h/2)*[1 1]'; % taking average %
 be     = be+T_env*(beta1*h/2)*[1 1]';
%    bc(va)  = bc(va)+be; % assemble the load vector bc (here)=f (in paper)
   K(va,va) = K(va,va)+Ke; % assemble the stiffness matrix
end % end of K and bc loop
%
% setting up for T_entry, which may differ for each time step
```

```
%
% K(1,2:nnr) = 0; K(1,1)= 1;% imposing dirichlet boundary condition, T, on
K(1,:) = 0; K(1,1)= 1; %

      Tf2    = (K\bc)'; %              (4)
      time(itme)   = tme/60/60; % for plotting later
      T_entry(itme) = Tf2(1); % plotting later
      T_exit(itme)  = Tf2(nnx); % for plotting later
      % To calculate Tm2
      P     = v*Tf1;
      Q     = (1/dt)*v*(Tf2-Tf1);
      % P and Q appear in equation:
      % dTm/dt=B*Tm+P+Q(t-t1), t1<=t<=t2
      R     = XI*(B*Tm1+P);
      S     = XI*Q;
      % R and S appear in equation (2)
      Beta  = -DI*S;
      Alpha = DI*(Beta-R);
      % alpha and beta appear in (3)
      Z     = Omexp*Alpha+dt*Beta; % see equation (3)
      Ta    = X*Z; % change of variable for decoupling system of DEs
      %     [upgrade sum(sum(abs(Ta)))]  % for testing
      Tm2   = Tm1+Ta; % compute Tm2 using Tm2-Tm1=Ta
      %
      Tms   = Tm2(nnr,:); % surface rock temperature at time t2
      %
   end  % of upgrade loop
   %
   Tm1   = Tm2; % what was Tm2 is now Tm1
   Tf1   = Tf2; % what was Tf2 is now Tf1
end   % of time loop
nt = length(T_entry);
figure(30)
hold on
axis on
grid on
plot(time,T_entry,'b-.')
plot(time, T_exit,'g--')
plot(t, md_air_out,'r' )
plot(t,ma*25)
legend('on entry', 'on exit', 'measured outlet', 0)
xlabel('time (hours)')
ylabel('temperature ( ^\circC)')
hold off


%%%%ground_coupling.m%%%%%
```

```
% method data
% nfe : number of fluid elements linear (were previously quadratic)
% nnx : number of nodes in the x-direction = nfe+1
% nnr : number of nodes in each rock
% nnt : number of times at which the initial temperature is recorded
%       this comes from the given or chosen data

nfe = 3;
nnx = nfe+1;
nnr = 8;

%%%%%%%%%%%%%%%%%%%%%%%%%%%%%%%%%%%%%%%%%%%%%%%
% Temperature data on entry to the rock store, Tf(1,t) , this may be read from the
%  data logger or set analytically  i.e. the inlet temperature which drives the storing
% dt   : the time step for computing (from the measured scheme) (secs)
% inte : inlet temperature at discrete times (deg)
% nnt  : number of time steps, which may be computed or read
%
dt   = 60;  % every 15 minutes
%
% setting time over "nd" days with steps of dt seconds and frequency etc
%nd   = 14;
final_tme_hrs = 30;
af   = (2*pi)/(24*60*60);
stme = 0; % start time
etme = final_tme_hrs*60*60;
%etme = nd*24*60*60; % end time

%%%%%%%%%%%%%%%%%%%%%%%%%%%%%%%%%%%%%%%%%%%%%%%
% Fuid (air)

% ma   : mass flow rate (kg/sec)
% rhof : density (kg/m^3)
% cf   : specific heat capacity (J/kgdegC)
% kf   : thermal conductivity  (W/mdegC)
% Sfr  : Surface frontal area (Cross sectional area of bed) (m^2)
%
m_a= 0.46;
cf= 1007;  kf   = 0.025;
Wb = 2.7; % Wb - Width of bed (m)
Db = 2; % Db - Depth of bed (m); for future use?
Sfr= Db*Wb; rhof= 1.106;
%
%%%%%%%%%%%%%%%%%%%%%%%%%%%%%%%%%%%%%%%%%%%%%%%
% Environment heat loss parameters
%
% U    : heat loss factor (W/m^2degC)
```

```
% P     : perimeter of bed (m)
% T_env : environment temperature (degC)
without_ground
T_without = T_exit1;
%
U = 2;
Lb= 2.31; % Lb - Length of bed (m)
P = 26.8;%9.4;%2*(Lb+Wb);

% %%%%%%%%Data file for the rock store %%%%%%%%%%
% A        - Area of convective heat transfer (m^2)
% hc       - convective film coefficient (W/m^2 degC)
% porosity - (void fraction or) porosity of bed = (volume of fluid)/(volume of bed)
% radius   - average sphere radius (m)
% A        - total surface area of convection (m^2)
% rpuv     - rocks per unit volume (/m^3)

hc       = 6.7;
porosity = 0.5;
radius   = 0.1;
rpuv     = 3*(1-porosity)/(radius); % rocks per unit volume (/m^3)
A        = rpuv*Sfr*Lb;
gamma    = kf*Sfr*porosity*Lb; % gamma=a
delta    = hc*A;
beta1    = U*P*Lb;
mu       = delta + beta1;
h        = Lb/(nfe); % length of each element
T_env    = 15;%0; % degree celsius: not wrong but not necessary since U=0

%%%%%%%%%%%%% Data on the rocks%%%%%%%%%%%%%%%%%%
% rm : rock density (kg/m^3)
% cm : specific heat capacity (J/kgdegC)
% km : thermal conductivity of rock material (W/mdegC)
%
% rm =2700; cm = 800; km =2.1;
rm = 1800; cm = 1000; km = 0.96;
% for plotting
nsteps  = round((etme-stme)/(dt)+1); % plot at how many t values?
T_entry = zeros(nsteps,1);
T_exit  = zeros(nsteps,1);
% end of data
% setting up the stepping matrices for the fluid and the rocks
% FLUID %%%using linear elements %%%%%%%%%%%%%%%%
%
% effectively independent of time because air flow is quick compared
% with the change in temperature in the rocks
Tms = zeros(1,nnx); % Temperature of rock surface in contact with the fluid
```

```
bc  = zeros(nnx,1);
K   = zeros(nnx,nnx);
%%
Be  = (gamma/h)*[1 -1
          -1  1]; % Be (here)=Kc (in paper)
Re  = (m_a*cf*Lb/2)*[-1  1
               -1  1]; % Re (here)=Km (in paper)
Ze  = (mu*h/6)*[2  1
          1  2]; % Ze (here)=Kh (in paper)
Ke  = Be+Re+Ze; % element stiffness matrix
% assembling K and bc in Ku=bc
for ia = 1:nnx-1
   va     = [ia ia+1];
   be     = ((Tms(ia)+Tms(ia+1))/2)*(delta*h/2)*[1 1]'; % taking average
   be     = be+T_env*(beta1*h/2)*[1 1]';
   bc(va)  = bc(va)+be; % assemble the load vector bc (here)=f (in paper)
   K(va,va) = K(va,va)+Ke; % assemble the stiffness matrix
end % end of K and bc loop

%setting up for T_entry, which may differ for each time step

% K(1,2:nnr) = 0; K(1,1)= 1;% imposing dirichlet boundary condition, T, on
K(1,:) = 0; K(1,1)= 1; % imposing dirichlet boundary condition, T_f(0,t)=T_fi(t), on
% LHS of FE equation(s) Ku=bc
%
% %%%%%%%%%%%%%ROCKS %%%%%%%%%%%%%%%%%%%%%
nts = nsteps;
Z   = zeros(nnr,nnx);
Z0  = zeros(nnr,1);
B   = zeros(nnr,nnr);
v   = zeros(nnr,1);
bv  = zeros(nnr,1);
hr  = radius/(nnr-1); % step size in radial direction
%
 %%%%%%%%%%%%The general rows%%%%%%%%%%%%%%%
% forming the iteration matrix B of FD equations:
%    dTm/dt=B*Tm-Tf*v                  (1)
for it = 2 : nnr-1
   rp = (it-1)*hr; % distance along radius from centre of rock
   at = (1/hr)*(1/hr-1/rp); % at=lambda_i
   bt = -2/hr/hr; % bt=theta
   ct = (1/hr)*(1/hr+1/rp); % ct=\tilde{lambda}_i
   B(it,it-1:it+1) = [at bt ct];
end
%
% for the first and last nodes
%
```

```
B(1,1:2) = (6/hr/hr)*[-1 1];
rp = radius; % last node
q  = 2*hr*hc/km; % phi=bt-q*ct
B(nnr,nnr-1:nnr)= [-bt bt-q*ct];
%
B           = (km/(rm*cm))*B; % had factored out alpha
% Eqn (1) transforms, under change of variable Ta=X*z, to
%   dz/dtau=D*z+R+S*tau              (2)
% Matrices X and D are given by
[X,D]    = eig(B); % X diagonalizes B
lamb     = diag(D); % eigenvalues
Omexp    = 1-exp(D*dt); % the solution of eqution (2) is
%   z=alpha*Omexp+beta*dt            (3)
XI       = inv(X); % R=X\(B*Tm1+P)
DI       = inv(D); % inv(D) related to beta
v(nnr)   = (2*hc/(rm*cm))*(1/hr+1/radius); % part of v in equation (1)
%
%%%%%%%%%%%%%%%%%%%%%%%%%%%%%%%%%%%%%%%%%%%%%%
% Semi-analytic solution
%
% Solve equation (1) on interval [t1,t2] on t-axis, where we assume
% linear variation of Tf(t), i.e
%
% Tf(t)=Tf1+(t-t1)*(Tf2-Tf1)/dt
%
% where
%
% Tf1 = fluid temperature at time t=t1
% Tf2 = fluid temperature at time t=t2
%  dt = t2-t1
%
% Similar notation:
%
% Tm1 = rock temperature at time t=t_1
% Tm2 = rock temperature at time t=t_2
% Ta  = Tm2-Tm1
%
% Setting the basic loop: progressing from time t1 to time t2 with the computation
% over the time range
%
Tf1 = 20*ones(1,nnx); %=zeros(1,nnx);
Tf2 = 20*ones(1,nnx); % is this used?
Tm1 = zeros(nnr,nnx); %;20*ones(nnr,nnx)
Tm2 = zeros(nnr,nnx);
Z   = zeros(nnr,nnx);
Z0  = zeros(nnr,nnx);
Ta  = zeros(nnr,nnx);
```

```
%
% Tf(1) is the inlet and Tf(nnx) the outlet temperatures
% Tm(nnr,:) is the temperature Tm(R,x,t) of the rock face in contact with
% the fluid at any time t and a distance x from entry into bed startng at time t1, with
%20 (why not 26?) temperature throughout and then setting in the given input
% temperature to obtain the temperatures at time t2; then recursively.
%
itme        = 1; % start at time level 1
%
tmes=stme:dt:etme;
%measured_0920_1004
measured_99_0217_0303
intes=md_air_in; % inlet temperatures or temperatures at entry
T_entry(itme) = intes(1); % Tf1(1); % initial air temperature at entry
T_exit(itme)  = intes(1); % initial air temperature at exit
tcounter=1;
for tme =tmes  % time stepping
   inte  = 20;% +10*sin(af*tme); %
   %inte      = intes(tcounter); tcounter=tcounter+1;
   time(itme) = tme/60/60; % can this be improved later?
   itme       = itme+1; % increase counter for time levels
   %
   % now at time t2
   %
   nup = 10;
   for upgrade = 1:nup
      % compute Tf2
      bc     = zeros(nnx,1); % begin with zeros in bc of K*Tf=bc
      % Tf2(1) = inte; % this does not seem necessary? replaced in (4) below
      %
      % forming the right hand side vector of the fluid equation
      %
      for ia = 1:nnx-1 % assemble bc in K*Tf=bc
         vt    = [ia ia+1];
         be    = ((Tms(ia)+Tms(ia+1))/2)*(delta*h/2)*[1 1]';
         be    = be+T_env*(beta1*h/2)*[1 1]';
         bc(vt) = bc(vt)+be;
      end
      bc(1)   = inte; % imposing bc T_f(0,t)=T_fi(t) on RHS of K*Tf=bc
      % K changes with time but how? any code that changes K comes here!
      Tf2     = (K\bc)'; %              (4)
      time(itme)    = tme/60/60; % for plotting later
      T_entry(itme) = Tf2(1); % plotting later
      T_exit(itme)  = Tf2(nnx); % for plotting later
      % To calculate Tm2
      P     = v*Tf1;
      Q     = (1/dt)*v*(Tf2-Tf1);
```

```
        % P and Q appear in equation:
        % dTm/dt=B*Tm+P+Q(t-t1), t1<=t<=t2
        R    = XI*(B*Tm1+P);
        S    = XI*Q;
        % R and S appear in equation (2)
        Beta  = -DI*S;
        Alpha = DI*(Beta-R);
        % alpha and beta appear in (3)
        Z    = Omexp*Alpha+dt*Beta; % see equation (3)
        Ta   = X*Z; % change of variable for decoupling system of DEs
        %      [upgrade sum(sum(abs(Ta)))]  % for testing
        Tm2  = Tm1+Ta; % compute Tm2 using Tm2-Tm1=Ta
        %
        Tms  = Tm2(nnr,:); % surface rock temperature at time t2
        %
    end  % of upgrade loop
    %
    Tm1  = Tm2; % what was Tm2 is now Tm1
    Tf1  = Tf2; % what was Tf2 is now Tf1
end  % of time loop
T_diff = T_without - T_exit;
% nt = length(T_entry);
 figure(1)
% hold on
% axis on
% grid on
plot(time, T_exit,'g')
hold on
plot(time,T_without,'b--')
legend('with','without' ,0)
xlabel('time (hours)')
ylabel('temperature (^\circC)')
hold off

figure(2)
plot(time,T_diff,'b--')
legend('difference',0)
xlabel('time (hours)')
ylabel('temperature (^\circC)')

%%%%Granite_store.m%%%%%

% method data
% nfe : number of fluid elements linear (were previously quadratic)
% nnx : number of nodes in the x-direction = nfe+1
% nnr : number of nodes in each rock
% nnt : number of times at which the initial temperature is recorded
```

```
%      this comes from the given or chosen data

nfe = 3;
nnx = nfe+1;
nnr = 10;

%%%%%%%%%%%%%%%%%%%%%%%%%%%%%%%%%%%%%%%%%%%%%%
% Temperature data on entry to the rock store, Tf(1,t) this may be read from the data
% logger or set analytically i.e. the inlet temperature which drives the storing
% dt   : the time step for computing (from the measured scheme) (secs)
% inte : inlet temperature at discrete times (deg)
% nnt  : number of time steps, which may be computed or read
%
dt   = 60; % every 15 minutes
%
% setting time over "nd" days with steps of dt seconds and frequency etc
%
%nd   = 1;
final_tme_hrs = 8;
af   = (2*pi)/(24*60*60);
stme = 0; % start time
etme = final_tme_hrs*60*60;
%etme = nd*24*60*60; % end time

% Fuid (air)
%
% ma   : mass flow rate (kg/sec)
% rhof : density (kg/m^3)
% cf   : specific heat capacity (J/kgdegC)
% kf   : thermal conductivity  (W/mdegC)
% Sfr  : Surface frontal area (Cross sectional area of bed) (m^2)
%
m_a =m_a;%volume_flow_rates;%0.6;
cf= 1007;  kf  = 0.025;
Wb = 2.7; % Wb - Width of bed (m)
Db = 2; % Db - Depth of bed (m); for future use?
Sfr= Db*Wb; rhof= 1.106;
%
% Environment heat loss parameters %%%%%%%%%%%%%%%
%
% U     : heat loss factor (W/m^2degC)
% P     : perimeter of bed (m)
% T_env : environment temperature (degC)
%
U = 0;
Lb= Lb;%2; % Lb - Length of bed (m)
P = 26.8;%2*(Lb+Wb);
```

```
% Data file for the rock store
%
% A        - Area of convective heat transfer (m^2)
% hc       - convective film coefficient (W/m^2 degC)
% porosity  - (void fraction or) porosity of bed = (volume of fluid)/(volume of bed)
% radius   - average sphere radius (m)
% A        - total surface area of convection (m^2)
% rpuv     - rocks per unit volume (/m^3)
%
hc       = 6;
porosity = 0.5;
radius   = 0.1;
rpuv     = 3*(1-porosity)/(radius); % rocks per unit volume (/m^3)
A        = rpuv*Sfr*Lb;
gamma    = kf*Sfr*porosity*Lb; % gamma=a
%
delta    = hc*A;
beta1    = U*P*Lb;
mu       = delta + beta1;
h        = Lb/(nfe); % length of each element
T_env    = 15;%0; % degree celsius: not wrong but not necessary since U=0
T_0      = 0;

% %%%%%%%%%%%Data on the rocks%%%%%%%%%
% rm : rock density (kg/m^3)
% cm : specific heat capacity (J/kgdegC)
% km : thermal conductivity of rock material (W/mdegC)
%
rm = 2700; cm = 800; km = 2.1;
%  for plotting
nsteps   = round((etme-stme)/(dt)+1); % plot at how many t values?
T_entry  = zeros(nsteps,1);
T_exit   = zeros(nsteps,1);
itime    = 1; % NB: not used elsewhere?
%  end of data
%  setting up the stepping matrices for the fluid and the rocks
%
% FLUID %%using linear element%%%%%%%%%%%%%%%%%%%
%  effectively independent of time because air flow is quick compared
%  with the change in temperature in the rocks
Tms = zeros(1,nnx); % Temperature of rock surface in contact with the fluid
bc  = zeros(nnx,1);
K   = zeros(nnx,nnx);
%%
Be  = (gamma/h)*[1 -1
            -1  1]; % Be (here)=Kc (in paper)
Re  = (m_a*cf*Lb/2)*[-1  1
```

```
            -1  1]; % Re (here)=Km (in paper)
Ze  = (mu*h/6)*[2  1
            1  2]; % Ze (here)=Kh (in paper)
Ke  = Be+Re+Ze; % element stiffness matrix
% assembling K and bc in Ku=bc
for ia = 1:nnx-1
   va     = [ia ia+1];
   be     = ((Tms(ia)+Tms(ia+1))/2)*(delta*h/2)*[1 1]'; % taking average
       be     = be+T_env*(beta1*h/2)*[1 1]';
   bc(va)    = bc(va)+be; % assemble the load vector bc (here)=f (in paper)
   K(va,va) = K(va,va)+Ke; % assemble the stiffness matrix
end % end of K and bc loop

%setting up for T_entry, which may differ for each time step

% K(1,2:nnr) = 0; K(1,1)= 1;% imposing dirichlet boundary condition, T, on
K(1,:) = 0; K(1,1)= 1; % imposing dirichlet boundary condition, T_f(0,t)=T_fi(t), on
% LHS of FE equation(s) Ku=bc
%
% ROCKS %%%%%%%%%%%%%%%%%%%%%%%%%%%%%%%%%
nts = nsteps;
Z   = zeros(nnr,nnx);
Z0  = zeros(nnr,1);
B   = zeros(nnr,nnr);
v   = zeros(nnr,1);
bv  = zeros(nnr,1);
hr  = radius/(nnr-1); % step size in radial direction
%
% the general rows
%
% forming the iteration matrix B of FD equations:
%    dTm/dt=B*Tm-Tf*v                (1)
for it = 2 : nnr-1
   rp = (it-1)*hr; % distance along radius from centre of rock
   at = (1/hr)*(1/hr-1/rp); % at=lambda_i
   bt = -2/hr/hr; % bt=theta
   ct = (1/hr)*(1/hr+1/rp); % ct=\tilde{lambda}_i
   B(it,it-1:it+1) = [at bt ct];
end
%
% for the first and last nodes
%
B(1,1:2)  = (6/hr/hr)*[-1 1];
rp = radius; % last node
q  = 2*hr*hc/km; % phi=bt-q*ct
B(nnr,nnr-1:nnr)= [-bt bt-q*ct];
%
```

```
B            = (km/(rm*cm))*B; % had factored out alpha
% Eqn (1) transforms, under change of variable Ta=X*z, to
%    dz/dtau=D*z+R+S*tau              (2)
% Matrices X and D are given by
[X,D]    = eig(B); % X diagonalizes B
lamb     = diag(D); % eigenvalues
Omexp    = 1-exp(D*dt); % the solution of eqution (2) is
%    z=alpha*Omexp+beta*dt            (3)
XI       = inv(X); % R=X\(B*Tm1+P)
DI       = inv(D); % inv(D) related to beta
v(nnr)   = (2*hc/(rm*cm))*(1/hr+1/radius); % part of v in equation (1)
%
%%%%%%%%%%%%%%%%%%%%%%%%%%%%%%%%%%%%%%%%%%%%%%%%%%
% Semi-analytic solution
% Solve equation (1) on interval [t1,t2] on t-axis, where we assume
% linear variation of Tf(t), i.e
%
% Tf(t)=Tf1+(t-t1)*(Tf2-Tf1)/dt
%
% where
%
% Tf1 = fluid temperature at time t=t1
% Tf2 = fluid temperature at time t=t2
% dt = t2-t1
%
% Similar notation:
%
% Tm1 = rock temperature at time t=t_1
% Tm2 = rock temperature at time t=t_2
% Ta  = Tm2-Tm1
%
% Setting the basic loop: progressing from time t1 to time t2
% with the computation over the time range
%
Tf1 = 20*ones(1,nnx); %zeros(1,nnx); %
Tf2 = zeros(1,nnx); % is this used?
Tm1 = zeros(nnr,nnx);%20*ones(nnr,nnx);
Tm2 = zeros(nnr,nnx);
Z   = zeros(nnr,nnx);
Z0  = zeros(nnr,nnx);
Ta  = zeros(nnr,nnx);
%
% Tf(1) is the inlet and Tf(nnx) the outlet temperatures
% Tm(nnr,:) is the temperature Tm(R,x,t) of the rock face in contact with the fluid at
% any time t and a distance x from entry into bed starting at time t1, with 20
% temperature throughout and then setting in the given input temperature to obtain
%the temperatures at time t2; then recursively.
```

```
%
itme        = 1; % start at time level 1
%
tmes=stme:dt:etme;
%measured_0920_1004
measured_99_0217_0303
intes=md_air_in; % inlet temperatures or temperatures at entry
T_entry(itme) = intes(1); % Tf1(1); % initial air temperature at entry
T_exit(itme)  = intes(1); % initial air temperature at exit
tcounter=1;
for tme =tmes  % time stepping
   inte  = 20;%20 +10*sin(af*tme); %
%     inte      = intes(tcounter); tcounter=tcounter+1;
   time(itme) = tme/60/60; % can this be improved later?
   itme       = itme+1; % increase counter for time levels
   %
   % now at time t2
   %
   nup = 10;
   for upgrade = 1:nup
      % compute Tf2
      bc     = zeros(nnx,1); % begin with zeros in bc of K*Tf=bc
      % Tf2(1) = inte; % this does not seem necessary? replaced in (4) below
      %
      % forming the right hand side vector of the fluid equation
      %
      for ia = 1:nnx-1 % assemble bc in K*Tf=bc
         vt    = [ia ia+1];
         be    = ((Tms(ia)+Tms(ia+1))/2)*(delta*h/2)*[1 1]';
         be    = be+T_env*(beta1*h/2)*[1 1]';
         bc(vt) = bc(vt)+be;
      end
      bc(1)  = inte; % imposing bc T_f(0,t)=T_fi(t) on RHS of K*Tf=bc
      Tf2    = (K\bc)'; %              (4)
      time(itme)    = tme/60/60; % for plotting later
      T_entry(itme) = Tf2(1); % plotting later
      T_exit(itme)  = Tf2(nnx); % for plotting later
      % To calculate Tm2
      P     = v*Tf1;
      Q     = (1/dt)*v*(Tf2-Tf1);
      % P and Q appear in equation:
      % dTm/dt=B*Tm+P+Q(t-t1), t1<=t<=t2
      R     = XI*(B*Tm1+P);
      S     = XI*Q;
      % R and S appear in equation (2)
      Beta  = -DI*S;
      Alpha = DI*(Beta-R);
```

```
      % alpha and beta appear in (3)
      Z    = Omexp*Alpha+dt*Beta; % see equation (3)
      Ta   = X*Z; % change of variable for decoupling system of DEs
      %      [upgrade sum(sum(abs(Ta)))]  % for testing
      Tm2  = Tm1+Ta; % compute Tm2 using Tm2-Tm1=Ta
      %
      Tms  = Tm2(nnr,:); % surface rock temperature at time t2
      %
    end  % of upgrade loop
    %
    Tm1  = Tm2; % what was Tm2 is now Tm1
    Tf1  = Tf2; % what was Tf2 is now Tf1
  end  % of time loop
  T_fo = T_exit;
  T_fi = 20;

%%%%%inputs_granite.m%%%%%%
%NUMERICAL DATA (inputs) FOR PHYSICAL CONSTANTS IN THE
% MATHEMATICAL MODEL FOR THE TRANSIENT BEHAVIOUR OF A
% PACKED BED DRIVEN BY THE FLUID INLET TEMPERATURE.
% * physical constants
% ** fluid
% symbol   -  meaning
% c_f      -  specific heat capacity (J/kg degC)
% rho_f    -  density (kg/m^3)
% k_f      -  thermal conductivity (W/m degC)
% V_f      -  volume flow rate (m^3/s)
% m_f      -  mass flow rate (kg/m^3)
%
c_f=1007;
rho_f=1.106;
k_f=.025;
m_a=m_a;
m_f=rho_f*m_a;
%
% ** solid (granite sphere)
% c_m      -  specific heat capacity (J/kg degC)
% rho_m    -  density (kg/m^3)
% k_m      -  thermal conductivity (W/m degC)
% alpha_m  -  thermal diffusivity (ms)
%
c_m=800;
rho_m=2700;
k_m=2.1;
alpha_m=k_m/(rho_m*c_m);
%
% ** other
```

```
% hc       - convective film coefficient (W/m^2degC)
% porosity -  porosity of bed=(volume of fluid)/(volume of bed)
% lb       - length of bed (m)
% S_fr     - frontal surface area (m^2)
% radius   - average sphere radius (m)
% A     - total surface area of convection (m^2)
% rpuv     - rocks per unit volume (/m^3)
%
hc=6;
porosity=0.5;
Lb=Lb;
S_fr=2*2.7;
radius=.1;
rpuv=3*(1-porosity)/(4*pi*radius^3);
A=rpuv*S_fr*Lb*4*pi*radius^2;
%

%%%%%%Brick_store.m%%%%%%
% method data

% nfe : number of fluid elements linear (were previously quadratic)
% nnx : number of nodes in the x-direction = nfe+1
% nnr : number of nodes in each rock
% nnt : number of times at which the initial temperature is recorded
%       this comes from the given or chosen data

nfe = 3;
nnx = nfe+1;
nnr = 8;
%%%%%%%%%%%%%%%%%%%%%%%%%%%%%%%%%%%%%%%%%%%%%%%%%%%%%%%%%%%%%%%%
% Temperature data on entry to the rock store, Tf(1,t)  this may be read from the data
% logger or set analytically i.e. the inlet temperature which drives the storing
%
% dt   : the time step for computing (from the measured scheme) (secs)
% inte : inlet temperature at discrete times (deg)
% nnt  : number of time steps, which may be computed or read
%
dt   = 60;  % every 15 minutes
%
% setting time over "nd" days with steps of dt seconds and frequency etc
%
%nd   = 1;%14;
final_tme_hrs = 8;
af   = (2*pi)/(24*60*60);
stme = 0; % start time
etme = final_tme_hrs*60*60;
%etme = nd*24*60*60; % end time
```

```
%
% Fuid (air) %%%%%%%%%%%%%%%%%%%%%
%
% ma   : mass flow rate (kg/sec)
% rhof : density (kg/m^3)
% cf   : specific heat capacity (J/kgdegC)
% kf   : thermal conductivity  (W/mdegC)
% Sfr  : Surface frontal area (Cross sectional area of bed) (m^2)
%
m_a =m_a;%volume_flow_rates;%0.6;
cf= 1007;  kf  = 0.025;
Wb = 2.7; % Wb - Width of bed (m)
Db = 2; % Db - Depth of bed (m); for future use?
Sfr= Db*Wb; rhof= 1.106;
%%%%%%%%%%%%%%%%%%%%%%%%%%%%%%%%%%%%%%%%%%%%
% Environment heat loss parameters
%
% U     : heat loss factor (W/m^2degC)
% P     : perimeter of bed (m)
% T_env : environment temperature (degC)
%
U = 0;
Lb= Lb;%2; % Lb - Length of bed (m)
P = 26.8;%2*(Lb+Wb); % Revisit formula when including loss to environment but
not important if U=0
%
% Data file for the rock store
% A         - Area of convective heat transfer (m^2)
% hc        - convective film coefficient (W/m^2 degC)
% porosity  - (void fraction or) porosity of bed = (volume of fluid)/(volume of bed)
% radius    - average sphere radius (m)
% A         - total surface area of convection (m^2)
% rpuv      - rocks per unit volume (/m^3)
%
hc       = 6;
porosity = 0.5;
radius   = 0.1;
rpuv     = 3*(1-porosity)/(radius); % rocks per unit volume (/m^3)
A        = rpuv*Sfr*Lb;
gamma    = kf*Sfr*porosity*Lb; % gamma=a
%
delta    = hc*A;
beta1    = U*P*Lb;
mu       = delta + beta1;
h        = Lb/(nfe); % length of each element
T_env    = 0; % degree celsius: not wrong but not necessary since U=0
T_0      = 0;
```

```
%
%%%%%%%%%%%%%%%%%%%%%%%%%%%%%%%%%%%%%%%%%%%
% Data on the rocks
% rm : rock density (kg/m^3)
% cm : specific heat capacity (J/kgdegC)
% km : thermal conductivity of rock material (W/mdegC)
%
rm = 1700; cm = 800; km = 0.73;
% for plotting
nsteps  = round((etme-stme)/(dt)+1); % plot at how many t values?
T_entry  = zeros(nsteps,1);
T_exit  = zeros(nsteps,1);
itime   = 1; % NB: not used elsewhere?
% end of data
% setting up the stepping matrices for the fluid and the rocks
%
%FLUID%%%using linear element%%%%%%%%%%%%%%%%%%%%%%%
% effectively independent of time because air flow is quick compared
% with the change in temperature in the rocks
Tms = zeros(1,nnx); % Temperature of rock surface in contact with the fluid
bc  = zeros(nnx,1);
K   = zeros(nnx,nnx);
%%
Be  = (gamma/h)*[1 -1
          -1  1]; % Be (here)=Kc (in paper)
Re  = (m_a*cf*Lb/2)*[-1  1
              -1  1]; % Re (here)=Km (in paper)
Ze  = (mu*h/6)*[2  1
          1  2]; % Ze (here)=Kh (in paper)
Ke  = Be+Re+Ze; % element stiffness matrix
% assembling K and bc in Ku=bc
for ia = 1:nnx-1
   va     = [ia ia+1];
   be     = ((Tms(ia)+Tms(ia+1))/2)*(delta*h/2)*[1 1]'; % taking average
   be     = be+T_env*(beta1*h/2)*[1 1]';
   bc(va)  = bc(va)+be; % assemble the load vector bc (here)=f (in paper)
   K(va,va) = K(va,va)+Ke; % assemble the stiffness matrix
end % end of K and bc loop

%setting up for T_entry, which may differ for each time step

% K(1,2:nnr) = 0; K(1,1)= 1;% imposing dirichlet boundary condition, T, on
K(1,:) = 0; K(1,1)= 1; % imposing dirichlet boundary condition, T_f(0,t)=T_fi(t), on
% LHS of FE equation(s) Ku=bc
%
% ROCKS %%%%%%%%%%%%%%%%%%%%%%%%
nts = nsteps;
```

```
Z  = zeros(nnr,nnx);
Z0  = zeros(nnr,1);
B  = zeros(nnr,nnr);
v  = zeros(nnr,1);
bv  = zeros(nnr,1);
hr  = radius/(nnr-1); % step size in radial direction
%
% the general rows
%
% forming the iteration matrix B of FD equations:
%   dTm/dt=B*Tm-Tf*v                    (1)
for it = 2 : nnr-1
   rp = (it-1)*hr; % distance along radius from centre of rock
   at = (1/hr)*(1/hr-1/rp); % at=lambda_i
   bt = -2/hr/hr; % bt=theta
   ct = (1/hr)*(1/hr+1/rp); % ct=\tilde{lambda}_i
   B(it,it-1:it+1) = [at bt ct];
end
%
% for the first and last nodes
%
B(1,1:2)  = (6/hr/hr)*[-1 1];
rp = radius; % last node
q  =  2*hr*hc/km; % phi=bt-q*ct
B(nnr,nnr-1:nnr)= [-bt bt-q*ct];
%
B           = (km/(rm*cm))*B; % had factored out alpha
% Eqn (1) transforms, under change of variable Ta=X*z, to
%   dz/dtau=D*z+R+S*tau                 (2)
% Matrices X and D are given by
[X,D]   = eig(B); % X diagonalizes B
lamb     = diag(D); % eigenvalues
Omexp   = 1-exp(D*dt); % the solution of eqution (2) is
%     z=alpha*Omexp+beta*dt             (3)
XI      = inv(X); % R=X\(B*Tm1+P)
DI      = inv(D); % inv(D) related to beta
v(nnr)  = (2*hc/(rm*cm))*(1/hr+1/radius); % part of v in equation (1)

%%%%%%%%%%%%%%%%%%%%%%%%%%%%%%%%%%%%%%%%%%%%%%%%%%
% Semi-analytic solution
% Solve equation (1) on interval [t1,t2] on t-axis, where we assume
% linear variation of Tf(t), i.e

% Tf(t)=Tf1+(t-t1)*(Tf2-Tf1)/dt
%
% where
%
```

```
% Tf1 = fluid temperature at time t=t1
% Tf2 = fluid temperature at time t=t2
% dt = t2-t1
% Similar notation:

% Tm1 = rock temperature at time t=t_1
% Tm2 = rock temperature at time t=t_2
% Ta = Tm2-Tm1

% Setting the basic loop: progressing from time t1 to time t2
% with the computation over the time range

Tf1 = 20*ones(1,nnx); %=zeros(1,nnx);
Tf2 = zeros(1,nnx); % is this used?
Tm1 = zeros(nnr,nnx);%20*ones(nnr,nnx);
Tm2 = zeros(nnr,nnx);
Z   = zeros(nnr,nnx);
Z0  = zeros(nnr,nnx);
Ta  = zeros(nnr,nnx);
%
% Tf(1) is the inlet and Tf(nnx) the outlet temperatures
% Tm(nnr,:) is the temperature Tm(R,x,t) of the rock face in contact with
% the fluid at any time t and a distance x from entry into bed
%
% starting at time t1, with 20 temperature throughout and then setting
% in the given input temperature to obtain the temperatures at time t2;
% then recursively.
%
itme        = 1; % start at time level 1
%
tmes=stme:dt:etme;
%measured_0920_1004
measured_99_0217_0303
intes=md_air_in; % inlet temperatures or temperatures at entry
T_entry(itme) = intes(1); % Tf1(1); % initial air temperature at entry
T_exit(itme)  = intes(1); % initial air temperature at exit
tcounter=1;
for tme =tmes  % time stepping
   inte  = 20;%20 +10*sin(af*tme); %
   %inte      = intes(tcounter); tcounter=tcounter+1;
   time(itme) = tme/60/60; % can this be improved later?
   itme       = itme+1; % increase counter for time levels
   %
   % now at time t2
   %
   nup = 10;
   for upgrade = 1:nup
```

```
        % compute Tf2
        bc    = zeros(nnx,1); % begin with zeros in bc of K*Tf=bc
        % Tf2(1) = inte; % this does not seem necessary? replaced in (4) below
        %
        % forming the right hand side vector of the fluid equation
        %
        for ia = 1:nnx-1 % assemble bc in K*Tf=bc
            vt    = [ia ia+1];
            be    = ((Tms(ia)+Tms(ia+1))/2)*(delta*h/2)*[1 1]';
            be    = be+T_env*(beta1*h/2)*[1 1]';
            bc(vt) = bc(vt)+be;
        end
        bc(1)  = inte; % imposing bc T_f(0,t)=T_fi(t) on RHS of K*Tf=bc
        Tf2    = (K\bc)'; %              (4)
        time(itme)   = tme/60/60; % for plotting later
        T_entry(itme) = Tf2(1); % plotting later
        T_exit(itme)  = Tf2(nnx); % for plotting later
        % To calculate Tm2
        P    = v*Tf1;
        Q    = (1/dt)*v*(Tf2-Tf1);
        % P and Q appear in equation:
        % dTm/dt=B*Tm+P+Q(t-t1), t1<=t<=t2
        R    = XI*(B*Tm1+P);
        S    = XI*Q;
        % R and S appear in equation (2)
        Beta  = -DI*S;
        Alpha = DI*(Beta-R);
        % alpha and beta appear in (3)
        Z    = Omexp*Alpha+dt*Beta; % see equation (3)
        Ta   = X*Z; % change of variable for decoupling system of DEs
        %      [upgrade sum(sum(abs(Ta)))]  % for testing
        Tm2  = Tm1+Ta; % compute Tm2 using Tm2-Tm1=Ta
        Tms  = Tm2(nnr,:); % surface rock temperature at time t2
        %
    end   % of upgrade loop
    %
    Tm1   = Tm2; % what was Tm2 is now Tm1
    Tf1   = Tf2; % what was Tf2 is now Tf1
end   % of time loop
T_fo = T_exit;
T_fi = 20;

%%%%%inputs_brick.m
%% NUMERICAL DATA (inputs) FOR PHYSICAL CONSTANTS IN THE
% MATHEMATICAL MODEL FOR THE TRANSIENT BEHAVIOUR OF A
% PACKED BED DRIVEN BY THE FLUID INLET TEMPERATURE.
% physical constants
```

```
% fluid
% symbol   -  meaning
% c_f      -  specific heat capacity (J/kg degC)
% rho_f    -  density (kg/m^3)
% k_f      -  thermal conductivity (W/m degC)
% m_a      -  volume flow rate (m^3/s)
% m_f      -  mass flow rate (kg/m^3)

c_f=1007;
rho_f=1.106;
k_f=.025;
m_a=m_a;
m_f=rho_f*m_a;

% ** solid (bricks 'rubble')
% c_m      -  specific heat capacity (J/kg degC)
% rho_m    -  density (kg/m^3)
% k_m      -  thermal conductivity (W/m degC)
% alpha_m  -  thermal diffusivity (ms)

c_m=800;
rho_m=1700;
k_m=0.73;
alpha_m=k_m/(rho_m*c_m);

% other

% hc       -  convective film coefficient (W/m^2degC)
% porosity -  porosity of bed=(volume of fluid)/(volume of bed)
% lb       -  length of bed (m)
% S_fr     -  frontal surface area (m^2)
% radius   -  average sphere radius (m)
% A        -  total surface area of convection (m^2)
% rpuv     -  rocks per unit volume (/m^3)

hc=6;
porosity=.5;
Lb=Lb;
S_fr=2*2.7;
radius=.1;
rpuv=3*(1-porosity)/(4*pi*radius^3);
A=rpuv*S_fr*Lb*4*pi*radius^2;

% EOF


%%%%%Concrete_store.m%%%%%%
```